ABSTRACT:

An improved parametric equation has been proposed by Dr. Kozicki for characterization of the flow geometry in the rectilinear flow of Non-Newtonian fluids, in open and closed conduits of arbitrary cross-section and in purely viscous, inelastic flow of Non-Newtonian fluids through packed beds and porous media. In the new formulation, an infinite number of geometric parameters characterize the flow geometry. The actual number required in a particular application is shown to be determined by the fluid model equation representing the rheological behaviour of the fluid. In the present work the third geometric coefficient ε_2' was evaluated for both the Ostwald-de-Waele and Ellis fluids with flow behaviour s=2 and α=2 integers. The value obtained for $\varepsilon_2=0.375$ using a power-law fluid model and $\varepsilon_2=0.3868$ for an Ellis fluid model. The maximum deviation is less than 5% which is within engineering accuracy.

The anomalous surface effects exhibited by these fluids at the solid boundary were also examined . Polymer adsorption and separation phenomena were observed for flow through both packed beds and capillary tubes. A mathematical model explaining the behaviour of the polymer for any fluid model satisfactorily correlated the available experimental data.

ACKNOWLEDGEMENT:

The author wishes to express his gratitude to Dr. William Kozicki for his constant encouragement in carrying out this work, which otherwise could not have been successfully achieved. He is also thankful to Mr. G. Gasperetti, Mr. Bonaldo for their assistance in the construction of the equipment.

TABLE OF CONTENTS

LIST OF FIGURES

LIST OF FIGURES

LIST OF FIGURES

LIST OF FIGURES

LIST OF TABLES

LIST OF TABLES

LIST OF TABLES

LIST OF TABLES

LIST OF TABLES

LIST OF TABLES

LIST OF TABLES

LIST OF TABLES

Chapter I

Introduction:

The flow of fluids through porous media has attracted the attention of many researchers due to its growing importance in the industries. Some of the technology pertinent to fluid flow through porous media includes soil mechanics, ground water hydrology, naval architecture, polymer processing, petroleum engineering and waste disposal applications.

The study of the flow of fluids through porous media may be separated into two categories, namely:

a) Newtonian: that is fluids for which the relation between shear stress and shear rate is a simple proportionality. This includes all gases and most homogeneous, nonpolymeric fluids.

b) Non-Newtonian: are fluids for which the relation between shear stress and shear rate is not a simple proportionality. Suspensions and solutions of polymers are examples of these fluids.

The former class of fluids has been studied more extensively than the latter one which is frequently encountered in many engineering branches.

A simple method was proposed in earlier papers (16) by Dr. Kozicki and his co-workers for prediction of non-

Newtonian flow in open and closed conduits of arbitrary cross-section utilizing a generalized Rabinowitsch-Mooney equation with two geometric parameters characterizing the flow geometry. The above technique was shown (14) to be successfully applicable to the interpretation and prediction of the flow characteristics in purely viscous inelastic flow through packed beds and porous media. Also the analytical results and experimental data was satisfactory for a broad range of fluid models and flow geometries including rectangular, triangular and elliptical ducts and concentric annuli over a wide range of aspect ratios, with a maximum deviation of 5 per cent. However, it was noted that for concentric annuli with aspect ratios in the range $0<k<0.2$, the former method was inapplicable. The aberrations encountered (32) which are a function of the fluid model as well as of the aspect ratio, are of greater magnitude than above with a maximum deviation of about 25% occurring at an aspect ratio of 0.01. Also the existing method becomes more inapplicable for correlating packed beds and porous media flow data when the fluids observed increase in Non-Newtonian behaviour.

Presently a more general formulation of the problem of characterization of flow geometries, with regards to flow of Non-Newtonian fluids has been derived by Dr. Kozicki, in which the above mentioned limitations of the previous generalization of the Rabinowitsch-Mooney equation are effectively eliminated. The purpose of the present work is to evaluate more geometric coefficients for two different Non-Newtonian fluid models and to test the validity of the improved formulation. However, in order to achieve this, one has to take into account the surface effects which are exhibited by these fluids on the solid boundary.

Chapter II

Literature Survey

Non-Newtonian flow through porous media

The most fundamental equation that governs the flow through porous media is that of Darcy. Darcy's law states that for a viscous flow of a Newtonian fluid through an isotropic, homogeneous, porous medium, the volumetric flow rate Q, through the medium is directly proportional to the cross-sectional area of the bed A, and to the pressure gradient $\Delta P/L$ causing flow i.e.

$$Q=kA\frac{(\Delta P)}{(L)} \qquad \ldots(1)$$

Unfortunately this law describes the flow through porous media only in a certain region and does not provide sufficient information concerning the property of permeability. Many attempted to relate the permeability to the properties of the porous medium theoretically and emperically despite these numerous attempts there is no universally accepted correlation.

The three fundamental theoretical approaches for studying the flow through porous media are:

(1) Hydraulic radius theory

(2) Drag theory

(3) Statistical theory

They all assume that the flow is based on the microscopic flow within pores. The analysis of the first two methods are based on the Navier Stoke's equations, while the third is based on statistical mechanics. The porous medium is envisaged as an assemblage of channels, in the first method, the second regards the particles to be obstacles to an otherwise straight flow of the fluid and the third considers the medium as intrinsically disordered.

The Hydraulic radius or capillary model is the most popular method used, among those that use this model are Kozicki et al (14), Mckinley et alia (20) Hassel and Bondi (12), Sadowski and Bird (28), Christopher, Middleman and Gaitonde (4, 5, 7, 8), Marshal and Metzner (21) and many others.

A generalized scale-up method based on the capillary model, Hydraulic Radius Concept

There are many methods established in predicting a Non-Newtonian flow behaviour in porous media, and for correlating results of porous media experiments with viscometric data. At the present time, there still does not seem to be a universally acceptable scale-up method. The previous method proposed for depicting the flow rate and maximum velocity in the isothermal, steady, uniform laminar flow of any incompressible, time-independent Non-Newtonian fluid in straight open channels of arbitrary cross-section utilizes the knowledge of two geometric coefficients in the Rabinowitch and Mooney equation. The generalization of the Rabinowitch and Mooney equation may be represented in the following form.

$$f(\tau_w) = a\,\tau_w \frac{\partial \frac{2(\langle u\rangle - u_w)}{rH}}{\partial \tau_w} + b\,\frac{2(\langle u\rangle - u_w)}{rH} \quad \ldots\ldots\ldots\ldots \quad (2)$$

This form takes into account the effective slip velocity and the variation of the velocity gradient $f(\tau_w)$, τ_w and u_w with distance around the wetted periphery, where

$$f(\tau_w) = \frac{1}{p} \oint f(\tau_w)\,dl \quad \ldots\ldots\ldots\ldots\ldots\ldots \quad (3)$$

$$f(\tau_w) = -\left(\frac{du}{dr}\right)_w = \frac{\tau_w}{\eta} \quad \ldots\ldots\ldots\ldots\ldots\ldots \quad (4)$$

$$\tau_w = \frac{1}{p} \oint \tau_w\,dl \quad \ldots\ldots\ldots\ldots\ldots\ldots \quad (5)$$

$$u_w = \frac{1}{p} \oint u_w\,dl \quad \ldots\ldots\ldots\ldots\ldots\ldots \quad (6)$$

a, b, are geometric coefficients characteristic of the shape of the flow cross-section which may be evaluated using a Newtonian fluid.

Integrating equation (2) gives the following general results,

$$\frac{\langle u\rangle - u_w}{rH} = \frac{1}{2a}\,\tau_w^{-\frac{b}{a}} \int_{\tau yT}^{\tau_w} \tau^{\frac{b}{a}-1} f(\tau)\,d\tau \quad \ldots\ldots \quad (7)$$

$$= \frac{1}{2a} \tau_w^{\frac{-b}{a}} \int_{\tau_y T}^{\tau_w} \frac{\tau}{\eta} \, d\tau \qquad \ldots\ldots\ldots\ldots\ldots\ldots \quad (8)$$

Using the Blake-Kozeny model for the packed bed, that is the porous medium is envisaged as a conduit or conduits of complicated cross-sectional geometry. Equation (8) is applicable to both packed beds and capillary tubes and may be written in terms of the aspect factor ξ and the impermeability factor k_i, where $\xi = \frac{b}{a}$ and $k_i = 2(a + b)$ the term T

$$\frac{\langle u\rangle - u_w}{rH} = \frac{(1+\xi)}{k_i} \tau_w^{-\xi} \int_{\tau_y T}^{\tau_w} \frac{\tau^{\xi}}{\eta} \, d\tau \qquad \ldots\ldots\ldots\ldots\ldots\ldots \quad (9)$$

is the tortuosity which accounts for the actual capillaries in the bed.

In the above equation, the average velocity through the pores <u> is related to the superficial velocity based on the cross-sectional area of the empty bed by

$$\langle u\rangle = \frac{Us}{\varepsilon} \qquad \ldots\ldots\ldots\ldots\ldots\ldots \quad (10)$$

this is the well known Dupuit-Forchheimer Assumption Scheidegger (39).

The average "slip velocity" u_w at the pore wall is similarly related to the superficial slip velocity by

$$u_w = \frac{u_{ws}}{\varepsilon} \qquad \text{(11)}$$

the hydraulic radius (for an isotropic bed) is given by

$$rH = \frac{\text{cross section available to flow}}{\text{wetted perimeter}}$$

$$= \frac{\text{volume available to flow}}{\text{total wetted surface}}$$

$$= \frac{\varepsilon}{(1 - \varepsilon) S'} \qquad \text{(12)}$$

where the specific surface per unit volume for a bed comprised of uniform spheres is

$$S' = \frac{6}{Dp} \qquad \text{(13)}$$

For a bed of irregular particles, equation (13) serves as the defining relation for the particle diameter.

τ_w is given by the following expression derived for straight conduits of arbitrary cross-sectional shape,

$$\tau_w = rH \left(\frac{-dp'}{dx}\right) \qquad \text{(14)}$$

The Non-Newtonian viscosity η is defined in accordance with the following relationship for the fluid expressed in the form of a "generalized Newtonian fluid" where τ_{ij} and γ_{ij}

$$\tau_{ij} = -\frac{\eta\partial U_j}{\partial x_i} + \frac{\partial U_i}{\partial x_j} = -\eta\gamma_{ij} \quad \ldots\ldots\ldots\ldots\ldots\ldots \quad (15)$$

are components of the stress tensor τ and rate of deformation γ rensor, respectively. It is presumed that the Non-Newtonian viscosity η is a scalar function of either of the scalar invariants.

$$\tau = +\sqrt{\tfrac{1}{2}}\,(\tau:\tau) = \sqrt{\tfrac{1}{2}}\,\sum_i \sum_j \tau_{ij}^2 \quad \ldots\ldots\ldots\ldots\ldots\ldots \quad (16)$$

or

$$\gamma = +\sqrt{\tfrac{1}{2}}\,(\gamma:\gamma) = \sqrt{\tfrac{1}{2}}\,\sum_i \sum_j \gamma_{ij}^2 \quad \ldots\ldots\ldots\ldots\ldots\ldots \quad (17)$$

Anomalous surface effects

Previous literature has shown that under appropriate conditions, some Non-Newtonian materials exhibit anomalous surface effects under steady flow behaviour. Most of the published literature concerning anomalous surface behaviour of Non-Newtonian flow through capillary tubes illustrates that the effective surface velocity U_W is positive, that is the viscosity of the material within a distance δ from the wall is lower than the bulk material outside the boundary. Some of the dilute solutions reported that exhibit this physical behaviour are aqueous solutions of the sodium salt of carboxymethycellulose (3) blood (11) GRS lattices (34) and moderately high molecular weight grade of poly(methylmethacrylate) in monochlorobenzene (33). Kozicki et alia.

(14) were the first to report adsorption effects, and to distinguish between negative and positive effective velocities from the studies of Non-Newtonian flow through porous media. The adsorption effect can be interpreted when the viscosity within the anomalous layer is greater than the bulk of material.

Many attempted to devise theories in order to predict the occurrences of macroscopic effects in certain flow geometries. Some of the first investigators who examined the surface effects were Oldroyd (25) Mooney (18) and Scott-Blair (29)

Evidently the past literature shows the existence of surface effects. These effects if not accounted for in the analysis of viscometric data can lead to false informations of rheological behaviour because of misinterpretation of viscometric data.

Chapter III

Theoretical Analysis

Improved parametric equations

The equation (2) given previously was obtained by a simple and straight-forward generalization of the analytical result derived for the closed circular and slit cross sections and semi-circular and inclined plane open channels, does not provide for interaction, in the general case, with second and higher derivatives of $\frac{2(\langle u\rangle - u_w)}{rH}$ with respect to τ_w. Therefore in the present analysis, Dr. Kozicki replaces equation (2), by the following basic differential equation of infinite order, which is postulated to govern the flow of Non-Newtonian fluids in conduits of arbitrary cross-section,

$$f(\tau) = \varepsilon_o w + \varepsilon_1 \tau \frac{dw}{d\tau} + \varepsilon_2 \tau^2 \frac{d^2 w}{d\tau^2} + \ldots. + \varepsilon_i \tau^i \frac{d^i w}{d\tau^i} + \ldots. \qquad (18)$$

where w is given by $\frac{2(\langle u\rangle - u_w)}{rH}$ and τ has been substituted for τ_w to make the equation simpler.

The ε_i's are now the new geometric parameters characterizing the shape of the arbitrary flow cross-section. In general an infinite number of geometric parameters are now required to characterize a flow geometry as compared with just two previously v.i.z., b and a in equation (2).

Equation (18) reduces to the same form as equation (2) for simple cases of circular and slit cross-sections and also for Newtonian fluids, $\frac{d^i w}{d\tau^i} = o$ for $i > 1$.

The infinite order differential equation is solved by a perturbation technique utilizing the assumption that $\varepsilon_i^2 < 1$ and the boundary condition that $w=0$ at $\tau=0$. The first step is to determine the solution to the i-th order differential equation obtained by truncating equation (18) at the ith term

$$f(\tau) = \varepsilon_o W_i + \varepsilon_1 \tau \frac{dW_i}{d\tau} + \varepsilon_2 \tau^2 \frac{d^2 W_i}{d\tau^2} + \ldots + \varepsilon_i \tau^i \frac{d^i W_i}{d\tau^i} \quad \ldots\ldots (19)$$

It is assumed that the solution $W_i(\tau)$ to equation (19) can be represented as a power series in the coefficient ε_i as follows

$$W_i = \sum_{j=o}^{\alpha} W_{ij}(\tau)\ \varepsilon_i^j \qquad W_{ij}\ (o) = 0 \text{ for all } j \ldots\ldots\ldots\ (20)$$

where the coefficients W_{ij} of the ε_i^j are functions of τ to be determined. Clearly the boundary condition $W_i = 0$ at $\tau = 0$ will be satisfied if a solution of the form of equation (22) can be found satisfying the condition $W_{ij}\ (0) = 0$ for all j.

Substituting equation (20), into (19) yields

$$f(\tau) = \varepsilon_o \sum_{j=o}^{\alpha} \varepsilon_i^{\ j}\, W_{ij} + \varepsilon_1 \tau \sum_{j=o}^{\alpha} \varepsilon_i^{\ j} \frac{dW_{ij}}{d\tau} + \varepsilon_i \tau^{i} \sum_{j=o}^{\alpha} \varepsilon_i^{\ j} \frac{dW_{ij}}{d\tau^i} \qquad (21)$$

which expanded, and equating coefficients of like powers of

ε_i, leads to the following infinite set of differential equation of (i-1) th order to be solved recursively for the functions w_{io} , w_{i1}, w_{i2} etc...

$$f(\tau) = \varepsilon_0 w_{io} + \varepsilon_1 \tau \frac{dw_{io}}{d\tau} + \varepsilon_2 \tau \frac{dw_{io}}{d\tau^2} + \ldots + \varepsilon_{i-1} \tau^{i-1} \frac{d^i w_{io}}{d\tau^{i-1}} \quad \ldots (22)$$

$$-\tau^i \frac{d^i w_{io}}{d\tau^1} = \varepsilon_0 w_{i1} + \varepsilon_i \tau \frac{dw_{i1}}{d\tau} + \varepsilon_2 \tau^2 \frac{d^2 w_{i1}}{d\tau^2} + \ldots + \varepsilon_{i-1} \tau^{i-1} \frac{d^{i-1} w_{i1}}{d\tau^{i-1}} \ldots \quad \ldots (23)$$

$$-\tau^i \frac{d^i w_{i(j-1)}}{d\tau^i} = \varepsilon_0 w_{ij} + \varepsilon_1 \tau \frac{d^i w_{ij}}{d\tau} + \varepsilon_2 \tau^2 \frac{d^2 w_{ij}}{d\tau^2} + \ldots + \varepsilon_{i-1} \tau^{i-1} \frac{d^{i-1} w_{ij}}{d\tau^{i-1}} \quad \ldots (24)$$

It is seen that the solution to the first equation in the above set is given by $w_{io} = w_{i-i}$ where w_{i-1} is the solution to the (i-1) th order differential equation formed by truncation of equation (18) at the (i-1)th term. The successive solutions w_{io}, w_{i1}, w_{i2} etc... of the above system of equations unables us to construct the solution w_i, represented by equation (20), to the ith order equation, equation (19). Clearly, this solution is also the zero-order solution to the (i-1)th order truncated equation (18), that is,

$$W_i = W_{(i+1)0}$$

A formal analytical procedure has thus been developed for obtaining the solution to equation (18), truncated to any order as well as to the untruncated equation of infinite order in the limit, by successively utilizing solutions to lower order truncations of equation (18) beginning with the second order differential equation

$$f(\tau) = \varepsilon_0 w_2 + \varepsilon_1 \tau \frac{dw_2}{d\tau} + \varepsilon_2 \tau^2 \frac{d^2 w_2}{d\tau} \quad \ldots\ldots\ldots\ldots\ldots\ldots \quad (25)$$

We pause briefly to illustrate the procedure just described by evaluating several terms of the solution to equation (25).

The zero-order solution w_{20} is given by the solution to the truncated first-order equation w_1 which is readily found (1) as

$$w_{20} = w_1 = \frac{1}{\varepsilon_1} \tau^{-\xi} \int_0^\tau \tau^{\xi-1} f(\tau)\, d\tau \quad \ldots\ldots\ldots\ldots \quad (26)$$

where the aspect factor is $\xi = \varepsilon_0 / \varepsilon_1$

Making use of this result in equation (23), we obtain the first order solution w_{21} as,

$$w_{21} = -\frac{1}{\varepsilon_1} \tau^{-\xi} \int_0^\tau \tau^{\xi+1} \frac{d^2 w_{20}}{d\tau^2}\, d\tau \quad \ldots\ldots\ldots\ldots \quad (27)$$

Similarly, any subsequent term, w_{2j} ,is readily obtained from the function representing the preceding term in the series by

$$w_{2j} = -\frac{1}{\varepsilon_1} \tau^{-\xi} \int_0^\tau \tau^{\xi+1} \frac{d^2\, w_{2(j-1)}}{d\tau^2}\, d\tau \quad \ldots\ldots\ldots \quad (28)$$

Applications to Various Fluid Models

We will now illustrate the usefulness of the method by performing actual integrations for some Non-Newtonian fluid models yielding the average velocity - pressure drop relationship for these fluids.

(1) Ostwald-de-Waele (power-law) fluid.

The Ostwald-de-Waele fluid is represented by the fluid model equation

$$f(\tau) = \frac{\tau}{\eta} = \left(\frac{\tau}{K}\right)^s \quad \ldots\ldots\ldots\ldots\ldots\ldots\ldots \quad (29)$$

where s is the reciprocal of the flow behaviour index, $s = \frac{1}{n}$.

Utilizing equation (29) the functions w_{20}, w_{21}. etc... are readily found from equations (26) - (28) as follows

$$w_{20} = \frac{1}{\varepsilon_0+\varepsilon_1 s} \left(\frac{\tau}{K}\right)^s \quad \ldots\ldots\ldots\ldots\ldots\ldots\ldots \quad (30)$$

$$w_{21} = -\frac{s\,(s-1)}{(\varepsilon_0+\varepsilon^1 s)^2} \left(\frac{\tau}{K}\right)^s \quad \ldots\ldots\ldots\ldots\ldots\ldots\ldots \quad (31)$$

$$w_{2j} = \frac{(-1)^j\, s^j\, (s-1)^j}{(\varepsilon_0+\varepsilon^1 s)^{j+1}} \left(\frac{\tau}{K}\right)^s \quad \ldots\ldots\ldots\ldots\ldots\ldots\ldots \quad (32)$$

Hence, the solution w_2 of the second order differential equation represented by equation (25), obtained for the Ostwald-de-Waele fluid by substitution of these functions is the appropriate form of equation (20) is given by

$$w_2 = \frac{(\tau/K)^s}{\varepsilon_0 + \varepsilon_1 s} \sum_{j=0}^{\infty} \left(\frac{-s(s-1)\varepsilon_2}{\varepsilon_0 + \varepsilon_1 s}\right)^j \quad \text{.........(33)}$$

The solution w_2 may be expressed finally in the following simple closed form

$$w_2 = \frac{(\tau/K)^s}{\varepsilon_0 + \varepsilon_1 s}\left(1 + \frac{s(s-1)\varepsilon_2}{\varepsilon_0 + \varepsilon_1 s}\right)^{-1} \quad \text{...............(34)}$$

$$= \frac{(\tau/K)^s}{\varepsilon_0 + \varepsilon_1 s + \varepsilon_2 s(s-1)} \quad \text{.............(35)}$$

which follows from equation (34) for $\frac{s(s-1)\varepsilon_2}{\varepsilon_0 + \varepsilon_1 s} < 1$

One can now set $w_2 = w_{30}$ and proceed in the same way to arrive at the solution for the third order equation w_3 and continuing further in the same manner obtain w_4, w_5 etc. Thus, the functions w_3 ,....., w_i ...., respectively, yielded by this procedure are as follows:

$$w_3 = \frac{(\tau/K)^s}{\varepsilon_0 + \varepsilon_1 s + \varepsilon_2 s(s-1) + \varepsilon_3 s(s-1)(s-2)} \quad \text{......(36)}$$

$$\vdots \qquad\qquad \vdots$$

$$w_i = \frac{(\tau/K)^s}{\varepsilon_0 + \varepsilon_1 s + \varepsilon_2 s(s-1) + \ldots + \varepsilon_i s(s-1)\ldots(s-i+1)} \quad \ldots\ldots\ldots(37)$$

By inspection, the solution w to the untruncated differential equation of infinite order, equation (18), representing the most general solution for the flow of power-law fluids in conduits of arbitrary cross-section, can therefore be written as

$$\frac{(\tau/K)^s}{w} = \varepsilon_0 + \varepsilon_1 s + \varepsilon_2 s(s-1) + \varepsilon_3 s(s-1)(s-2) + \ldots\ldots\ldots$$

$$\ldots + \varepsilon_i s(s-1)\ldots(s-i+1) + \ldots \quad \ldots\ldots\ldots\ldots\ldots\ldots(38)$$

Some interesting and useful properties which equation (38) has are when $s = \frac{1}{n}$ has the values 0, 1, 2, ..., the right hand side of equation (38) becomes $\varepsilon_0, \varepsilon_0 + \varepsilon_1, \varepsilon_0 + 2\varepsilon_1 + 2\varepsilon_2 \ldots$, respectively, and we see that for the s integral, the number of geometric parameters appearing in the general solution increases with the degree of Non-Newtonianess of the fluid and is given by s+1. Further, for the s integral, equation (38) becomes the following:

$$\frac{(\tau/K)^s}{w} = \sum_{j=0}^{s} \varepsilon_j \frac{s!}{(s-j)!} = \sum_{j=0}^{s} \varepsilon_j \binom{s}{j} j! \quad \ldots\ldots\ldots\ldots\ldots(39)$$

which also corresponds to the solution w_s to the truncated differential equation or orders represented by equation (19) with i = s.

Therefore, when $n = \frac{1}{2}$, $s = 2$ the average velocity pressure-drop relationship according to equation (39) is described by the simple equation

$$\frac{(\tau/K)^2}{W} = \varepsilon_0 + 2\varepsilon_1 + 2\varepsilon_2 \quad \ldots\ldots\ldots\ldots\ldots\ldots \quad (40)$$

This property of the general solution for power-law fluids provides a convenient means for evaluation the geometric parameters. Thus, if one has access to an independent source of information describing power-law fluids flow for a particular geometry, obtained either by experiment or analytically by the conventional method, ε_0 is obtained directly from the flow characteristics for $s = 1$ with ε_0 and ε_1 known, ε_2 is determined from the data for $s = 2$, and so on. Since the geometric parameters are independent of the fluid, they can be used to predict the flow of fluids described by other fluid model equations.

<u>Ellis fluids</u>

The ellis fluid model is given as

$$f(\tau) = \frac{\tau}{\eta_0}\left[1 + (\tau/\tau_{\frac{1}{2}})^{\alpha-1}\right] \quad \ldots\ldots\ldots\ldots\ldots\ldots\ldots \quad (41)$$

Using the same procedure, the solution, w_2, is found to be:

$$W_{20} = W_1 = \frac{\tau}{\eta_0}\left(\frac{1}{\varepsilon_0+\varepsilon_1} + \frac{1}{\varepsilon_0+\alpha\varepsilon_1} \quad (\tau/\tau_{1/2})^{\alpha-1}\right) \quad \text{........(42)}$$

$$W_{21} = \frac{-\tau\alpha(\alpha-1)}{\eta_0 \ (\varepsilon_0+\alpha\varepsilon_1)}(\tau/\tau_{1/2})^{\alpha-1} \quad \text{.....................(43)}$$

$$W_{2j} = \frac{(-1)^j \tau \ \alpha^j \ (\alpha-1)^j \ (\tau/\tau_{1/2})^{\alpha-1}}{\eta_0 \ (\varepsilon_0 + \alpha\varepsilon_1)^{j+1}} \quad \text{.....................(44)}$$

The infinite series resulting on substitution of these functions in the appropriate form of equation (20) can be transformed to the following closed form solution for W_2:

$$W_2 = \frac{\tau}{\eta_0}\left(\frac{1}{\varepsilon_0+\varepsilon_1} + \frac{1}{\varepsilon_0+\alpha\varepsilon_1+\alpha(\alpha-1)\ \varepsilon_2} \quad (\tau/\tau_{1/2})^{\alpha-1}\right) \text{...........(45)}$$

Similarly, the function $W_3, \ldots, W_i \ldots$, yielded successively for the Ellis fluids, are given by

$$W_3 = \frac{\tau}{\eta_0}\left(\frac{1}{\varepsilon_0+\varepsilon_1} + \frac{1}{\varepsilon_0+\alpha\varepsilon_1+\alpha(\alpha-1)\varepsilon_2+\alpha(\alpha-1)(\alpha-2)\varepsilon_3} \ (\tau/\tau_{1/2})^{\alpha-1}\right) \text{(46)}$$

$$W_i = \frac{\tau}{\eta_0}\left(\frac{1}{\varepsilon_0+\varepsilon_1} + \frac{1}{\varepsilon_0+\alpha\varepsilon_1+\alpha(\alpha-1)\ \varepsilon_2+\ldots+\alpha(\alpha-1)\ldots\ (\alpha i+1)\ \varepsilon_i} (\tau/\tau_{1/2})^{\alpha-1}\right)$$

(47)

and the general relationship describing the flow of the Ellis fluid can be therefore be represented as

$$w = \frac{\tau}{\eta_0}\left[\frac{1}{\varepsilon_0+\varepsilon_1} + \frac{1}{\varepsilon_0+\alpha\varepsilon_1+\alpha(\alpha-1)\ \varepsilon_2+..(\alpha)\ (\alpha-1)..\ (\alpha-i+1)\ \varepsilon_i+.}(\tau/\tau_{\frac{1}{2}})^{\alpha-1}\right] \quad ....(48)$$

For a fluid for which $\alpha=2$, equation (48) simplifies to

$$w = \frac{\tau}{\eta_0}\left[\frac{1}{\varepsilon_0+\varepsilon_1} + \frac{1}{\varepsilon_0+2\varepsilon_1+2\varepsilon_2}\ (\tau/\tau_{\frac{1}{2}})\right] \quad ....(49)$$

We see that when α is an integer, the number of geometric parameters needed to specify the flow geometry with an Ellis fluid which is also governed by the degree of Non-Newtonian behaviour of the fluid, as exhibited in the value of the flow behaviour index α.

Equation (49) may be rewritten in the following form applicable for integral values of α

$$w = \frac{\tau}{\eta_0}\left[\frac{1}{\varepsilon_0+\varepsilon_1} + \frac{1}{\sum_{j=0}^{\alpha} \varepsilon_j \binom{\alpha}{j} j!}(\tau/\tau_{\frac{1}{2}})^{\alpha-1}\right] \quad ....(50)$$

This equation may be transformed into equations (46) and (47) when $i=\alpha$ and when $\alpha=2$ it gives equation (49).

Analysis of anomalous flow

One of the main problems of Non-Newtonian flow through porous media is the frequent occurrence of surface effects. This has to be accounted for in order to predict flow through porous media more precisely. Oldroyd (25) was the first to propose a method for determining the mean effective velocity u_w for Non-Newtonian flow through a circular tube. Substantially, the same procedure is applied to an arbitrary cross-section.

In steady, uniform, isothermal, laminar flow of a time-independent fluid through an arbitrary cross-section, the average velocity <u> , is determined by equation (9) rewritten in the following form,

$$\frac{2\langle u\rangle}{rH} = \frac{2u_w}{rH} + \frac{2\ (1+\xi\ )}{k_i}\ \tau w^{-\xi} \int_{\tau_y}^{\tau_w} \frac{\tau^{\xi}}{\eta}\ d\tau \ \ldots\ldots\ldots\ldots (51)$$

According to this expression a unique relationship exists between $\frac{2\langle u\rangle}{rH}$ when $u_w = 0$ and τw which is independent of the hydraulic radius. In the presence of a surface effect, plots of $\frac{2\langle u\rangle}{rH}$ versus τw are expected to yield separate curves for different values of the hydraulic radius, rH. From these curves, at a selected value of a plot of $\frac{2\langle u\rangle}{rH}$ versus $\frac{1}{rH}$ can be constructed. The curve obtained is a straight line with slope $2u_w$. By repeating the procedure at different values of τ_w, the effective velocity at the wall can be determined as a function of the contour integrated average shear stress. The same procedure is applicable to flow through packed beds and porous media. It should be mentioned that in the above procedure for calculating u_w, it is assumed that u_w is independent of rH being a function only of τ_w. It was Oldroyd (19) who defined a slip coefficient.

$$\xi' = \frac{\overline{U}_w}{\tau_w} \quad \ldots\ldots\ldots\ldots\ldots\ldots\ldots \quad (52)$$

presumed to be a function only of shear stress to represent the functional relationship between the effective velocity at the wall and the shear stress at the wall. Introducing (52) in equation (51) yields

$$\frac{2\langle u\rangle}{rH} = \frac{2\xi'\overline{\tau}_w}{rH} + \frac{2(1+\xi)}{k_i}\,\tau_w^{-\xi}\int_{\tau_y}^{\tau_w}\frac{\tau^{\xi}}{\eta}\,d\tau \quad \ldots\ldots\ldots\ldots\ldots \quad (53)$$

In the most general case, the effective wall velocity may vary with both hydraulic radius and shear stress. This was found by Jastrezebski (13) in a study of the flow of concentrated suspensions and also by Kozicki et alia. The latter indicates that there exists a critical shear stress, τ_c, which marks the transition from a negative effective velocity to a positive one at the wall for values of wall shear stress greater than τ_c.

Thus a new slip coefficient ξ'' which is a function of both shear stress and hydraulic radius is defined by

$$\xi''(\tau_w, rH) = \frac{\overline{U}_w}{\tau_w - \tau_c(rH)} \quad \ldots\ldots\ldots\ldots\ldots\ldots\ldots \quad (54)$$

where the critical shear stress, τ_c, which is a function of the hydraulic radius, is introduced.

Further, an explicit dependence of ξ" on rH, which permits a successful resolution of the experimental data, is introduced by setting the slip coefficient inversely proportional to the hydraulic radius to a power β. Thus one can define a modified slip coefficient ξ", analogously to Jastrezebski (13) by

$$\varepsilon''' = rH^{\beta}\ \xi''\ (\tau_w,\ rH) \qquad \text{.................... (55)}$$

which varies only with shear stress and is independent of the hydraulic radius.

Inserting equations (54) and (55) into (51) yields

$$\frac{2\langle u\rangle}{rH} = \frac{2\xi'''(\overline{\tau}_w - \overline{\tau}c)}{rH^{\beta+1}} + \frac{2(1+\xi)\ \overline{\tau}_w^{\ -\xi}}{k_i} \int_{\overline{\tau}_y}^{\overline{\tau}_w} \frac{\tau}{\eta}\ d\tau \qquad \text{........... (56)}$$

according to equation (56), a plot of the flow data in the form of $\frac{2\langle u\rangle}{rH}$ vs $\frac{2(\tau_w - \tau c)}{rH^{\beta+1}}$ for a particular value of τ_w producing a straight line with slope ξ''' . However since τc and β are not known before hand, but must also be determined, it is necessary to set up an iterative algorithm as follows. Referring to fig. (12) for convenience, a trial curve for τ_w vs $2(\langle u\rangle - \overline{u}w)/rH$ is first assumed, which intersects the τw vs $\frac{2\langle u\rangle}{rH}$ curves determined for different rH values. The τ_w values corresponding to the points of intersection of this trial curve with τ_w vs $\frac{2\langle u\rangle}{rH}$ curves, obtained for the different hydraulic radius, represent the trial values for τc for each tube diameter, corresponding to the trial curve selected. Using these values of τc, we next select a value of τw and determine β such that the plot of $\frac{2\langle u\rangle}{rH}$ vs $\frac{2(\tau_W-\tau c)}{rH^{\beta+1}}$, at the chosen τw is linear. We determine ξ''' from the slope of this line. By repeating this procedure at different values of shear stress, ξ''' can be determined as a function of τw. Having found ξ''', the effective velocity u_w can be evaluated from equation (54) and (55). One can then correct the measured average velocity or flow rate and calculate the quantity $\frac{2(\langle u\rangle-\bar{U}_W)}{rH}$ as a function of shear stress for each tube diameter. These quantities when plotted should lie on the assumed τw vs $\frac{2(\langle u\rangle-\bar{u}_W)}{rH}$ curve; if not, a different trial curve yielding a new set of values of τc is assumed and the procedure repeated from the beginning. The complete algorithm is repeated until the resulting τw vs $\frac{2(\langle u\rangle-\bar{u}_W)}{rH}$ curve coincides with the assumed one.

Estimation of the Anomalous layer Thickness

Based on Oldroyd's analysis (19), the velocity gradient in the anomalous layer within a normal distance δ from the solid boundary may be represented by

$$\frac{du}{dy} = f(\tau) + g(\delta,\tau,y) \qquad (57)$$

where y is the distance measured from the wall, $f(\tau)$ is the

FIG 1

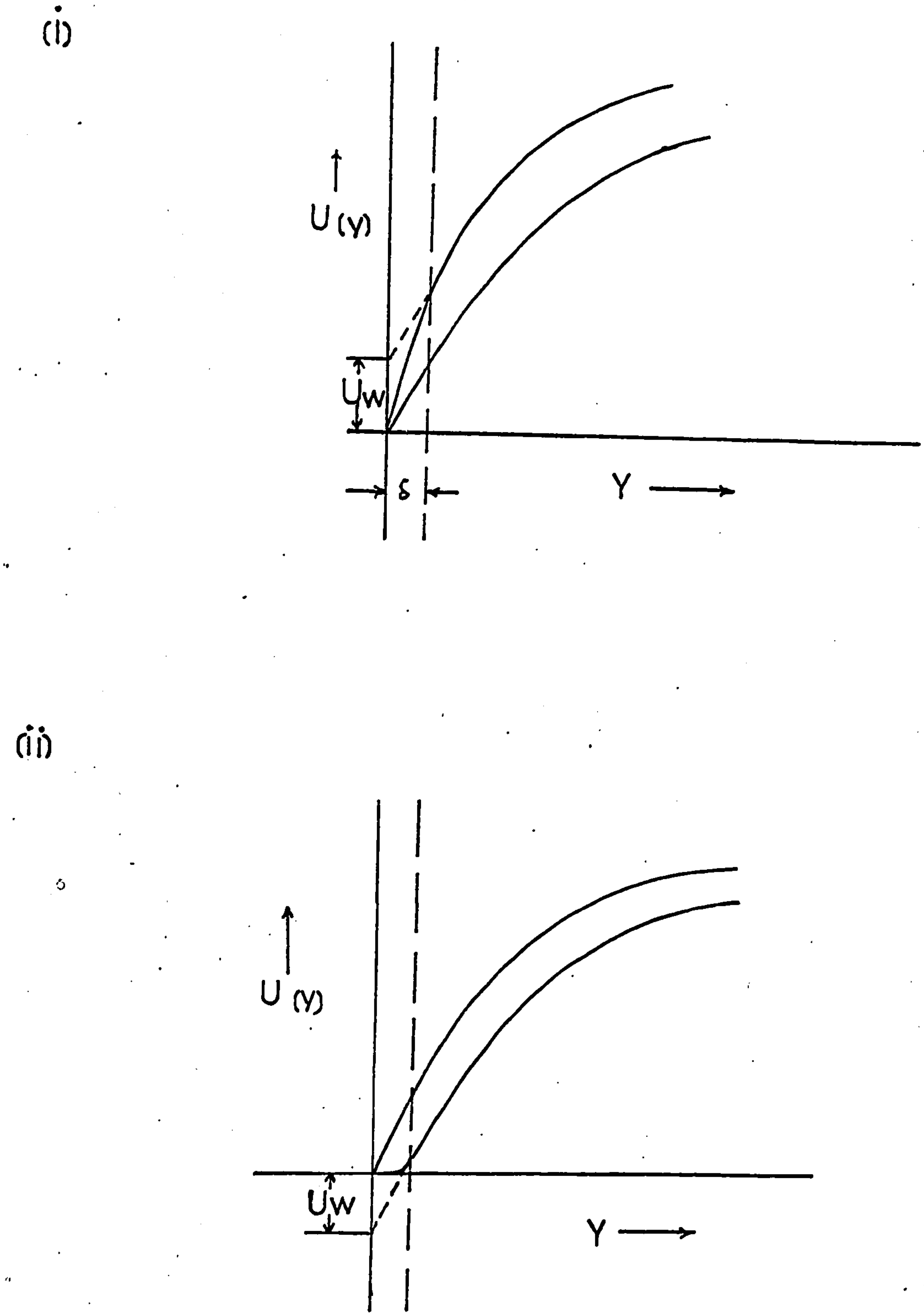

velocity gradient characteristically ascribable to the fluid under laminar conditions, and $g(\delta,\tau,y)$ is a correction term accounting for the anomalous behaviour in the vicinity of the solid wall. Outside the anomalous layer, at $y>\delta$ $g(\delta,\tau,y)=0$ and the velocity gradient is given by the characteristic function of shear stress ascribable to the main stream fluid such that $f(\tau)$ is approximated by $f(\tau_W)$ which yields the velocity beyond the anomalous layer given by the relation

$$u - u_W = f(\tau_W)\, y \quad \ldots\ldots\ldots\ldots\ldots\ldots\ldots \quad (58)$$

and

$$u_W = \int_0^\delta g(\delta,\tau,y)\, dy \quad \ldots\ldots\ldots\ldots\ldots\ldots\ldots \quad (59)$$

equation (59) is the defining equation for the "effective surface velocity at the wall".

As mentioned previously in the introduction there are two possible cases of anomalous behaviour, namely

(i) Positive effective velocity of slip at the wall

(ii) Negative effective velocity at the wall

the two cases are shown in fig. 1.

An estimate of the thickness of the anomalous layer is simple to perform once u_W is known. For case (i) which is also called the "separation phenomena" that is a pure solvent layer is formed adjacent to the wall then the velocity gradient in this layer is given as

$$\frac{du}{dy} = \frac{\tau_w}{\mu s} \qquad \text{.................... (60)}$$

Inserting equation (60) into (58) yields

$$U_w = \delta \frac{\tau_w}{\mu s} - f(\tau_w) = \delta\ \tau_w\left(\frac{1}{\mu s} - \frac{1}{\eta_w}\right) \qquad \text{............ (61)}$$

where μs is the viscosity of the pure solvent.

In the second case when the effective velocity is negative that is a certain amount of polymer adsorption and gel formation occur at the surface, the velocity gradient in the anomalous layer is so small that it can be assumed to be zero i.e. $\frac{du}{dy} = 0$.

The anomalous layer thickness is then found from equation (58) to be

$$U_w = \delta\ f(\tau_w) = -\delta \frac{\tau_w}{\eta w} \qquad \text{.................... (62)}$$

The above procedure is applicable to both packed bed and capillary tube data, also to conduits of arbitrary cross-sections, except τ_w and u_w are replaced by the contour integrated average quantities $\overline{\tau}_w$ and $\overline{u}_w$ respectively.

Friction factor-Reynolds number relationship for laminar flow

In laminar flow, the Fanning friction factor and Reynolds number are related according to the following relationship:

$$f = \frac{2\,\tau_w}{\rho\,(\langle u\rangle - u_w)^2} = \frac{16}{Re} \qquad (63)$$

The Reynolds number, expressed in terms of the apparent viscosity is given by:

$$Re = \frac{4rH\,(\langle u\rangle - \bar{u}_w)\,\rho}{(a + b)\,\eta ap} = \frac{8rH\,(\langle u\rangle - \bar{u}_w)\,\rho}{k_i\,\eta ap} \qquad (64)$$

Employing indices analogous to those originally defined for the circular tube by Metzner and Reed (21) the Reynolds number can also be expressed alternatively by

$$Re = \frac{\rho\,(\langle u\rangle - u_w)^{2-n^*}\,rh^{n^*}}{2^{n^*-3}\,K^*} \qquad (65)$$

where n* and K* are defined respectively by

$$n^* = \frac{\partial \ln \tau_w}{\partial \ln \dfrac{2(\langle u\rangle - u_w)}{rH}} \qquad (66)$$

and

$$K^* = \bar{\tau}_w \left(\frac{2(\langle u\rangle - \bar{u}_w)}{rH}\right)^{n^*} \qquad (67)$$

The partial differentiation in equation (66) is performed at constant values of geometric parameters, corresponding to a fixed flow geometry.

The general flow equation (7) may be used to express ηap, n* and K* in terms of the Non-Newtonian viscosity, η, of the fluid and the geometric parameters, ξ and k_i, of the flow channel as follows:

$$\eta ap = \frac{\tau_w^{1+\xi}}{(1+\xi)\int_{\bar{\tau}_y}^{\bar{\tau}_w} \frac{\tau^{\xi}}{\eta}\, d\tau} \quad \ldots\ldots\ldots\ldots\ldots\ldots\ldots \quad (68)$$

$$n^* = \frac{\eta_w \int_{\bar{\tau}_y}^{\bar{\tau}_w} \frac{\tau^{\xi}}{\eta}\, d\tau}{\bar{\tau}_w^{1+\xi}\,\xi\eta w \int_{\bar{\tau}_y}^{\tau_w} \frac{\tau}{\eta}\, d\tau} \quad \ldots\ldots\ldots\ldots\ldots\ldots\ldots \quad (69)$$

and

$$K^* = \bar{\tau}_w^{1+\xi n^*} \left(\frac{k_i}{2(1+\xi)}\right)^{n^*} \int_{\bar{\tau}_y}^{\bar{\tau}_w} \frac{\tau^{\xi}}{\eta}\, d\tau \quad \ldots\ldots\ldots\ldots\ldots \quad (70)$$

where η_w is the value of η evaluated at τ_w. All these three expressions are applicable to flow through porous media and packed beds, provided the proper modification is made of the lower integration limits, that is τ_y is replaced by $\tau_y T$ to account for the tortuosity of the actual capillary inside the porous medium. Thus we see that the relationships between the friction factor and Reynolds number presented here are applicable to any time-independent fluid, characterized by the Non-Newtonian viscosity η, and to any shape of flow channel, characterized by the geometric parameters "ξ" and k_i (or "a" or "b")

Application to Power Law fluids

In the simple case where there are no surface effects for the flow of power law fluids, and when n and K values remain constant over considerable ranges of shear rate, the Reynolds number may be represented as

$$Re = \frac{D^{n} \cdot \langle u\rangle^{2-n} \cdot \rho}{8^{n-1} \cdot K'} \qquad \text{.....................(71)}$$

which was defined by Metzner and Reed

where $n^* = n' = n$ ....(72)

and $K^* = K' = \frac{K(3n+1)}{4n}$ ....(73)

For a Newtonian fluid equation (71) reduces to the conventional Reynolds number in a circular pipe by setting $n = 1$ and $K' = \mu$

Generally, power law fluids may be represented by

$$\tau = K \left(\frac{-du}{dr}\right)^{n} = K\, f\, (\tau)^{n} \qquad \text{.....................(74)}$$

where n and K may vary continuously with shear rate. Expressing equation (74) in logarithmic form one gets

$$\log \tau = \log K + n \log f(\tau) \qquad \text{.....................(75)}$$

if n and K are assumed to be constant over at least a differential range of shear rate, then equation (75) may be differentiated as follows, within this range:

$$n = \frac{d \log \tau}{d \log f\ (\tau)} \qquad \text{.....................(76)}$$

The shear rate at the wall $\left(- \frac{du}{dr} \right)_w$ or more generally $f\ (\tau_w)$, can be shown to be related to the average velocity and the geometric parameters by the general flow equation (77) as follows:

$$f(\overline{\tau}_w) = \frac{2\ (\langle u\rangle - \overline{u}_w)}{rH} \frac{(a + bn^*)}{(n^*)} \qquad \text{.....................(77)}$$

converting equation (77) in logarithmic form

$$\log f\,(\bar{\tau}_w) = \log \frac{2(\langle u\rangle - u_w)}{rH} + \log \frac{(a + bn^*)}{n^*} \quad \ldots\ldots\ldots\ldots\ldots (78)$$

and differentiating this result with respect to $\log \tau_w$ at constant values of geometric parameters, one obtains:

$$\frac{\partial \log f\,(\bar{\tau}w)}{\partial \log \tau_w} = \frac{\partial \log \frac{2(\langle u\rangle - \bar{u}_w)}{rH}}{\partial \log \tau_w} + \frac{\partial \log \frac{(a+bn^*)}{n^*}}{\partial \log \tau_w} \quad \ldots\ldots\ldots (79)$$

Substituting the definitions of n and n*, given by equation (76) and (69) respectively, in the above equation yields

$$\frac{1}{n} = \frac{1}{n^*} + \frac{\partial \log \frac{(a+bn^*)}{n^*}}{\partial \log \tau_w} \quad \ldots\ldots\ldots\ldots\ldots\ldots\ldots (80)$$

Rearranging equation (80) one may obtain the expression for n in the following form

$$n = \frac{1}{\frac{1}{n^*} + \frac{\partial \log (a+bn^*)/n^*}{\partial \log \tau}} \quad \ldots\ldots\ldots\ldots\ldots\ldots\ldots (81)$$

$$= \frac{n^*}{1 - \frac{a}{a+bn^*}\,\frac{\partial n^*}{\partial \log \tau}} \quad \ldots\ldots\ldots\ldots\ldots\ldots\ldots (82)$$

or in terms of the aspect factor ξ, n is equal to

$$n = \frac{n^*}{1 - \frac{1}{1 + \xi n^*}\,\frac{\partial n^*}{\partial \log \tau}} \quad \ldots\ldots\ldots\ldots\ldots\ldots\ldots (83)$$

equation (83) represents the relationship between n and n^* for a power law fluid at any particular shear stress when the plot of $2(\langle u\rangle - \bar{u}_w)/rH$ versus $\bar{\tau}_w$ is not linear.

Prediction of Transition from Laminar to Turbulent Flow:

Metzner and Reed (21) proposed a correlation of the laminar, transition and turbulent flow regions for the flow of Non-Newtonian fluids. However in their analysis, it was assumed that there was no slip at the wall. It was, however necessary to take the slip into account because of the increased evidence of its occurrence in the tube flow. Kozicki et al (14) redefined the Reynolds number - friction factor relationships accounting for the anomalous wall effects. The expressions for the critical values of the friction factor, fc, and the Reynolds number Re_c, are given by the following relationships:

$$fc = \frac{1}{404}\left|\frac{3n+1}{n+1}\,(1-\lambda c)^{\frac{n+1}{n}} + \frac{Uw}{\langle u\rangle - u_w}\right|\frac{3n+1}{n}\,(\lambda c)^{\frac{1}{n}} \quad .....(84)$$

and

$$\lambda c = \frac{1}{n+2}^{\frac{n}{n+1}} \quad 1 + \left|\frac{(n+1)}{(3n+1)}\,\frac{Uw}{(\langle u\rangle - u_w}\right|^{\frac{n}{n+1}} \quad ....(85)$$

$$Re_c = \frac{16}{fc} \quad ....(86)$$

It is necessary to calculate the Re in order to ensure that the flow conditions are laminar since the mathematical model, discussed in the previous sections is for laminar flow of Non-Newtonian fluids.

Chapter IV

Viscometric experiment

In this chapter we shall give a brief discussion of the polymeric fluids used and their preparation. A description of the viscometer and the experimental procedure shall also be given. The equations suitable for representing tube-flow of Non-Newtonian fluids were given previously in Chapter III. They are applicable to the viscometric data, so they shall not be mentioned again.

(i) Fluids

The polymeric fluids chosen in the present work were Hydroxycelluloses (natrosol 250 GR and 250 HR) These were obtained in powder form from Hercules Powder Company. These polymers have molecules which are slightly rigid, due to this they have a slightly extended rod configuration, shown by Sitaramaiah and Goring (38). Their probable structure is

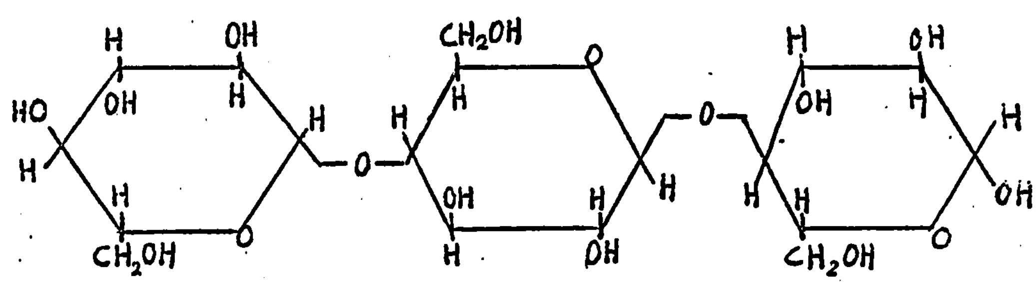

For standardization the fluids selected were 42% by wt sugar solution and distilled water which are definitely Newtonian.

The preparation of the fluids was relatively simple. An appropriate amount of polymer was added to a weighed amount of warm water contained in a 40 gallon container. The solution was stirred with an electric stirrer. The polymer was added at short intervals while being stirred. It took approximately two hours for the polymer to dissolve completely. The sugar solution was prepared similarly, and was used for standardizing the viscometer. The packed beds were calibrated with distilled water instead of the sugar solution since the latter might have ruined the circulating pump.

(ii) Viscometer and Procedure:

The viscometer used was a capillary viscometer. This is a device from which one can obtain the rheological properties for a Non-Newtonian fluid system such as the power-Law fluid. One obtains measurements of the pressure gradient and volumetric flow rate from a cylindrical tube of precisely known dimensions. A plot of shear rate $\bar{\tau}w$ versus shear stress $\frac{2 (\langle u \rangle - \bar{u}_W)}{rH}$, allows one to determine the power law shear stress fluid parameters.

The important components of the viscometer are

(i) Capillary tube

(ii) Reservoir tanks

(iii) Driving force

(iv) Thermal regulating device

In fig. 3 a schematic diagram of the viscometer is represented. Reservoir B is a stainless steel tank with dimensions 16.0 cm in diameter and 21.5 cm in height. The temperature of the solution in B was controlled at 25°C by means of a cooling coil through which water from the constant temperature bath was circulated. The solution was allowed to flow down to reservoir A which has a water-jacket around the exterior to keep the solution at the required temperature. The height of the level of the solution in A was always kept constant by means of the overflow outlet K. The construction material of A is brass, painted inside in order to prevent corrosion, the dimensions are 14 cm in diameter and 17.2 cm in height. The capillary tube was connected to A by means of a hexagonal nut welded to the bottom of A as indicated by H. The capillary tube extended into an airtight glass jacket connected to a graduated burrette which was used to measure the volumetric flow rate. The means of driving the fluid down the capillary was by vacuum. The regulating valve M was used to obtain the appropriate driving force desired. The pressure drop was measured by means of a mercury manometer with one arm opened to the atmosphere.

A series of capillary tubes were used with diameters which ranged from 0.0890 cm - 0.24546 cm, and with lengths from 79.8 cm to 84.6 cm. The dimensions of the diameters were obtained by mercury displacement with an error which ranged from 2% - 5% compared to the diameters provided from the manufacturer. The L/D ratio employed was greater than 300, so as to make the entrance effect negligible.

It was pointed out earlier that the viscometer was standardized with 42% sugar solution. The plot of shear rate versus shear stress curve is shown in fig. 4, indicated no wall effects since a unique curve was obtained for capillary tubes with different diameters. The slope obtained was n = 1.016 close to unity, showed the fluid to be Newtonian, further the viscosity was experimentally determined to be μ = 6.03 centipoise compared with that obtained theoretically in Perry's handbook shown in fig. 6. The deviation was less than 0.5% error. Fig. 5 shows the plot of f versus Re which indicated laminar flow. The different concentrations of Non-Newtonian fluids employed were 0.8, 1.2, 1.6, 2, 2.2, 2.4, 2.6, per cent by weight of Nat-250GR, and 0.2, 0.3, 0.4, 0.5, 0.6, 0.7 per cent by weight of Nat-250HR.

The raw experimental viscometer data consisted of flow rate versus pressure drop. These can be converted into shear stress and shear rate data. However, before doing so, some corrections must be made to obtain the true pressure gradient. The corrections are for the following effects.

(1) Head of fluid about tube exit

(2) Kinetic energy effects

(3) Tube entrance effects

A total mechanical energy balance yields the expression for the frictional pressure drop across the capillary tube in fully developed flow

$$\frac{-dp}{dx} = \frac{\Delta h \rho g}{L} \frac{g}{g_c} + \left(\frac{Ho + L}{L}\right) \rho \frac{g}{g_c} - \frac{\rho \langle u \rangle^2}{L} \left(\frac{1}{2\alpha'} + \frac{Kc}{2}\right) \quad \text{.............. (87)}$$

For Newtonian fluids in fully developed laminar flow, α' has the value of ½. The cut end of the capillary tube is usually trimmed to result in a slightly rounded entrance. For such cases, Foust et al (36) quote a value of 0.23 for K_c for Newtonian fluids. Thus the final expression for Newtonian fluids

$$\frac{-dp}{dx} = \frac{\Delta h \rho g}{L} \frac{g}{g_c} + \left(\frac{Ho + L}{L}\right) \rho \frac{g}{g_c} - 1.12 \frac{\rho \langle u \rangle^2}{L} \quad \text{............ (88)}$$

It was pointed out earlier that L/D has been taken very large such that the entrance effect is negligible. Equation (87) is used to obtain the true pressure gradient and equivalent shear stress.

FIG 3

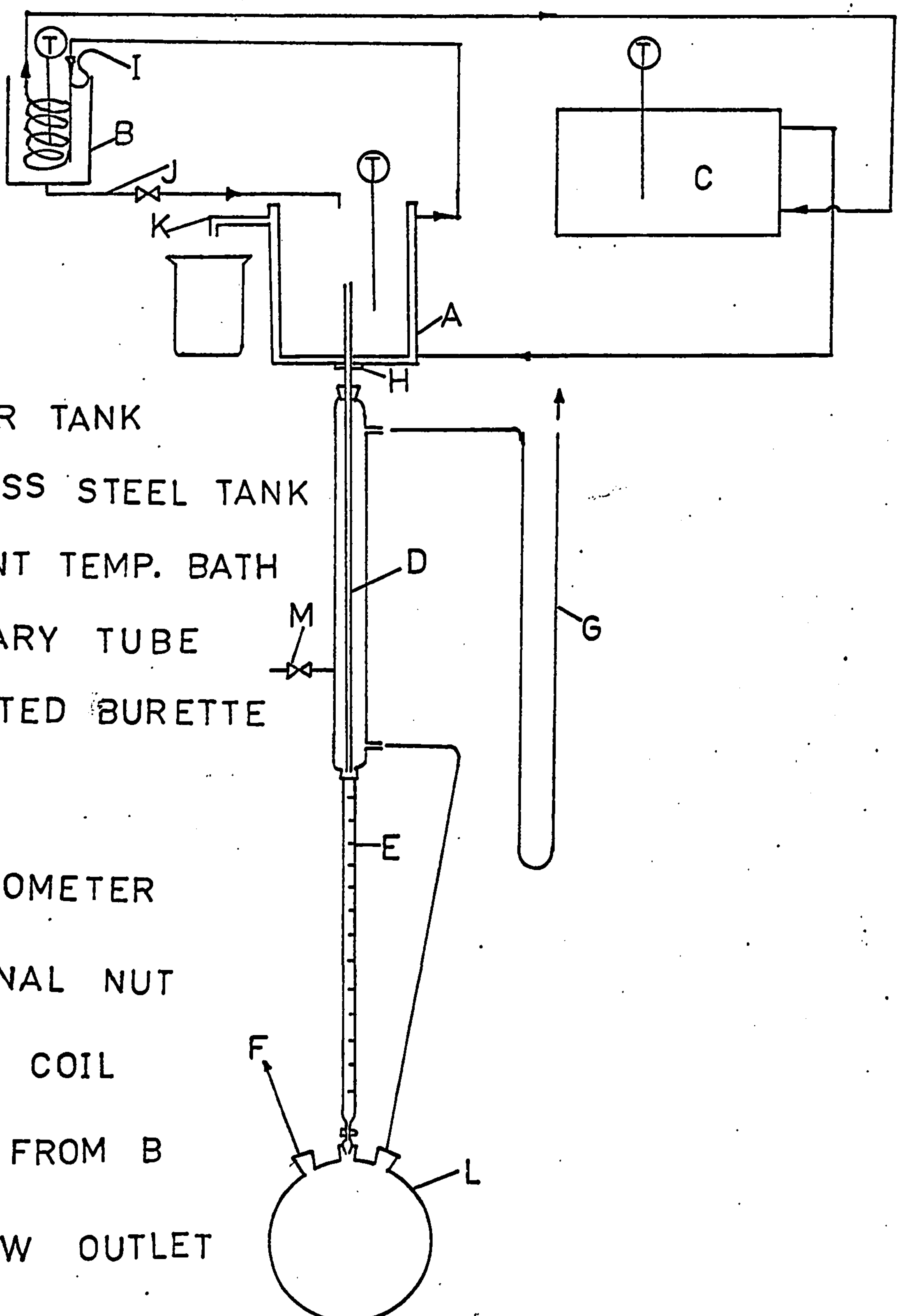

A: RESERVOIR TANK

B: STAINLESS STEEL TANK

C: CONSTANT TEMP. BATH

D: CAPILLARY TUBE

E: GRADUATED BURETTE

F: VACUUM

G: Hg MANOMETER

H: HEXAGONAL NUT

I: COOLING COIL

J: OUTLET FROM B

K: OUTLET OVERFLOW

L: GLASS SPHERE

CAPILLARY VISCOMETER

FIG 4

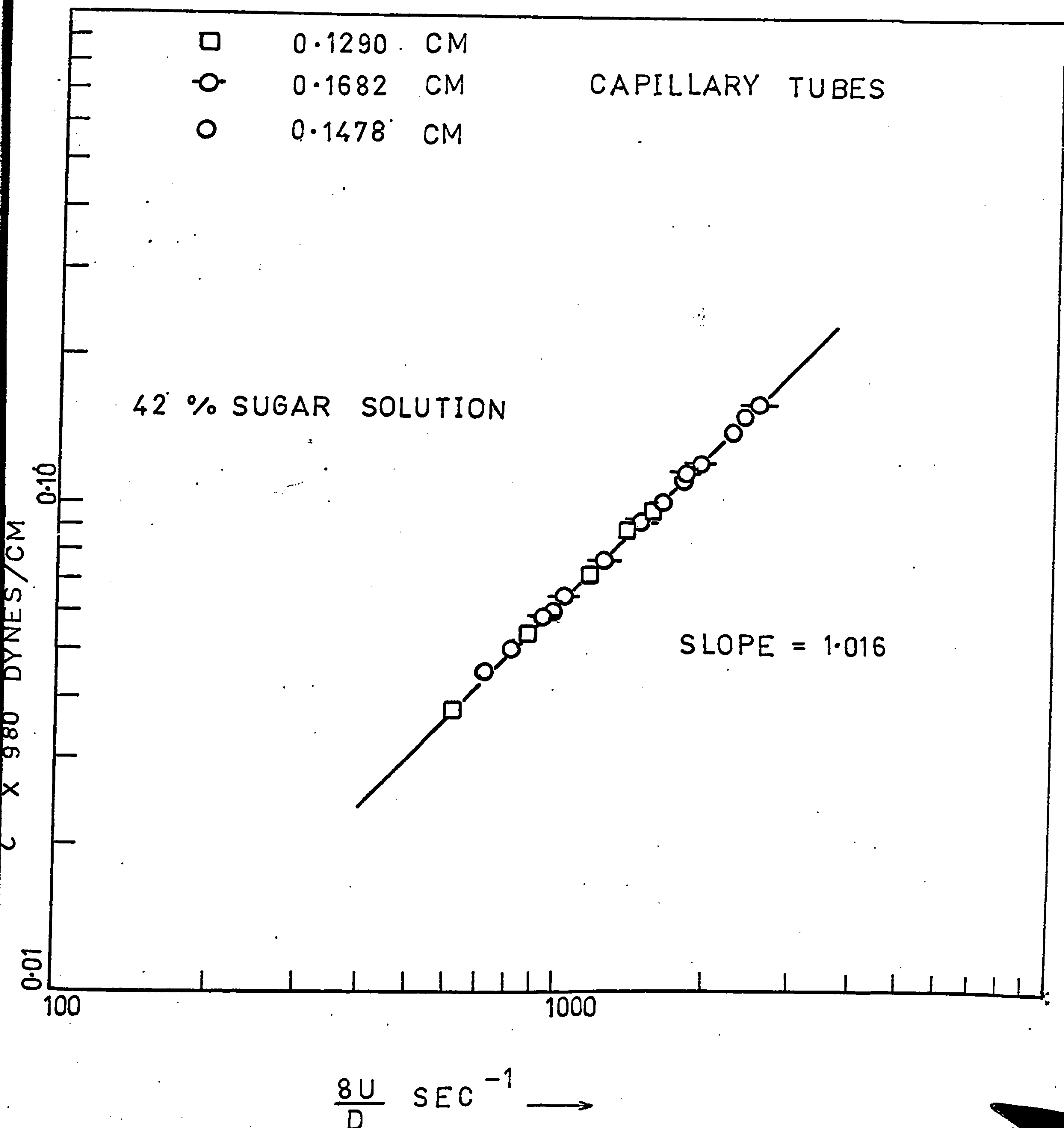

□ 0·1290 CM
-o- 0·1682 CM
o 0·1478 CM
CAPILLARY TUBES
42 % SUGAR SOLUTION
SLOPE = 1·016
0·10
0·01
X 980 DYNES/CM
100
1000
8U/D SEC^{-1}

FIG 5

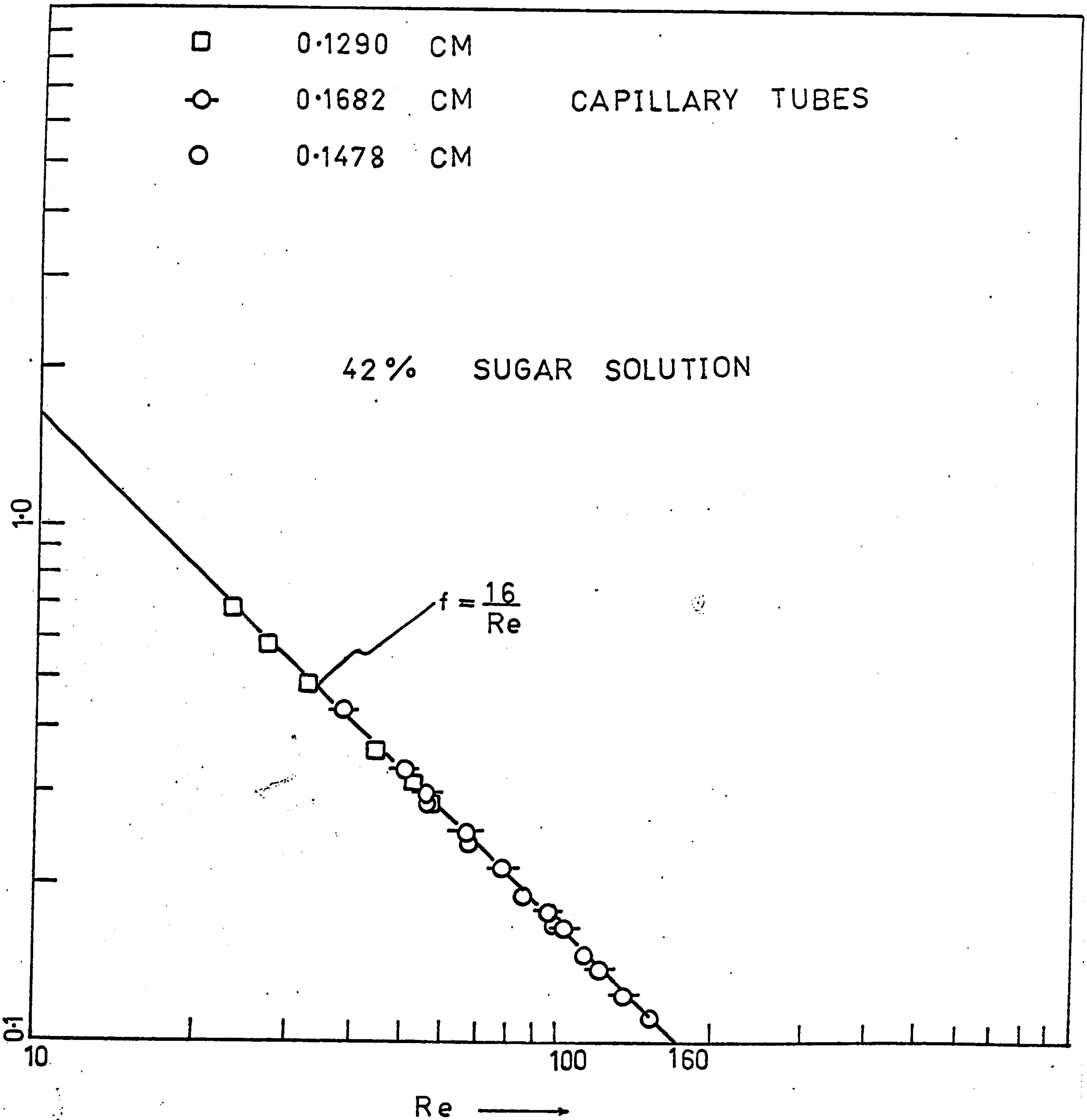

0·1290 CM
0·1682 CM
0·1478 CM
CAPILLARY TUBES
42% SUGAR SOLUTION
f = 16/Re
1·0
0·1
10
100
160
Re

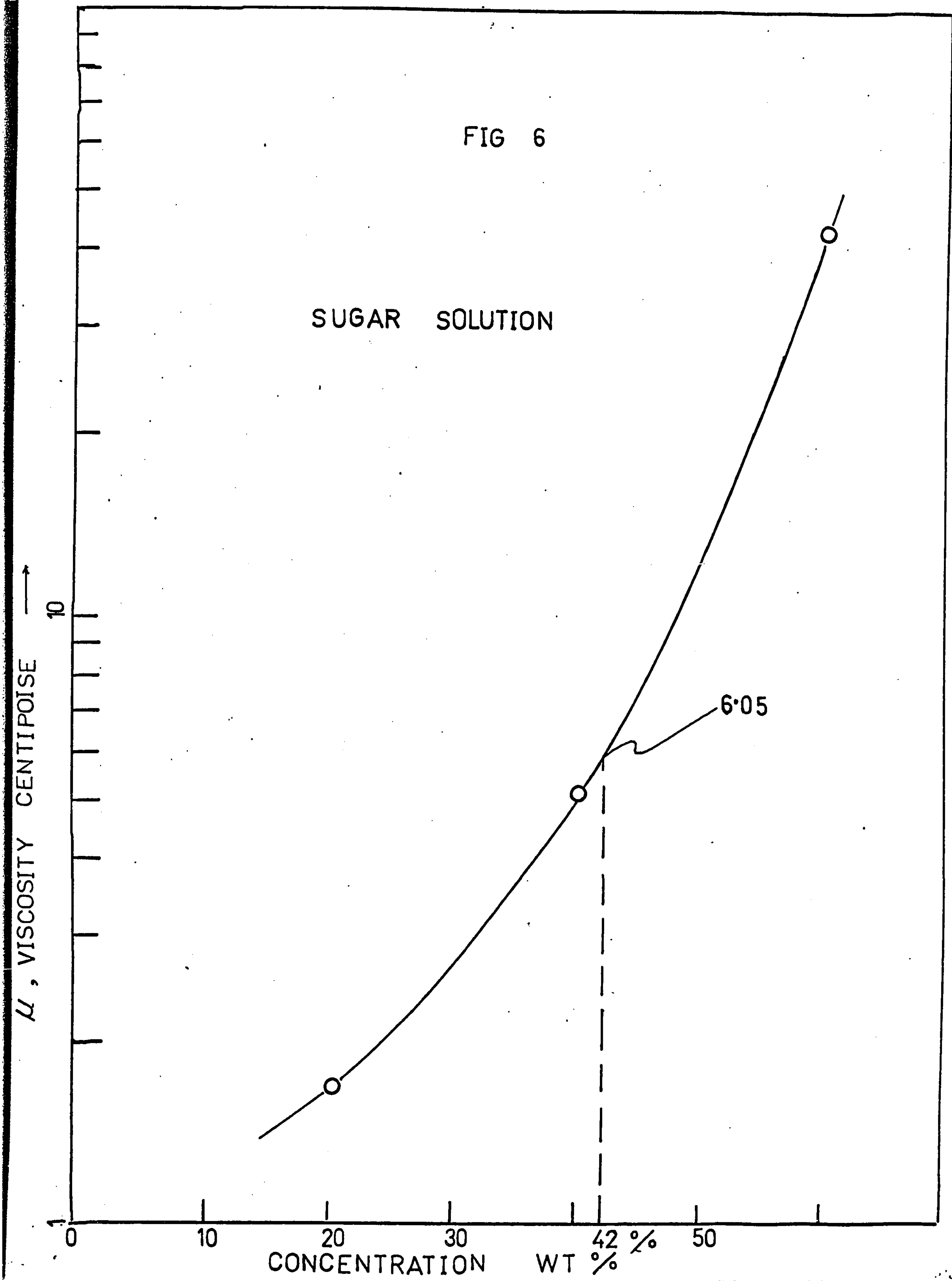
FIG 6
SUGAR SOLUTION
6·05
10
1
μ, VISCOSITY CENTIPOISE
0
10
20
30
42 %
50
CONCENTRATION WT %

Chapter V

Packed Beds Experiments

In this chapter a brief description of the experimental apparatus and procedure will be given. The analysis of the standardization is similar to that of the viscometer, in terms of shear rate vs shear stress and friction factor, and Reynolds number relationship.

(i) Materials

The Non-Newtonian solutions used were Natrosol 250 GR and 250 HR. The concentrations were identical to those of the viscometric experiment. These fluids were selected due to their anomalous behaviour, as indicated by Sadowski (28) and Pasari (26).

There is a variety of "porous media" used in flow studies involving rheologically complex fluids. Some of the models of porous media are sand packs, and matrices of uniformly alundum plugs, sandstone cores, porous metal discs and compressed glass wool. Each of these models is in itself somewhat unique in its geometric morphology. The porous media chosen in the present work consists of stainless steel spheres. Three different sizes were used with diameters 0.3175 cm, 0.2394 cm and 0.1592 cm. These measurements were determined with a vernier caliper and a micrometer. The deviations of the diameters compared with those supplied from the manufacturer was less than 3%.

The columns, valves and pipelines ($\frac{1}{2}$ " diam.) were all stainless steel except for the pump. The test-section is made of plexiglass.

(ii) Equipment and Procedure

A schematic diagram of the packed beds was shown in fig. 7. The solution to be studied was pumped from the 10 gallon capacity tank S by means of a gear pump. The solution in the reservoir was controlled by a cooling coil, at 25°C. There were three test sections namely I, II and III. Each of these was connected to a mercury manometer when reading was taken.

The dimensions of the test sections were given in Table 46. The ratio of diameter of column to the length of test section is from 6.336 - 6.7664, for the test sections in order to assure geometric similarity.

Each test section was filled with the particles in essentially the same manner. An exact amount of spheres were weighed to provide the required porosity for the section. The section was then bolted to the column. The fluid was first allowed to flow upward into the column, until it was completely filled. Then closing and opening the appropriate valves, the solution was then pumped downward into the column, until some fluid was overflowing from the top three valves to assure that no air remained in the flow system. The Bypass line E was used to regulate the flow rate and to allow steady flow into the test section. The entire system was held at equilibrium for at least ten to fifteen minutes before the flow rate and pressure drop were taken of the sample.

The equipment was standardized using distilled water. The results are shown in fig. 8 and 9 and they show no evidence of surface effects being present.

FIG 7

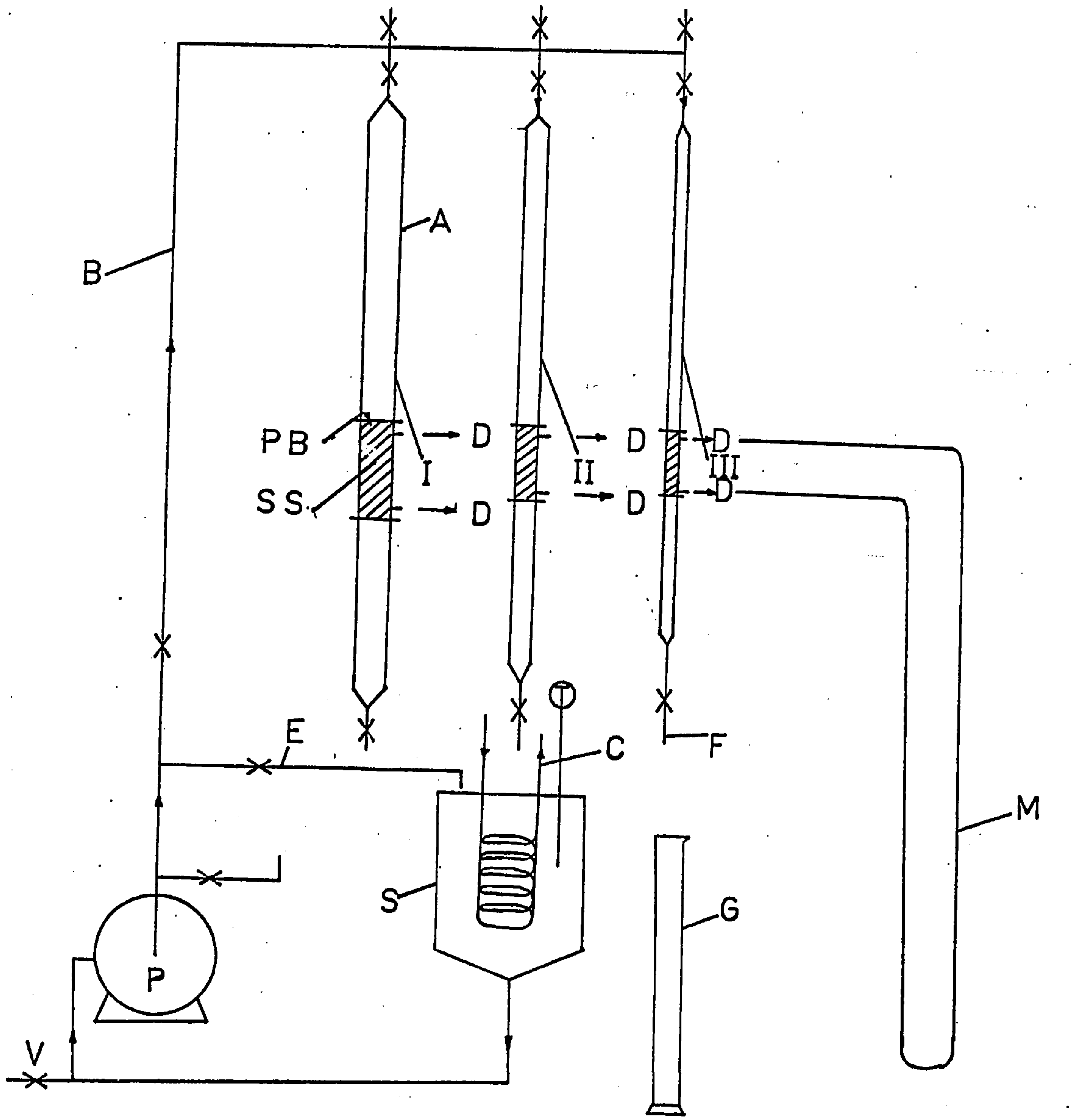

PACKED BEDS

A : INCOMING SECTION
B : STAINLESS STEEL PIPE
C : COOLING COIL
D : CONNECTION TO MANOMETER
E : BY PASS
F : OUTLET
G : GRADUATED CYLINDER
M : MANOMETER
P : CIRCULATING PUMP
PB : PACKED BED
SS STAINLESS STEEL SPHERE
T THERMOMETER
V VALVE
S TANK SS

FIG 8

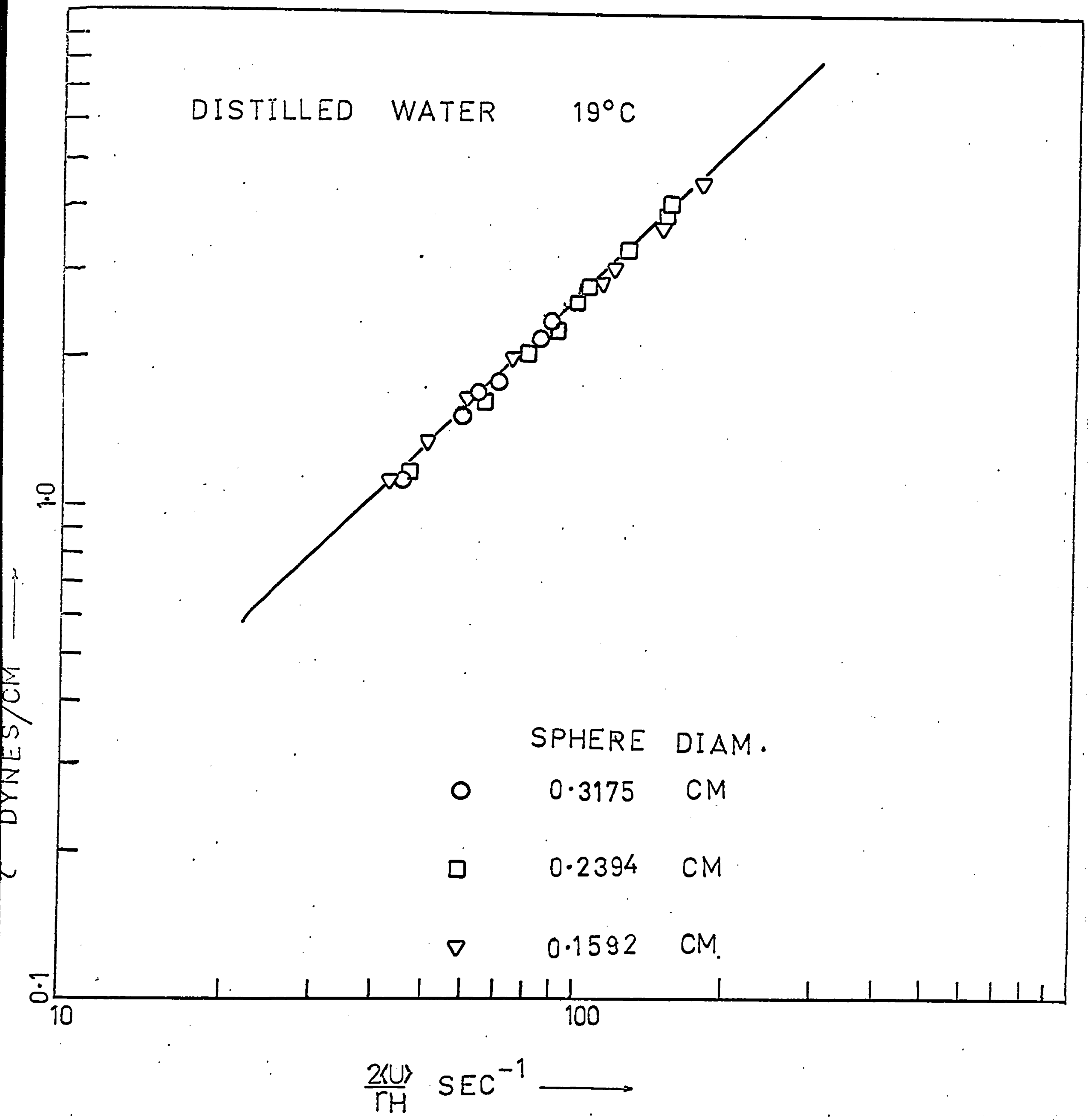
DISTILLED WATER 19°C
SPHERE DIAM.
0·3175 CM
0·2394 CM
0·1592 CM
τ DYNES/CM
1·0
0·1
10
100
2⟨U⟩/rH SEC⁻¹

FIG 9

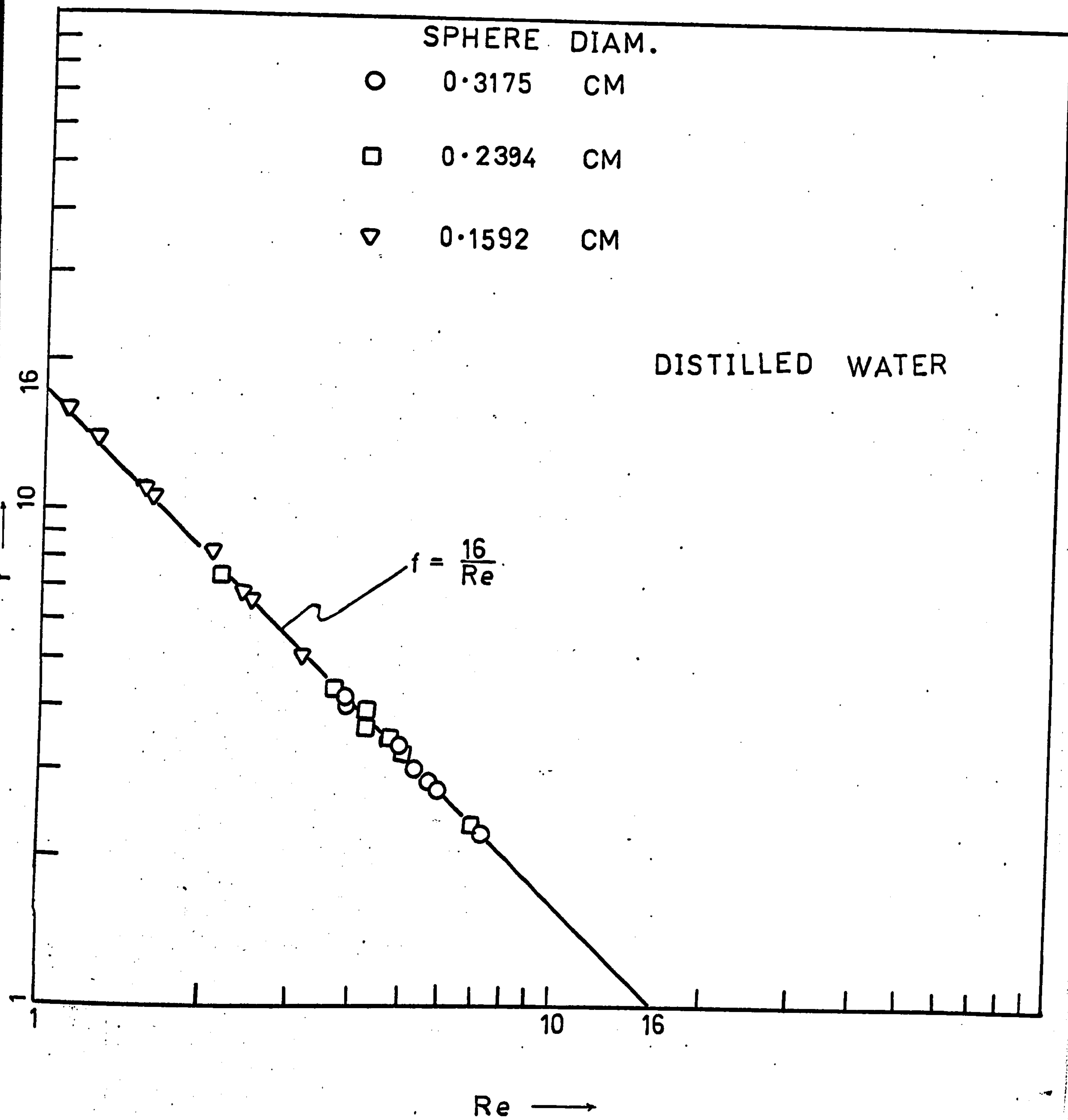
SPHERE DIAM.
0·3175 CM
0·2394 CM
0·1592 CM
DISTILLED WATER
f = 16/Re
16
10
1
10
16
Re

TABLE 1

VALUES OF CRITICAL SHEAR STRESS

CAPILLARY NO.	DYNES/CM^2						
	0.8% NAT-250GR	1.2% NAT-250GR	1.6% NAT-250GR	2.0% NAT-250GR	2.2% NAT-250GR	2.4% NAT-250GR	2.6% NAT-250GR
1			732	1270	1450	1820	2400
2		408	575	850	900	1450	2000
3	116						
6		710	620	950	1245	1650	2300
7	217.5	340	541	750	850	1100	1800
8		330					
9	71.5						
10	27.5						
12							

TABLE 2

VALUES OF CRITICAL SHEAR STRESS

PACKED BED NO.	DYNES/CM² 0.8% NAT-250GR	1.2% NAT-250GR	1.6% NAT-250GR	2% NAT-250GR	2.2% NAT-250GR	2.4% NAT-250GR
1		5000	6500	9300	13000	22200
11		1050	3200	5000	7800	11100
III		910	1300	2550	5000	6500

TABLE 3

PACKED BED I

SOLUTION: Distilled water at 19°C

ε : 0.3810

rH : 0.03257

u cm/sec	τwdynes/cm^2	$\frac{2<u>}{RH}$ sec^{-1}	f	Re
0.7310	1.1490	44.887	4.2712	3.8449
0.7560	1.2170	45.808	4.0468	3.8449
0.946	1.5430	58.089	3.4276	4.9739
1.023	1.7150	62.817	3.0363	5.2730
1.100	1.7500	67.545	2.9023	5.8067
1.136	1.8040	69.756	2.7745	5.9779
1.147	1.8430	70.432	2.8007	6.0472
1.163	1.8620	71.414	2.7507	6.1336
1.360	2.2010	83.511	2.3785	7.1712
1.406	2.4430	86.335	2.2891	7.2440

TABLE 4

PACKED BED II

SOLUTION: Distilled water at 19°C

ε : 0.38174

rH : 0.024636

u cm/sec	τ dynes/cm^2	$\frac{2<u>}{rH}$ sec^{-1}	f	Re
0.560	1.198	45.462	7.5083	2.1930
0.795	1.654	64.540	5.1354	3.1150
0.969	2.059	78.666	4.3927	3.6942
1.109	2.256	90.031	3.6728	4.2781
1.215	2.626	98.636	3.5546	4.7247
1.293	2.773	104.969	3.3146	5.0288
1.517	3.334	123.153	2.8985	5.7868
1.847	3.932	149.944	2.3050	7.1802
1.869	4.119	151.730	2.3594	7.1286

TABLE 5

PACKED BED III

SOLUTION: Distilled water at 19°C

ε : 0.3835

rH : 0.0165

u cm/sec	τ dynes/cm^2	$\frac{2\langle u\rangle}{rH}$ sec^{-1}	f	Re
0.1670	0.4770	20.242	34.9718	0.4325
0.3406	1.155	41.285	19.9097	0.8873
0.4080	1.358	49.455	16.3097	1.0628
0.4880	1.688	59.152	14.1472	1.2725
0.6050	2.029	73.333	11.0666	1.5773
0.6140	2.029	74.424	10.7498	1.6004
0.8007	2.696	97.055	8.4037	2.0860
0.9181	2.864	111.285	6.9414	2.3780
0.9693	3.091	117.491	6.6295	2.5317
1.2050	3.633	146.061	5.1107	3.1211
1.4470	4.522	175.394	4.3505	3.78

TABLE 6

RESULTS FOR PACKED BED I

SOLUTION: 1.2% Natrosol-250GR

τ_W dynes/cm^2	u_W cm/sec	$\frac{2(\langle u \rangle - u_W)}{rH}$ sec^{-1}	$\delta \times 10^{-4}$cm
744.5035	-2.22357	1374.1	4.3599
521.3960	-1.62412	949.3	4.8052
357.2150	-1.06920	617.9	5.0914
230.2190	-0.61613	372.3	5.0296
124.9200	-0.23402	180.7	4.0349
69.5900	-0.131957	93.55	4.7130
54.8600	-0.0759	70.61	6.966

SOLUTION: 1.6% Natrosol-250GR

τ_W dynes/cm^2	u_W cm/sec	$\frac{2(\langle u \rangle - u_W)}{rH}$ sec^{-1}	$\delta \times 10^{-4}$
80.979	-0.3300	61.500	21.8540
90.812	-0.3642	70.900	20.8110
237.490	-0.7766	197.800	12.7311
363.857	-0.9670	314.990	0/2095

TABLE 6 (cont'd)

SOLUTION: 1.6% Natrosol-250GR

τw dynes/cm^2	u_W cm/sec	$\frac{2(\langle u\rangle - u_W)}{rH}$ sec^{-1}	$\delta \times 10^{-4}$
554.624	-1.3248	515.7430	7.6138
712.885	-1.5549	700.620	6.3463
956.066	-1.8796	995.000	5.29465
1153.435	-2.1134	1256.000	4.6448

SOLUTION: 2% Natrosol-250GR

τw dynes/cm^2	u_W cm/sec	$\frac{2(\langle u\rangle - u_W)}{rH}$ sec^{-1}	$\delta \times 10^{-4}$cm
178.789	-0.5302	83.1700	25.9918
333.400	-1.1004	181.5270	24.4535
549.166	-1.8652	337.6970	22.9707
910.402	-3.0666	637.9930	20.9038

SOLUTION: 2.4% Natrosol-25GR

τw dynes/cm^2	uw cm/sec	$\frac{2(\langle u\rangle - uw)}{rH}$ sec^{-1}	$\delta \times 10^{-4}$cm
153.0190	-0.2049	33.1500	16.3920

TABLE 6 (cont'd)

SOLUTION: 2.4% Natrosol-250GR

τ_w dynes/cm^2	u_W cm/sec	$\frac{2(\langle u\rangle - u_W)}{rH}$ sec^{-1}	$\delta \times 10^{-4}$ cm
237.3500	-0.3352	57.6700	15.0990
376.6000	-0.5666	90.1600	14.3456
532.3000	-0.8201	161.5700	12.8145
637.8800	-0.9609	202.8700	11.8638
814.8800	-1.2154	278.7000	11.0395

SOLUTION: 2.2% Natrosol-250GR

τ_w dynes/cm^2	u_W cm/sec	$\frac{2(\langle u\rangle - u_W)}{rH}$ sec^{-1}	$\delta \times 10^{-4}$ cm
179.760	-0.2782	50.1620	19.8736
272.790	-0.4439	85.9250	17.7564
381.462	-0.6357	131.8540	15.8934
500.288	-0.8316	186.3690	14.0947
703.004	-1.1501	286.2200	12.4876
945.700	-1.5883	434.6350	11.5097

TABLE 7

RESULTS FOR PACKED BED II

SOLUTION: 1.2% Natrosol-250GR

τw dynes/cm^2	u_W cm/sec	$\frac{2(<u> - u_W)}{rH}$ sec^{-1}	$\delta \times 10^{-4}$cm
774.79	-0.199307	1454.81	0.36909
580.79	-0.24814	1056.46	0.65300
411.300	-0.23132	709.445	0.92531
228.40	-0.140382	358.600	1.1602
114.88	-0.053076	159.800	1.0207
67.38	-0.035308	90.900	1.3029
48.32	-0.014564	60.000	0.80911

SOLUTION: 1.6% Natrosol-250GR

τw dynes/cm^2	u_W cm/sec	$\frac{2(<u> - u_W)}{rH}$ sec^{-1}	$\delta \times 10^{-4}$cm
88.1970	-0.2292	65.25	13.4823
150.7380	-0.3547	115.53	10.7489
230.4860	-0.4731	187.00	8.0877
332.3870	-0.5699	276.295	6.0628

TABLE 7 (cont'd)

SOLUTION: 1.6% Natrosol-250GR (cont'd)

τ_w dynes/cm^2	u_W cm/sec	$\frac{2(\langle u\rangle - u_W)}{rH}$ sec^{-1}	$\delta \times 10^{-4}$ cm
501.9800	-0.7279	449.73	4.7022
738.5469	-0.8961	716.00	3.5141
1087.2137	-1.0569	1173.00	2.52243

SOLUTION: 2% Natrosol-250GR

τ_w dynes/cm^2	u_W cm/sec	$\frac{2(\langle u\rangle - u_W)}{rH}$ sec^{-1}	$\delta \times 10^{-4}$ cm
123.820	-0.2339	52.200	18.2742
206.128	-0.4271	98.200	17.1519
298.943	-0.6685	158.800	16.9660
424.720	-0.9798	244.870	16.3303
577.489	-1.3259	357.900	15.4181
756.940	-1.7010	499.251	14.3427
967.080	-2.0728	678.000	13.2026

TABLE 7 (cont'd)

SOLUTION: 2.2% Natrosol-250GR

τw dynes/cm²	u_w cm/sec	$\frac{2(\langle u\rangle - u_w)}{rH}$ sec⁻¹	δ x 10⁻⁴ cm
184.970	-0.2218	51.9960	15.2958
294.139	-0.3729	94.8636	13.3664
446.976	-0.5795	163.9800	11.5898
726.903	-0.9076	307.4200	9.4447
859.550	-1.0702	379.9540	8.9180
1004.770	-1.3039	476.1740	8.7510

SOLUTION: 2.4% Natrosol-250GR

τw dynes/cm²	u_w cm/sec	$\frac{2(\langle u\rangle - u_w)}{rH}$ sec⁻¹	δ x 10⁻⁴ cm
162.520	-0.1424	35.0000	10.7077
261.390	-0.2488	63.2000	9.9135
370.150	-0.3639	98.8950	9.3329
570.050	-0.5638	169.6800	8.0423
692.510	-0.6722	216.9170	7.3870
859.355	-0.8071	293.6400	6.7255

TABLE 8

RESULTS FOR PACKED BED III

SOLUTION: 1.2% Natrosol-250GR

τ_w dynes/cm^2	u_w cm/sec	$\frac{2(\langle u\rangle - u_w)}{rH}$ sec^{-1}	$\delta \times 10^{-4}$cm
878.910	-0.033313	1687.030	0.05246
641.730	-0.202065	1175.685	0.46992
443.400	-0.28005	780.390	1.01468
262.010	-0.19839	424.568	1.36820
136.800	-0.08993	199.136	1.38350
94.750	-0.05465	130.770	1.33300
65.240	-0.03623	87.455	1.38809

SOLUTION: 1.6% Natrosol-250GR

τ_w dynes/cm^2	u_w cm/sec	$\frac{2(\langle u\rangle - u_w)}{rH}$ sec^{-1}	$\delta \times 10^{-4}$cm
133.85	-0.186224	107.1000	6.6508
269.366	-0.2761	224.8800	3.8672
426.080	-0.3152	373.4180	2.4664
664.478	-0.31927	618.2800	1.4447

TABLE 8 (cont'd)

SOLUTION: 1.6% Natrosol-250GR (cont'd)

τ_w dynes/cm^2	u_w cm/sec	$\frac{2(\langle u\rangle - u_w)}{rH}$ sec^{-1}	$\delta \times 10^{-4}$ cm
946.322	-0.2654	954.2600	0.7583
1257.249	-0.03635	1342.0000	0.0713

SOLUTION: 2% Natrosol-250GR

τ_w dynes/cm^2	u_w cm/sec	$\frac{2(\langle u\rangle - u_w)}{rh}$ sec^{-1}	$\delta \times 10^{-4}$ cm
224.880	-0.3534	110.870	12.8514
401.140	-0.6588	224.300	11.6397
677.158	-0.9988	413.000	9.6037
920.544	-1.2006	590.650	8.1014
1124.648	-1.2926	740.400	6.9345

SOLUTION: 2.2% Natrosol-250GR

τ_w dynes/cm^2	u_w cm/sec	$\frac{2(\langle u\rangle - u_w)}{rH}$ sec^{-1}	$\delta \times 10^{-4}$ cm
225.442	-0.2815	67.1900	14.6598
380.810	-0.5019	118.060	12.5470

TABLE 8 (cont'd)

SOLUTION: 2.2% Natrosol-250GR (cont'd)

τ_w dynes/cm^2	u_w cm/sec	$\frac{2(\langle u\rangle - u_w)}{rH}$ sec^{-1}	$\delta \times 10^{-4}$ cm
518.063	-0.9862	196.086	16.1665
631.613	-1.3337	253.100	16.6713
797.660	-1.9091	343.463	17.5144
977.643	-2.6035	455.084	18.464

SOLUTION: 2.4% Natrosol-250GR

τ_w dynes/cm^2	u_w cm/sec	$\frac{2(\langle u\rangle - u_w)}{rH}$ sec^{-1}	$\delta \times 10^{-4}$ cm
183.740	-0.1448	48.890	9.1662
191.980	-0.1511	43.94	8.9433
258.840	-0.2122	64.77	8.5583
337.175	-0.2858	90.90	8.2123
482.510	-0.4108	142.00	7.3493
592.080	-0.4946	185.74	6.6840
783.440	-0.6259	262.30	5.7955
982.290	-0.7463	352.30	5.1116

TABLE 9

DATA FOR CAPILLARY NO. 3

SOLUTION: 42% by wt. sugar solution at 25°C

Q c.c./sec	u cm/sec	$\frac{8}{D}\langle u\rangle sec^{-1}$	τ_w dynes/cm^2	f	Re
0.1115	9.5477	615.977	37.1939	0.6855	23.37
0.1369	11.3414	731.7033	45.5606	0.5451	27.76
0.1611	13.3519	861.4170	52.6974	0.4966	32.68
0.2186	18.1156	1168.752	70.6607	0.3617	44.34
0.26064	21.5939	1393.160	86.2622	0.3108	52.86
0.28585	23.6824	1527.897	94.7766	0.2839	57.97

TABLE 10

DATA FOR CAPILLARY NO. 7

SOLUTION: 42% by wt. sugar solution at 25°C

Q c.c/sec	u cm/sec	$\frac{8}{D}\langle u\rangle sec^{-1}$	τ dynes/cm^2	f	Re
0.3797	17.099	813.273	49.5450	0.2888	55.975
0.4585	20.645	981.944	59.042	0.2360	67.585
0.5807	26.148	1243.681	74.624	0.1859	85.599
0.6736	30.330	1442.654	87.665	0.1624	99.294
0.7654	34.464	1639.204	100.0384	0.1435	112.822
0.8316	37.444	1780.970	110.0700	0.1338	122.579
1.0384	46.7575	2223.904	137.8252	0.1074	153.065

TABLE 11

DATA FOR CAPILLARY NO. 8

SOLUTION: 42% by wt. sugar solution at 25°C

Q c.c./sec	u cm/sec	$\frac{8}{D}\langle u\rangle$ sec^{-1}	τ dynes/cm^2	f	Re
0.22573	13.1637	712.5142	44.747	0.43376	38.4085
0.29509	17.2084	931.4461	58.290	0.33071	50.21
0.32467	18.9335	1024.8175	63.734	0.29870	55.24
0.39024	22.7570	1231.7800	77.175	0.25038	66.38
0.46162	26.9198	1457.0977	91.676	0.21250	78.54
0.56899	33.1807	1795.9817	114.297	0.1744	96.81
0.60927	35.5298	1923.1329	120.820	0.1608	103.66
0.80515	46.9526	2541.4154	156.968	0.1196	136.99

TABLE 12

SOLUTION: 1.6% Natrosol-250GR

RESULTS FOR CAPILLARY 1

τw dynes/cm^2	u_W cm/sec	$\frac{8(\langle u\rangle - u_W)}{D}$ sec^{-1}	$\delta \times 10^{-3}$cm
61.8420	-0.4095	100.4469	3.6565
80.8118	-0.5570	131.3713	3.6887
101.6218	-0.7242	183.9500	3.6029
126.7325	-0.9000	245.4290	3.4351
156.4465	-1.0903	322.0027	3.1600
181.9555	-1.2324	383.0937	2.9273
216.4650	-1.4050	474.2763	2.6018
246.2460	-1.5158	561.4350	2.3684
278.3550	-1.6041	668.7810	2.1410
303.7057	-1.6663	750.1549	1.9836
340.2740	-1.7230	872.8100	1.7855
359.2810	-1.7310	923.2670	1.6800
405.0840	-1.7180	1083.497	1.4317
446.2480	-1.6646	1232.488	1.2376

TABLE 12 (cont'd)

SOLUTION: .2% Natrosol 250-GR

τw dynes/cm^2	u_W cm/sec	$\frac{8(\langle u\rangle - u_W)}{D}$ sec^{-1}	$\delta \times 10^{-3}$cm
77.0470	-0.63178	68.6290	8.6545
114.479	-0.89914	110.6687	7.8186
162.674	-1.23156	171.5799	6.8040
210.862	-1.55336	244.0909	6.1887
268.062	-1.82459	330.4310	5.2887
327.304	-2.0354	414.4200	4.6154

SOLUTION: 2.2% Natrosol-250GR

τw dynes/cm^2	u_W cm/sec	$\frac{8(\langle u\rangle - u_W)}{D}$ sec^{-1}	$\delta \times 10^{-3}$cm
62.70	-0.25998	36.2873	7.2217
84.20	-0.33385	51.3559	6.3580
105.70	-0.42170	68.7060	6.1159
128.40	-0.50073	88.4090	5.6261
176.40	-0.67452	130.784	4.8878
202.56	-0.76739	161.127	4.5950

TABLE 12 (cont'd)

SOLUTION: 2.2% Natrosol-250GR (cont'd)

τ_w dynes/cm^2	u_w cm/sec	$\frac{8(\langle u\rangle - u_w)}{D}$ sec^{-1}	$\delta \times 10^{-3}$ cm
232.30	-0.87807	192.299	4.39036
262.00	-0.96798	224.572	4.06713
292.94	-1.05118	270.522	3.7949
335.26	-1.18077	331.713	3.5141
358.85	-1.24467	347.206	3.3822

SOLUTION: 2.4% Natrosol-250GR

τ_w dynes/cm^2	u_w cm/sec	$\frac{8(\langle u\rangle - u_w)}{D}$ sec^{-1}	$\delta \times 10^{-3}$ cm
78.279	-0.34057	33.6400	7.5683
113.13	-0.53541	55.9400	6.6926
145.92	-0.69563	78.1318	6.1019
172.57	-0.84549	95.8560	5.8309
191.020	-0.96498	110.050	5.7439
227.92	-1.17391	140.960	5.4600
258.66	-1.33570	168.233	5.3643

TABLE 12 (cont'd)

SOLUTION: 2.4% Natrosol-250GR (cont'd)

τ_w dynes/cm^2	u_W cm/sec	$\frac{8(\langle u\rangle - u_W)}{D}$ sec^{-1}	$\delta \times 10^{-3}$ cm
284.29	-1.45143	188.105	4.9735
312.99	-1.57165	224.353	4.97357
335.02	-1.63337	240.984	4.7344
362.20	-1.69256	273.333	4.4533

SOLUTION: 2.6% Natrosol-250GR

τ_w dynes/cm^2	u_W cm/sec	$\frac{8(\langle u\rangle - u_W)}{D}$ sec^{-1}	$\delta \times 10^{-3}$ cm
87.187	-0.25439	24.8936	9.9764
109.325	-0.28929	32.8650	7.8187
132.080	-0.36957	43.4348	7.3914
168.970	-0.47263	59.9200	6.5643
194.907	-0.58392	75.1075	6.5609
224.322	-0.71792	94.8020	6.3533
250.457	-0.86686	113.322	6.6172
279.668	-0.99751	132.700	6.5197

TABLE 12 (cont'd)

SOLUTION: 2.6% Natrosol-250GR (cont'd)

τ_w dynes/cm^2	u_w cm/sec	$\frac{8(\langle u \rangle - u_w)}{D}$ sec^{-1}	$\delta \times 10^{-3}$ cm
310.108	-1.14939	153.4600	6.3855
337.880	-1.26853	173.218	6.1879
358.380	-1.40562	189.6128	6.3032

TABLE 13

SOLUTION: 1.2% Natrosol-250GR

RESULTS FOR CAPILLARY 2

τ_w dynes/cm^2	u_w cm/sec	$\frac{8(\langle u\rangle - u_w)}{D}$ sec^{-1}	$\delta \times 10^{-3}$ cm
66.59499	-0.99001	262.5702	3.6667
93.30699	-1.11856	390.5754	2.8681
135.9749	-1.24653	586.2900	2.0775
174.5699	-1.28695	783.9398	1.5505
209.4599	-1.26213	917.3292	1.2136
248.6400	-1.160580	1211.6070	0.8778

SOLUTION: 1.6% Natrosol-250GR

τ_w dynes/cm^2	u_w cm/sec	$\frac{8(\langle u\rangle - u_w)}{D}$ sec^{-1}	$\delta \times 10^{-3}$ cm
49.8488	-0.2954	77.710	3.3191
65.1159	-0.4224	107.382	3.5203
89.8320	-0.6004	163.000	3.5317
113.657	-0.7645	219.577	3.3237
135.704	-0.8897	271.400	3.1217

TABLE 13 (cont'd)

SOLUTION: 1.6% Natrosol-250GR (cont'd)

τw dynes/cm^2	u_w cm/sec	$\frac{8(\langle u\rangle - u_w)}{D}$ sec^{-1}	$\delta \times 10^{-3}$ cm
158.797	-1.1047	330.580	2.8787
176.1577	-1.08313	369.620	2.6744
195.8520	-1.1595	432.200	2.4935
218.7753	-1.2242	495.740	2.2545
247.2610	-1.2906	579.180	2.0166
264.7680	-1.3042	632.490	1.8631
298.4840	-1.3293	735.960	1.6310
321.0689	-1.3142	796.680	1.4600
344.8560	-1.2829	865.900	1.30908
377.0026	-1.2120	986.050	1.1018

SOLUTION: 2% Natrosol-250GR

τw dynes/cm^2	u_w cm/sec	$\frac{8(\langle u\rangle - u_w)}{D}$ sec^{-1}	$\delta \times 10^{-3}$ cm
73.7358	-0.5738	67.9330	8.1972
117.3580	-0.7494	111.537	6.2449

TABLE 13 (cont'd)

SOLUTION: 2% Natrosol-250GR (cont'd)

τ_w dynes/cm²	u_w cm/sec	$\frac{8(\langle u\rangle - u_w)}{D}$ sec⁻¹	$\delta \times 10^{-3}$ cm
158.7177	-0.9545	164.2930	5.4545
205.5670	-1.1535	225.6310	4.7083
246.0340	-1.2757	275.1700	4.1151
296.9130	-1.3860	357.3670	3.5539
352.0686	-1.4515	438.2353	3.0239

SOLUTION: 2.2% Natrosol-250GR

τ_w dynes/cm²	u_w cm/sec	$\frac{8(\langle u\rangle - u_w)}{D}$ sec⁻¹	$\delta \times 10^{-3}$ cm
74.3380	-0.2238	44.2200	5.0292
92.9000	-0.2807	61.0000	4.7573
109.040	-0.3236	72.7000	4.4947
125.177	-0.3606	85.5000	4.1930
151.560	-0.4240	111.300	3.8106
169.880	-0.4705	124.400	3.6191
197.800	-0.5387	153.740	3.3668

TABLE 13 (cont'd)

SOLUTION: 2.2% Natrosol-250GR (cont'd)

τ_w dynes/cm^2	u_W cm/sec	$\frac{8(\langle u\rangle - u_W)}{D}$ sec^{-1}	$\delta \times 10^{-3}$cm
220.393	-0.5874	176.130	3.1244
246.376	-0.5874	204.200	2.884
268.000	-0.6318	225.600	2.7156
286.150	-0.6626	249.000	2.5580
320.050	-0.7355	286.400	2.3500
352.300	-0.7619	327.500	2.1164
399.125	-0.7941	391.200	1.8467

TABLE 14

SOLUTION: 2.4% Natrosol-250GR

τ_w dynes/cm^2	u_W cm/sec	$\frac{8(\langle u\rangle - u_W)}{D}$ sec^{-1}	$\delta \times 10^{-3}$cm
101.265	-0.45534	45.310	6.8780
120.067	-0.54413	56.040	6.2540
137.980	-0.65087	66.170	6.1986
160.250	-0.78493	84.645	5.9918
189.860	-0.93449	106.484	5.6294
212.620	-1.06947	126.907	5.5702
233.920	-1.15656	142.900	5.2811
266.920	-1.31909	173.290	5.1327
287.180	-1.39754	189.215	4.9209
311.470	-1.46733	210.257	4.6879
336.890	-1.53694	234.183	4.4549
364.560	-1.59320	260.885	4.1926

SOLUTION: 2.6% Natrosol-250GR

τ_w dynes/cm^2	u_W cm/sec	$\frac{8(\langle u\rangle - u_W)}{D}$ sec^{-1}	$\delta \times 10^{-3}$cm
87.210	-0.24945	24.440	9.7822

TABLE 14 (cont'd)

SOLUTION: 2.6% Natrosol-250GR (cont'd)

τ_w dynes/cm^2	u_W cm/sec	$\frac{8(\langle u\rangle - u_W)}{D}$ sec^{-1}	$\delta \times 10^{-3}$ cm
109.078	-0.29979	34.100	8.1025
139.660	-0.39008	45.460	7.2506
161.770	-0.47006	56.663	6.9629
182.600	-0.55768	67.737	6.8009
209.150	-0.65136	84.170	6.5136
230.400	-0.78753	97.594	6.7890
260.620	-0.92515	119.122	6.6000
287.330	-1.05121	134.045	6.5292
310.800	-1.16626	154.597	6.4790
338.080	-1.29191	177.358	6.3020
368.420	-1.46861	198.667	6.3852

TABLE 15

SOLUTION: 0.8% Natrosol-250GR

RESULTS FOR CAPILLARY 3

τ_w dynes/cm^2	u_W cm/sec	$\frac{8(\langle u\rangle - u_W)}{D}$ sec^{-1}	$\delta \times 10^{-3}$cm
40.8599	-0.56234	382.270	1.3388
61.6700	-0.41010	579.870	0.6614
82.0799	-0.25905	795.370	0.3084
101.549	-0.11152	990.060	0.10723
136.3599	0.16025	1401.19	0.01159
159.9099	0.34986	1681.77	0.021606
179.6799	0.51303	1882.66	0.028211

TABLE 16

SOLUTION: 1.2% Natrosol-250GR

RESULTS FOR CAPILLARY 6

τw dynes/cm^2	u_W cm/sec	$\frac{8(\langle u\rangle - u_W)}{D}$ sec^{-1}	$\delta \times 10^{-3}$ cm
74.976	-1.71598	304.7997	5.535419
114.48	-2.10417	485.0064	4.294220
150.456	-2.39978	669.5549	3.529088
189.870	-2.65382	877.3143	2.919490
216.288	-2.79331	1024.016	2.539370
259.923	-2.98765	1360.2307	1.965560

SOLUTION: 1.6% Natrosol-250GR

τw dynes/cm^2	u_W cm/sec	$\frac{8(\langle u\rangle - u_W)}{D}$ sec^{-1}	$\delta \times 10^{-3}$ cm
57.2025	-0.34267	93.1961	3.2635
70.8487	-0.4441	116.667	3.3900
91.5447	-0.5870	161.090	3.2611
114.069	-0.7240	212.4565	3.1478
114.187	-0.8987	286.4410	2.8992

TABLE 16 (cont'd)

SOLUTION: 1.6% Natrosol-250GR (cont'd)

τ_w dynes/cm^2	u_w cm/sec	$\frac{8(\langle u \rangle - u_w)}{D}$ sec^{-1}	$\delta \times 10^{-3}$ cm
175.670	-1.0466	368.2650	2.6165
191.959	-1.10719	408.9310	2.4334
209.637	-1.16724	412.7910	2.2887
248.3010	-1.27360	567.6850	1.9900
280.0250	-1.32966	659.0550	1.76816
308.2480	-1.3467	760.6690	1.58430
340.2970	-1.33630	869.4698	1.38470
371.9720	-1.30070	971.5900	1.2043
399.6026	-1.24590	1074.110	1.0558

SOLUTION: 2% Natrosol-250GR

τ_w dynes/cm^2	u_w cm/sec	$\frac{8(\langle u \rangle - u_w)}{D}$ sec^{-1}	$\delta \times 10^{-3}$ cm
81.2440	-0.52124	70.1270	6.6825
122.827	-0.75364	115.629	6.0290
166.148	-0.97545	167.879	5.1885

TABLE 16 (cont'd)

SOLUTION: 2% Natrosol-250GR (cont'd)

τ_W dynes/cm^2	u_W cm/sec	$\frac{8(<u> - u_W)}{D}$ sec^{-1}	$\delta \times 10^{-3}$ cm
208.184	-1.17090	220.914	4.7024
257.447	-1.32354	297.959	4.0229
310.639	-1.44919	380.563	3.4920
373.342	-1.53250	476.372	2.9757

SOLUTION: 2.4% Natrosol-250GR

τ_W dynes/cm^2	u_W cm/sec	$\frac{8(<u> - u_W)}{D}$ sec^{-1}	$\delta \times 10^{-3}$ cm
72.1730	-0.29447	30.6220	7.51195
89.7500	-0.40922	42.5967	7.32054
115.745	-0.54551	59.0260	6.65259
114.950	-0.67559	77.8310	6.03230
163.250	-0.79279	88.8980	5.82930
191.6300	-0.95279	114.847	5.63780
218.4500	-1.268380	140.398	6.34190
247.1030	-1.24700	163.638	5.30630

TABLE 16 (cont'd)

SOLUTION: 2.4% Natrosol-250GR (cont'd)

τ_w dynes/cm^2	u_w cm/sec	$\frac{8(\langle u \rangle - u_w)}{D}$ sec^{-1}	$\delta \times 10^{-3}$ cm
277.5000	-1.37855	203.515	5.08690
314.3000	-1.50191	220.0500	4.70820
340.2000	-1.57760	240.1815	4.50730
371.0500	-1.64838	269.1090	4.21580

SOLUTION: 2.6% Natrosol-250GR

τ_w dynes/cm^2	u_w cm/sec	$\frac{8(\langle u \rangle - u_w)}{D}$ sec^{-1}	$\delta \times 10^{-3}$ cm
90.42000	-0.20328	23.0800	7.528910
109.2770	-0.29696	32.4580	8.02600
131.7900	-0.37582	41.9900	7.66980
159.2570	-0.47572	55.7290	7.20790
187.8170	-0.57262	70.6900	6.65840
213.4500	-0.70478	85.6000	6.77680
235.4200	-0.81665	104.5000	6.80547
258.4800	-0.90825	116.0000	6.53420

TABLE 16 (cont'd)

SOLUTION: 2.6% Natrosol-250GR (cont'd)

τw dynes/cm^2	u_W cm/sec	$\frac{8(\langle u\rangle - u_W)}{D}$ sec^{-1}	$\delta \times 10^{-3}$cm
278.6200	-1.05111	131.5500	6.87000
300.5900	-1.15520	149.4110	6.71630
321.8300	-1.23964	160.5100	6.50730
343.2490	-1.37405	177.8900	6.54305

TABLE 17

SOLUTION: 0.8% Natrosol-250GR

RESULTS FOR CAPILLARY 7

τ_w dynes/cm^2	u_W cm/sec	$\frac{8(\langle u\rangle - u_W)}{D}$ sec^{-1}	$\delta \times 10^{-3}$ cm
53.4399	-0.9096	504.200	1.65284
77.2599	-0.78708	739.000	0.99004
104.8999	-0.64132	1049.40	0.59381
139.4299	-0.45347	1467.30	0.30848
175.7339	-0.24781	1910.90	0.13195

SOLUTION: 1.2% Natrosol-250GR

τ_w dynes/cm^2	u_W cm/sec	$\frac{8(\langle u\rangle - u_W)}{D}$ sec^{-1}	$\delta \times 10^{-3}$ cm
58.46599	-0.88712	229.8856	3.77498
79.79999	-0.97614	308.3000	3.050437
105.6799	-1.05040	440.2000	2.33422
133.0199	-1.08535	568.0000	1.83336
159.0799	-1.07993	703.4000	1.43089
183.0000	-1.04169	824.8000	1.03677
213.1740	-0.91236	999.8000	0.73644

TABLE 17 (cont'd)

SOLUTION: 1.6% Natrosol-250GR

τ_w dynes/cm^2	u_W cm/sec	$\frac{8(\langle u\rangle - u_W)}{D}$ sec^{-1}	$\delta \times 10^{-3}$cm
61.15470	-0.42788	98.0200	3.7865
75.34070	-0.55367	142.732	3.8990
99.29770	-0.72740	177.955	3.8284
115.1560	-0.83548	217.0524	3.5550
132.7540	-0.9441	250.6350	3.3717
152.9600	-1.0496	299.1957	3.0870
178.1160	-1.1650	359.8650	2.8414
214.5067	-1.2790	457.8700	2.4132
235.9100	-1.3222	514.6180	2.2037
262.996	-1.3553	589.5370	1.9585
293.000	-1.3560	676.4680	1.6950

SOLUTION: 2% Natrosol-250GR

τ_w dynes/cm^2	u_W cm/sec	$\frac{8(\langle u\rangle - u_W)}{D}$ sec^{-1}	$\delta \times 10^{-3}$cm
69.4260	-0.48151	60.47	7.4076
108.1747	-0.6944	105.63	6.3711

TABLE 17 (cont'd)

SOLUTION: 2% Natrosol-250GR

τw dynes/cm^2	u_W cm/sec	$\frac{8(\langle u\rangle - u_W)}{D}$ sec^{-1}	$\delta \times 10^{-3}$cm
147.9900	-0.89478	155.768	5.6275
189.4820	-1.0697	209.085	4.8844
244.1535	-1.2204	276.980	4.0013
335.1490	-1.34419	429.039	2.9542

SOLUTION: 2.2% Natrosol-250GR

τw dynes/cm^2	u_W cm/sec	$\frac{8(\langle u\rangle - u_W)}{D}$ sec^{-1}	$\delta \times 10^{-3}$cm
90.6729	-0.29795	56.17	5.2272
105.8399	-0.34067	67.98	4.9372
126.7530	-0.39558	81.80	4.4953
146.7970	-0.45570	102.15	4.29907
168.5780	-0.50843	123.90	3.9110
186.8860	-0.55193	138.00	3.6796
205.6200	-0.59763	156.80	3.5155
232.9880	-0.64561	182.45	3.1804
265.0590	-0.70269	224.40	2.9037

TABLE 17 (cont'd)

SOLUTION: 2.2% Natrosol-250GR (cont'd)

τ_w dynes/cm^2	u_W cm/sec	$\frac{8(\langle u\rangle - u_W)}{D}$ sec^{-1}	$\delta \times 10^{-3}$ cm
286.1060	-0.74089	243.91	2.7440
309.5990	-0.70787	270.89	2.5595
337.420	-0.79233	306.22	2.3304

SOLUTION: 2.4% Natrosol-250GR

τ_w dynes/cm^2	u_W cm/sec	$\frac{8(\langle u\rangle - u_W)}{D}$ sec^{-1}	$\delta \times 10^{-3}$ cm
93.81	-0.3589	41.2510	6.0322
117.47	-0.4673	54.0665	5.5632
141.988	-0.5696	73.7500	5.1779
162.970	-0.6684	89.0200	4.9879
184.300	-0.7621	107.2800	4.7635
208.300	-0.8588	123.3200	4.5685
239.14	-0.9775	148.7150	4.3837
264.30	-1.0681	165.5500	4.2216
283.60	-1.1212	184.1070	4.0043

TABLE 17 (cont'd)

SOLUTION: 2.4% Natrosol-250GR

τw dynes/cm^2	u_W cm/sec	$\frac{8(\langle u \rangle - u_W)}{D}$ sec^{-1}	$\delta \times 10^{-3}$cm
300.30	-1.1648	196.7627	3.8699
329.30	-1.2140	220.4435	3.6240

SOLUTION: 2.6% Natrosol-250GR

τw dynes/cm^2	u_W cm/sec	$\frac{8(\langle u \rangle - u_W)}{D}$ sec^{-1}	$\delta \times 10^{-3}$cm
141.6780	-0.41409	46.000	7.5563
165.7980	-0.49549	58.525	7.0785
193.1922	-0.61616	74.583	6.9231
216.5770	-0.74369	87.670	6.98306
238.4900	-0.83551	103.429	6.90506
264.4170	-0.95859	118.499	6.75068
283.5260	-1.072891	132.074	6.7055
301.0980	-1.14957	149.546	6.6642
317.4670	-1.225158	156.511	6.5516
394.1940	-1.35021	175.320	6.4296
372.8600	-1.51876	204.946	6.4354

TABLE 18

RESULTS FOR CAPILLARY No. 8

SOLUTION: 1.2% Natrosol-250GR

τw dynes/cm^2	u_W cm/sec	$\frac{8(\langle u\rangle - u_W)}{D}$ sec^{-1}	$\delta \times 10^{-3}$ cm
52.1297	-0.60173	198.8384	2.73513
80.0799	-0.64157	300.1025	1.94415
102.4149	-0.63620	410.2464	1.445909
141.8100	-0.55074	574.3052	0.8653
178.2000	-0.03834	750.953	0.045649
203.8470	-0.21499	1121.4094	0.21077

TABLE 19

RESULTS FOR CAPILLARY No. 9

SOLUTION: 0.8% Natrosol-250GR

τw dynes/cm^2	u_W cm/sec	$\frac{8(\langle u \rangle - u_W)}{D}$ sec^{-1}	$\delta \times 10^{-3}$cm
30.000	-0.37591	295.89	1.2126
38.810	-0.29772	374.62	0.7443
49.000	-0.20598	461.67	0.4119
67.3756	-0.03817	650.83	0.0553
93.2800	0.20470	921.77	0.0215
120.0000	0.46252	1233.89	0.038013
146.7549	0.72843	1500.87	0.049016
175.2199	1.02063	1837.50	0.05754

TABLE 20

RESULTS FOR CAPILLARY No. 10

SOLUTION: 0.8% Natrosol-250GR

τ_W dynes/cm^2	u_W cm/sec	$\frac{8(\langle u\rangle - u_W)}{D}$ sec^{-1}	$\delta \times 10^{-3}$ cm
30.200	0.02785	275.04	0.00907
44.794	0.17999	423.76	0.038980
57.799	0.31763	543.630	0.05400
71.429	0.46421	682.40	0.06392
81.700	0.57608	755.11	0.06930
115.450	0.94715	1144.96	0.11556
162.200	1.51203	1691.87	0.18822
192.950	1.95642	2065.47	0.10038

TABLE 21

Fluid Parameters of Natrosol-250GR

Concentration wt %	Shear Stress Range dynes /cm^2	n'	Max K dynes-sec'/cm^2
0.8	26.112 - 227.158	0.8928 - 0.99890	0.20456
1.2	60.000 - 500.000	0.704225-0.86538	1.58440
1.6	40.000 -1000.000	0.7500 - 0.96212	2.44803
2.0	60.000 -1000.000	0.78750- 0.88207	2.63157
2.2	50.000 -2000.000	0.72000- 0.82500	5.17400
2.4	70.000 -2000.000	0.64450- 0.76190	6.09905

TABLE 22

Highest Reynolds Numbers and Their Corresponding Critical Points for each solution and Tube diameter

I. 0.8% Natrosol-250GR

Tube	Diam. cm	τw dynes/cm^2	<u>, cm/sec	u_W cm/sec	Re	Re_c
3	0.1240	179.6799	41.31816	0.51303	57.5488	3363.229
7	0.1682	175.7339	75.64627	-0.24781	150.1768	2054
9	0.1014	175.2199	31.73913	1.02063	35.115	10852.928
10	0.0890	192.95188	24.93369	1.95642	22.6627	8290.25

II. 1.2% Natrosol-250GR

Tube	Diam. cm	τw dynes/cm^2	<u>, cm/sec	u_W cm/sec	Re	Re_c
2	0.19553	248.6400	28.45263	-1.16058	16.1346	12778.99
6	0.22500	272.639	35.26883	-2.98765	24.8205	15058.12
7	0.16820	244.98599	24.58296	-0.79536	11.8813	12394.11
8	0.14780	269.3279	23.97489	0.40525	9.8563	10417.37

TABLE 23

Highest Reynolds Numbers and Their Corresponding Critical Points for each Solution and Tube Diameter

I. 1.6% Natrosol-250GR

Tube	Diam. cm	τw dynes/cm^2	<u>, cm/sec	u_w cm/sec	Re	Re_c
1	0.24546	446.2480	36.1518	-1.66460	27.723	16819.6
2	0.19553	377.0026	22.8883	-1.21200	13.225	17396.7
6	0.22500	399.6026	28.9633	-1.24590	19.536	16574.8
7	0.16820	293.0000	12.8666	-1.3560	6.044	22651.2

II. 2% Natrosol-250GR

Tube	Diam. cm	τw dynes/cm^2	<u>, cm/sec	u_w cm/sec	Re	Re_c
1	0.24546	327.3040	10.6800	-2.0354	4.223	36753.3
2	0.19553	352.0686	9.2595	-1.4515	2.855	29126.5
6	-.22500	373.3420	11.86574	-1.5325	4.157	24652.5
7	0.16820	335.1490	7.571255	-1.34419	2.035	33446.1

TABLE 24

Highest Reynolds Numbers and Their Corresponding Critical Points for each Solution and Tube Diameter

I. 2.2% Natrosol-250GR

Tube	Diam. cm	τ_w dynes/cm^2	$\langle u \rangle$, cm/sec	u_w cm/sec	Re	Re_c
1	0.24546	358.8500	9.408568	-1.24467	2.6314	69779.7
2	0.19553	399.1250	8.768392	-0.7941	1.9409	40010.1
6	0.22500	368.3226	8.785200			
7	0.16820	337.4200	5.646095	-0.79233	1.0547	80657.8

II. 2.4% Natrosol-250GR

Tube	Diam. cm	τ_w dynes/cm^2	$\langle u \rangle$, cm/sec	u_w cm/sec	Re	Re_c
1	0.24546	362.2000	6.694121	-1.69256	1.98347	266855
2	0.19553	364.5600	4.782759	-1.59320	1.18543	105280
6	0.22500	371.0500	5.920743	-1.64838	1.6337	1395137
7	0.16820	329.3000	3.420897	-1.2140	0.70679	78570

TABLE 25

Highest Reynolds Numbers and Their Corresponding Critical Points for each Solution and Tube Diameter

I. 2.6% Natrosol-250GR

Tube	Diam. cm	τw dynes/cm^2	<u>, cm/sec	u_w cm/sec	Re	Re_c
1	0.24546	358.3800	4.412299	-1.40562	0.83307	32815.1
2	0.19553	368.4200	3.387028	-1.46861	0.56295	21246.1
6	0.22500	343.2990	3.629303	-1.37405	0.642232	25245
7	0.16820	372.8600	1.790243	-1.51876	0.43445	16695.5

TABLE 26

Highest Reynolds Numbers and Their Corresponding Critical Points for each Solution and Tube Diameter

I. 1.2% Natrosol-250GR

Packed Bed No.	Hydraulic radius cm	τ_w dynes/cm^2	<u> cm/sec	u_w cm/sec	Re	Re_c
I	0.032582	744.5035	20.162005	-2.22357	16.277	20317.4
II	0.024531	1290.574	30.15467	0.296720	18.118	12200.9
III	0.0163222	1573.5448	26.42907	1.49248	10.489	8212.4

II. 1.6% Natrosol-250GR

Packed Bed No.	Hydraulic radius cm	τ_w dynes/cm^2	<u> cm/sec	u_w cm/sec	Re	Re_c
I	0.03257652	1153.43535	18.34717	-2.1134	8.8842	16251.9
II	0.02453188	1087.21366	12.97363	-1.0569	4.5355	14101.2
III	0.01632725	1257.2496	10.92339	-0.03635	2.4046	10755.5

TABLE 27

Highest Reynolds Numbers and Their Corresponding Critical Points for each Solution and Tube Diameter

III. 2% Natrosol-250GR

Packed Bed No.	Hydraulic radius cm	τw dynes/cm^2	<u> cm/sec	u_w cm/sec	Re	Re_c
I	0.03257819	910.402	7.324252	-3.0666	1.93244	310469
II	0.0245268	967.080	6.243633	-2.0728	1.17650	115462
III	0.0163273	1124.648	4.751707	-1.2926	0.5777	55057.8

IV. 2.2% Natrosol-250GR

Packed Bed No.	Hydraulic radius cm	τw dynes/cm^2	<u> cm/sec	u_w cm/sec	Re	Re_c
I	0.0325705	945.73429	5.489096	-1.58830	0.86804	24121815
II	0.0245214	1004.77044	4.53572	-1.3039	0.55036	111680
III	0.01626236	977.64363	2.5936	-2.6035	0.3468	3646

TABLE 28

Highest Reynolds Numbers and Their Corresponding Critical Points for each Solution and Tube Diameter

V. 2.4% Natrosol-250GR

Packed Bed No.	Hydraulic radius cm	τ_w dynes/cm^2	<u> cm/sec	u_w cm/sec	Re	Re_c
I	0.03258529	814.88	3.32489	-1.2154	0.9217	159861.7
II	0.02452163	859.355	2.7942	-0.8071	0.3544	220774.6
III	0.01634449	982.29143	2.131922	-0.7463	0.1972	70876.9

Power Law Fluid Results:

TABLE 29

SOLUTION: 1.2% (by wt) Natrosol-250GR

Data for capillary tubes

τw dynes/cm^2	n'	w sec^{-1}	$f(\tau w) = \left(\frac{1+3n'}{4n'}\right) w$ sec^{-1}	n
60	0.825	225	236.9318	0.7800
90	0.820	360	379.7561	0.7615
150	0.814	650	687.1314	0.8591
200	0.807	930	985.6041	0.8734
300	0.795	1550	1649.9214	0.8937
500	0.772	2940	3157.0725	0.9412

Data for packed beds

τw dynes/cm^2	n'	$K \frac{\text{dynes-sec}^n}{cm_2}$	$f(\tau w) = \left(\frac{1+3n'}{4n'}\right) w$ sec^{-1}	$\frac{(\tau/K)^s}{w}$
60	0.823	0.6665	79.80	2.969
90	0.832	0.6428	126.00	3.014
150	0.847	0.5931	225.00	3.054
200	0.863	0.5217	315.00	3.129
300	0.892	0.4047	500.00	3.299
500	0.948	0.2408	895.00	3.527

TABLE 30

SOLUTION: 1.6% (by wt) Natrosol-250GR

Data for capillary tubes

τw dynes/cm^2	n'	w sec^{-1}	$f(\tau w)=\frac{(1+3n')}{4n'}w$ sec^{-1}	n
40	0.9621	62.0	62.61	0.7522
80	0.7854	137.0	146.36	0.8125
120	0.7500	231.0	250.24	0.8173
200	0.800	441.0	468.56	0.8214
400	0.7210	1070.0	1173.47	0.8621
600	0.8045	1800.0	1909.26	0.8571
800	0.7846	2550.0	2724.98	0.8949

Data for packed bed

τw dynes/cm^2	n'	K dynes-sec^n/cm^2	w sec^{-1}	$\frac{(\tau/K)^s}{w}$
80	0.8125	1.3921	60	2.4393
120	0.8173	1.3152	94	2.6621
200	0.8260	1.2444	164	2.8571
400	0.8490	0.9910	350	2.8269
600	0.8700	0.8391	570	3.3496
800	0.8920	0.6898	800	3.4063

TABLE 31

SOLUTION: 2% (by wt) Natrosol-250GR

Data for capillary tubes

τ dynes/cm^2	n'	w sec^{-1}	$f(\tau)=\frac{(1+3n')}{4n'}$ w sec^{-1}	n
60	0.7946	49.0	52.1667	0.755
80	0.8023	71.5	75.9037	0.758
100	0.7875	95.0	101.4087	0.761
200	0.8208	230.0	242.5534	0.778
400	0.8627	540.0	561.4758	0.815
600	0.8546	880.0	917.4149	0.850
800	0.8675	1220.0	1266.567	0.875

Data for packed beds

τ dynes/cm^2	n	K dynes-sec /cm^2	w sec^{-1}	$\frac{(\tau/k)^s}{w}$
60	0.755	3.035	20.7	2.5151
80	0.758	3.005	30	2.5304
100	0.761	2.989	39.5	2.5507
200	0.778	2.786	97	2.5057
400	0.815	2.281	230	2.4640

TABLE 31 (cont'd)

Data for packed beds (cont'd)

τ dynes/cm^2	n	K dynes-sec /cm^2	w sec^{-1}	$\frac{(\tau/K)^s}{w}$
600	0.850	1.819	380	2.4140
800	0.875	1.546	540	2.3399

TABLE 32

SOLUTION: 2.2% (by wt) Natrosol-250GR

Data for capillary tubes

τ dynes/cm^2	n'	w sec^{-1}	$f(\tau)=\frac{(1+3n')}{4n'}w$ sec^{-1}	n
90	0.775	56	60.0645	0.745
150	0.770	109	117.1396	0.746
200	0.765	155	166.9036	0.784
300	0.758	262	282.9116	0.730
400	0.750	387	419.2500	0.750
500	0.740	521	566.7635	0.756
600	0.733	678	735.7415	0.760
800	0.717	970	1065.7148	0.776
1000	0.700	1300	1439.2857	0.7669

Data for packed beds

τ dynes/cm	n	K dynes-sec^n/cm	w sec^{-1}	$\frac{(\tau/K)^s}{w}$
90	0.745	4.2577	20.5	2.9299
150	0.747	4.2734	40	2.9285
200	0.749	4.3291	57	2.9281

TABLE 32 (cont'd)

Data for packed beds (cont'd)

τ dynes/cm	n	K dynes-sec^n/cm^2	w sec^{-1}	$\frac{(\tau/k)^s}{w}$
300	0.750	4.3489	97.5	2.9016
400	0.755	4.1888	141.0	2.9733
500	0.756	4.1438	189.0	2.9987
600	0.76	3.9596	240.0	3.0822
800	0.764	3.8902	345.0	3.0890
1000	0.770	3.7002	470.0	3.0623

TABLE 33

SOLUTION: 2.4% (by wt) Natrosol-250GR

Data for capillary tubes

τdynes/cm	n'	w sec^{-1}	$f(\tau)=\left(\frac{1+3n'}{4n'}\right) w\ sec^{-1}$	n
70	0.695	29.1	32.2926	0.704
90	0.695	40.0	44.3781	0.713
150	0.696	80.0	88.7356	0.751
300	0.700	200.0	221.4286	0.748
500	0.705	395.0	436.3209	0.796
700	0.710	605.0	666.7782	0.829
900	0.712	860.0	946.9663	0.908

Data for packed beds

τdynes/cm^2	n	K dynes-sec^n/cm^2	w sec^{-1}	$\frac{(\tau/k)^s}{w}$
150	0.694	5.8693	32.0	2.773
300	0.751	5.1982	78.0	2.838
500	0.79	4.1069	151.0	2.889
700	0.805	3.7307	233.0	2.862
900	0.820	3.2632	321.0	2.950

TABLE 34

Ellis Fluid Results

conc % by wt	$\delta \times 10^{-3}$ cm max	D cm	τ_c dynes/cm^2	ε'''^0 cm^6/dynes -sec	η poise	η_0 poise ave
	9.45	0.2250	710	70×10^{-7}	0.42782	
1.2	6.80	0.19553	408		0.46555	0.4044
	5.00	0.14780	330		0.31991	
	4.82	0.19553	575		0.74500	
1.6	4.75	0.24546	732	22×10^{-7}	0.72400	0.7316
	4.40	0.22500	620		0.72580	
	11.0	0.24546	1270		1.25060	
2.0	10.7	0.19553	850	17×10^{-7}	1.44780	1.308
	8.80	0.22500	950		1.22600	
	8.30	0.24546	1450		1.89870	
2.2	7.40	0.16820	850	7.4×10^{-7}	1.97880	1.9404
	6.62	0.19553	900		1.94350	

TABLE 34 (cont'd)

Ellis Fluid Results (cont'd)

Conc % by wt.	$\delta_{max} \times 10^{-3}$ cm	D cm	τ_c dynes/cm^2	ε'''_o cm^6/dynes^2-sec	η_o poise	η_o poise ave
	10.0	0.24546	1820		2.46710	
2.4	9.70	0.19553	1450	5.466×10^{-7}	2.39270	2.4404
	8.80	0.16820	1100		2.46150	

Data for Capillary Tubes:

TABLE 35

SOLUTION: 1.2% (by wt) Natrosol-250GR

$\eta o_{ave} = 0.4044$ poise

$\tau_{1/2} = 200$ dynes/cm^2

τ dynes/cm	η poise	$\left(\frac{\eta_o}{\eta} - 1\right)$	$(\tau/\tau_{1/2})$
60	0.2479	0.6308	0.30
90	0.2370	0.7063	0.45
150	0.2221	0.8207	0.75
200	0.2046	0.9764	1.00
300	0.1751	1.3089	1.50
500	0.1581	1.5581	2.50

$\alpha - 1 = 0.40196$

TABLE 36

SOLUTION: 1.6% (by wt) Natrosol-250GR

$\eta o_{ave} = 0.7316$ poise

$\tau_{1/2} = 400$ dynes/cm^2

τ dynes/cm	η pose	$\frac{\eta o}{\eta} - 1$	$(\tau/\tau_{1/2})$
40	0.6389	0.1451	0.1
80	0.5466	0.3385	0.2
120	0.4795	0.5256	0.3
200	0.4268	0.7140	0.5
400	0.3409	1.1463	1.0
600	0.3142	1.3280	1.5
800	0.2936	1.4920	2.0
1000	0.2759	1.6519	2.5

$\alpha - 1 = 0.5098$

TABLE 37

SOLUTION: 2% (by wt) Natrosol-250GR

ηo_{ave} = 1.308 poise

$\tau_{1/2}$ = 700 dynes/cm^2

τ dynes/cm	η pose	$\frac{\eta o}{\eta} - 1$	$(\tau/\tau_{1/2})$
60	1.1525	0.1351	0.0857
80	1.0538	0.2413	0.1143
100	0.9925	0.3180	0.1428
200	0.8228	0.5897	0.2857
400	0.7059	0.8532	0.5714
600	0.6541	0.9999	0.8571
800	0.6331	1.0662	1.1428
1000	0.6108	1.1416	1.4286

$\alpha - 1 = 0.4431$

TABLE 38

SOLUTION: 2.2% (by wt) Natrosol-250GR

ηo_{ave} = 1.9404 poise

$\tau_{1/2}$ = 412 dynes/cm^2

τ dynes/cm	η poise	$\frac{\eta o}{\eta} - 1$	$(\tau/\tau_{1/2})$
60	1.7143	0.1319	0.1456
90	1.5000	0.2936	0.2184
200	1.1765	0.6493	0.4854
300	1.0526	0.8433	0.7281
400	0.9592	1.0228	0.9709
600	0.8571	1.2637	1.4563

$\alpha - 1 = 0.6078$

TABLE 39

SOLUTION: 2.4% (by wt) Natrosol-250GR

ηo_{ave} - 2.4404 poise

$\tau_{1/2}$ = 460 dynes/cm^2

τ dynes/cm	η poise	$\frac{\eta o}{\eta} - 1$	$(\tau/\tau_{1/2})$
70	2.1677	0.1258	0.1522
90	2.0280	0.2033	0.1956
150	1.6904	0.4437	0.3261
300	1.3548	0.8012	0.6522
500	1.1459	1.1296	1.0869
700	1.0498	1.3246	1.5217
900	0.9504	1.5677	1.9565

$\alpha - 1 = 0.71568$

TABLE 40

SOLUTION: 1.2% (by wt) Natrosol-250GR

$\eta o_{ave} = 0.40443$ poise

$\tau_{1/2} = 200$ dynes/cm^2

α-1= 0.40196

τ dynes/cm^2	w sec^{-1}	$\frac{w\eta o}{\tau}$	$(\tau/\tau_{1/2})^{\alpha-1}$
50	65	0.5257	0.5728
70	95	0.5488	0.6557
100	141	0.5702	0.7568
200	315	0.6369	1.0000
300	500	0.6740	1.1770
400	699	0.7067	1.3213
500	899	0.7272	1.4453
600	1100	0.7414	1.5552
700	1300	0.7511	1.6546
1000	1900	0.7684	1.9097

TABLE 41

SOLUTION: 1.6% (by wt) Natrosol-250GR

ηo_{ave} = 0.7316 poise

$\tau_{1/2}$ = 400 dynes/cm^2

α-1= 0.5098

τ dynes/cm^2	w sec^{-1}	$\frac{w\eta o}{\tau}$	$(\tau/\tau_{1/2})^{\alpha-1}$
70	52	0.5435	0.4112
90	69	0.5609	0.4674
150	120	0.5853	0.6065
200	164	0.5999	0.7023
300	255	0.6219	0.8636
400	350	0.64016	1.0000
500	459	0.6716	1.1205
600	565	0.6889	1.2296
700	680	0.7107	1.3301
800	800	0.7316	1.4238
10000	1040	0.7609	1.5954

TABLE 42

SOLUTION: 2% (by wt) Natrosol-250GR

$\tau o_{ave} = 1.3081$ poise

$\tau_{\frac{1}{2}} = 700$ dynes/cm^2

α-1= 0.4431

τ dynes/cm^2	w sec^{-1}	$\frac{w\eta o}{\tau}$	$(\tau/\tau_{\frac{1}{2}})^{\alpha-1}$
70	25.2	0.4709	0.3605
90	34.8	0.5058	0.4029
150	67.5	0.5887	0.5053
200	97.0	0.6344	0.5739
300	159.0	0.6933	0.6869
400	230.0	0.7522	0.7804
500	300.0	0.7849	0.8615
600	380.0	0.8285	0.9339
700	460.0	0.8596	0.9999
800	537.0	0.8781	1.0609
1000	700.0	0.9157	1.1712

TABLE 43

SOLUTION: 2.2% (by wt) Natrosol-250GR

ηo_{ave} = 1.9404 poise

$\tau_{1/2}$ = 412 dynes/cm^2

α-1= 0.6078

τ dynes/cm^2	w sec^{-1}	$\frac{w\eta o}{\tau}$	$(\tau/\tau_{1/2})^{\alpha-1}$
150	40	0.5174	0.5411
300	97	0.6274	0.8246
400	141	0.6839	0.9822
500	189	0.7334	1.1249
600	240	0.7761	1.2567
700	290	0.8039	1.3801
900	410	0.8839	1.6079
1000	470	0.9119	1.7143

TABLE 44

SOLUTION: 2.4% (by wt) Natrosol-250GR

$\eta o_{ave} = 2.4404$ poise

$\tau^{1/2} = 460$ dynes/cm^2

α-1= 0.7157

τ dynes/cm^2	w sec^{-1}	$\frac{w\eta o}{\eta}$	$(\tau/\tau_{1/2})^{\alpha-1}$
100	18.6	0.4539	0.3355
200	46.2	0.5637	0.5509
300	78.0	0.6345	0.7364
400	113.0	0.6894	0.9048
500	150.0	0.7321	1.0615
600	190.0	0.7728	1.2094
700	235.0	0.8193	1.3505
800	280.0	0.8541	1.4859
900	320.0	0.8077	1.6166
1000	370.0	0.9029	1.7432

TABLE 45

Conc % (by wt)	α for Ellis Model	$\frac{1}{\varepsilon_0+\varepsilon_1\alpha+\alpha(\alpha-1)\varepsilon_2+\ldots}$
1.2	1.40196	0.20879
1.6	1.50980	0.22000
2.0	1.44314	0.42727
2.2	1.60784	0.27434
2.4	1.71568	0.28000

Chapter VI

Results of Analysis:

The primary aim of analyzing the data is to evaluate the geometric coefficient ϵ_2 using the Ostwald-de-Waele fluid model, for the Non-Newtonian fluid, followed by the Ellis fluid model, in order to check the value obtained for ϵ_2 from the former fluid. However before evaluating the geometric parameter one has to eliminate the surface effects. Therefore the analysis consists of two parts, the first part is to examine the surface effects and the second to evaluate the geometric parameter. The analysis of the data is based on the theory developed by Dr. Kozicki given previously in Chapter III.

Fig. 10, 11, 12, 13, 14 represent the flow curves for five different concentrations of Nat-250-GR at (1.2%, 1.6%, 2%, 2.2%, 2.4% wt) respectively, obtained from both the packed beds and capillary viscometer. In these plots of τ_w versus $\frac{2\langle u\rangle}{rH}$ for different sized packings and capillary tubes, separate curves were obtained. This indicated that these fluids exhibit anomalous surface effects in the vicinity of the solid boundary. Some of these curves intersect or tend to intersect, which suggests the presence of a critical shear stress, τ_c, which marks the transition from a positive effective velocity when the shear stress is greater than τ_c, to a negative effective velocity when the shear stress is less than τc. The critical shear stress also represents the value of a wall shear stress for a particular solution concentration and hydraulic radius at which the effective velocity at the wall is zero.

The values of τc's were obtained by a trial and error procedure pointed out earlier in chapter III. These values were used to determine the final curves (broken line) of τ_w versus $\frac{2(\langle u\rangle - u_w)}{rH}$. These final curves are characteristic for each Natrosol concentration. When the effective slip velocities are calculated the corrections are applied to the experimental points. These corrected points for different hydraulic radius merge on the single, final curve of τ_w vs $\frac{2(\langle u\rangle - u_w)}{rH}$. These final curves for the various concentrations indicate that the surface effects increase as the concentration increases since the fluids become more Non-Newtonian. At a very low concentration the behaviour approaches that of the solvent (water) which is definitely Newtonian and do not exhibit any surface effects as shown by the calibration curve.

The final τc values for the various concentrations and hydraulic radius for both the packed beds and the viscometer are tabulated in table 1 & 2 respectively. A plot of τc vs concentrations with the diameter as parameter is shown in fig. 15 & 16. The plot shows that τc decreases with a decrease in hydraulic radius and concentration. This result

FIG 10

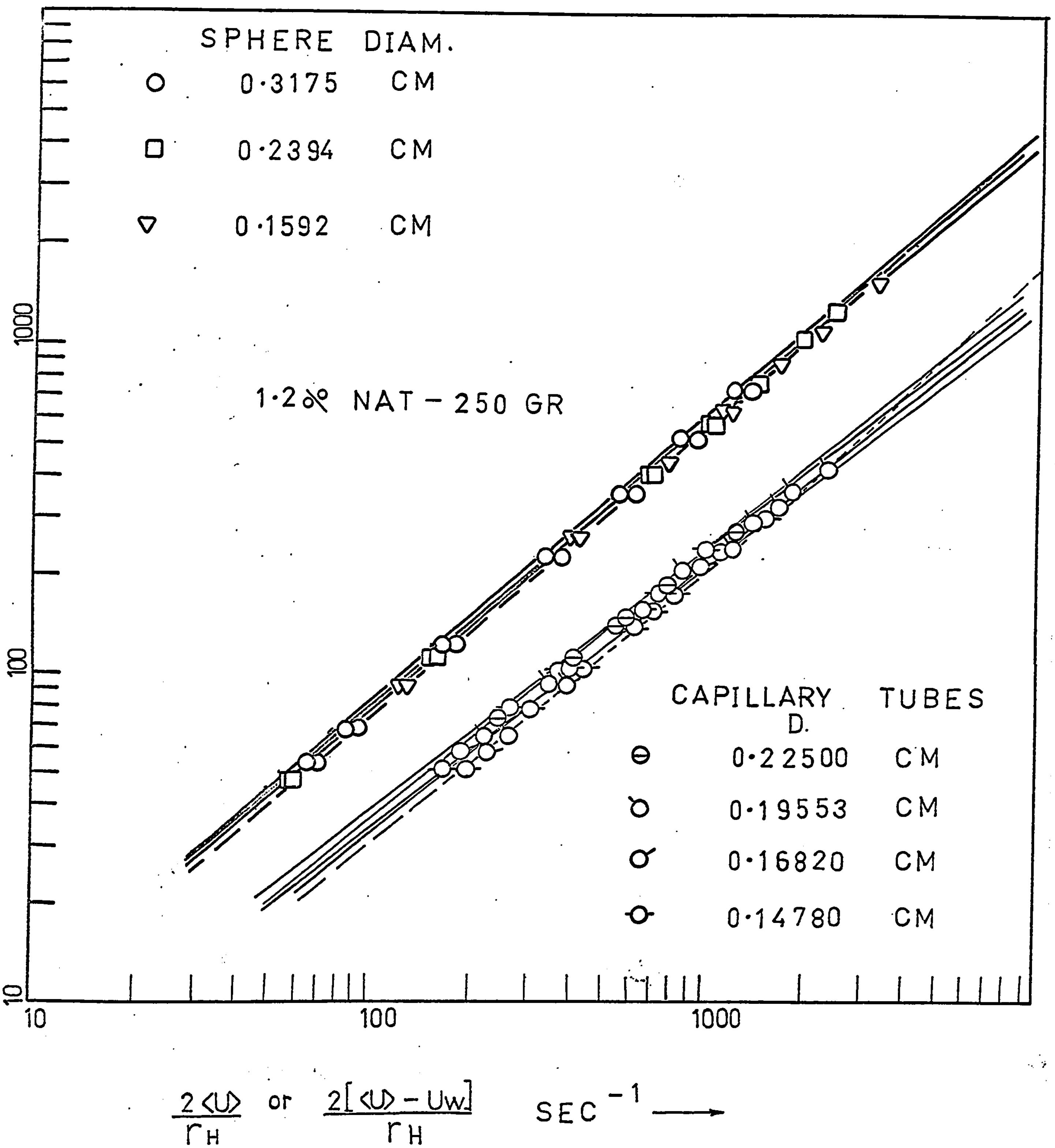
SPHERE DIAM.
0·3175 CM
0·2394 CM
0·1592 CM
1·2% NAT – 250 GR
CAPILLARY TUBES
D.
0·22500 CM
0·19553 CM
0·16820 CM
0·14780 CM
τw DYNES/CM²
10
100
1000
10
100
1000
2⟨U⟩/r_H or 2[⟨U⟩ – Uw]/r_H SEC⁻¹

FIG 11

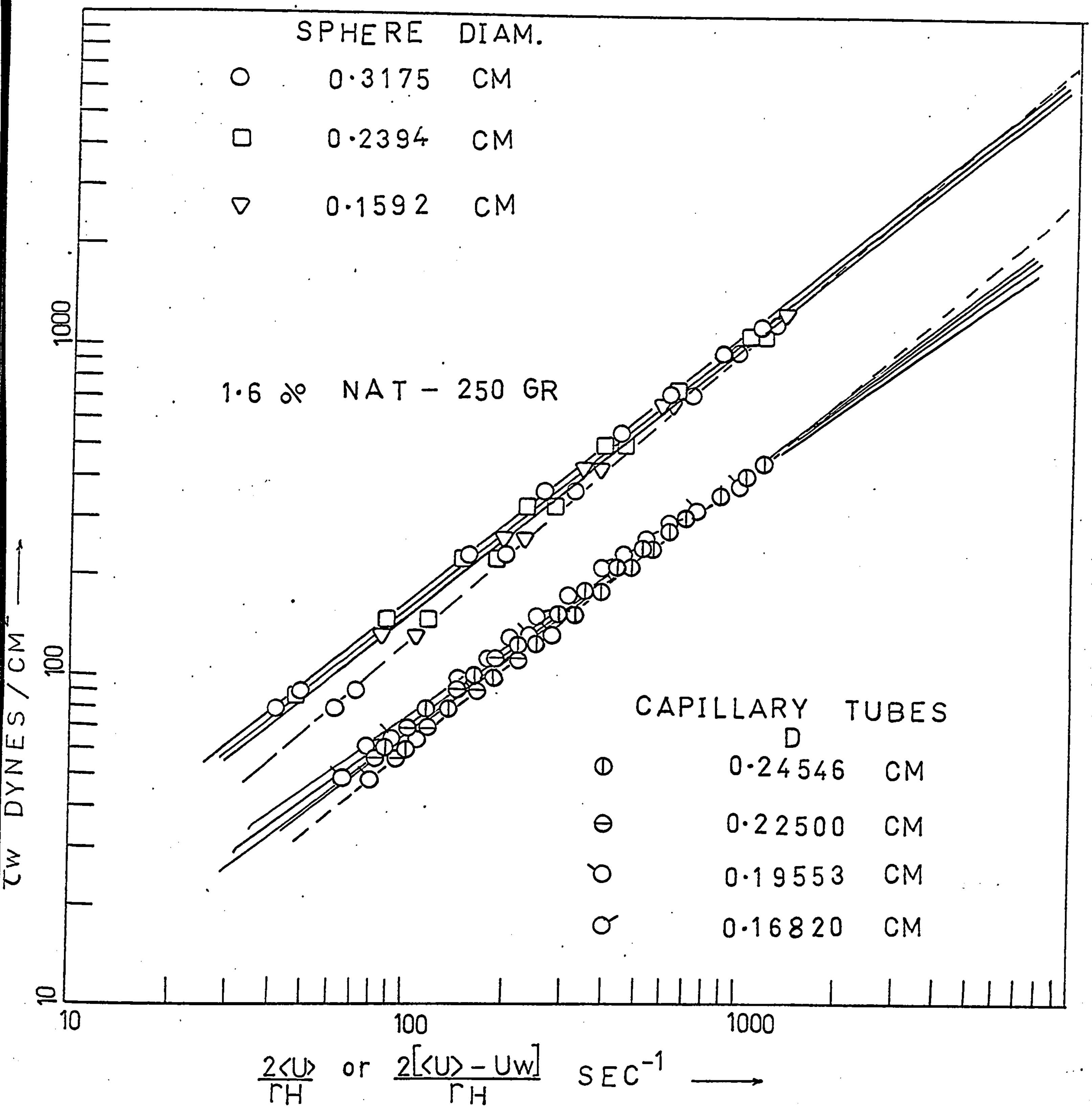
SPHERE DIAM.
0·3175 CM
0·2394 CM
0·1592 CM
1·6 % NAT - 250 GR
CAPILLARY TUBES
D
0·24546 CM
0·22500 CM
0·19553 CM
0·16820 CM
10
100
1000
10
100
1000
τw DYNES / CM²
2⟨U⟩ / rH or 2[⟨U⟩ - Uw] / rH SEC⁻¹

FIG 12

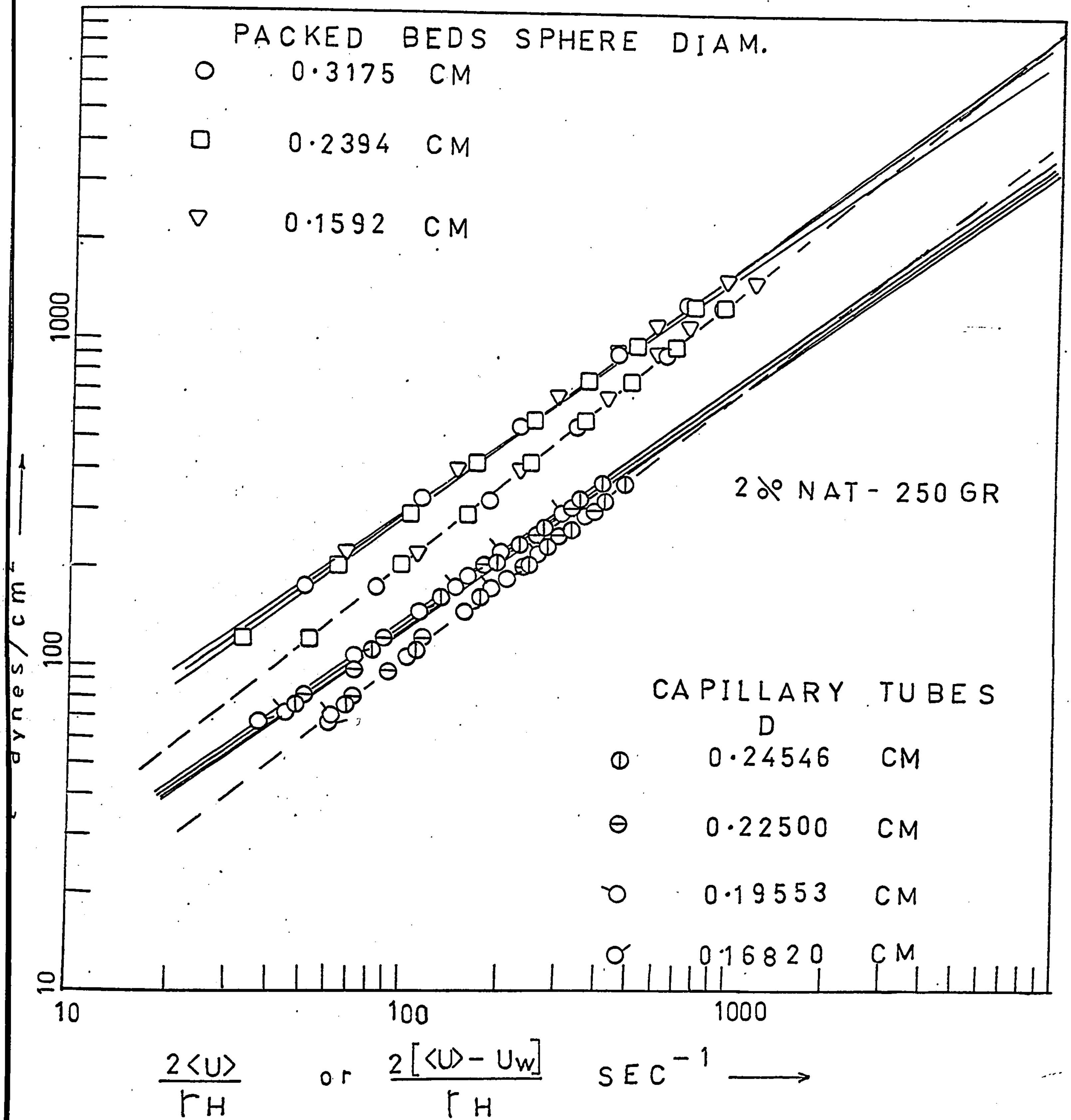
PACKED BEDS SPHERE DIAM.
0·3175 CM
0·2394 CM
0·1592 CM
2% NAT - 250 GR
CAPILLARY TUBES
D
0·24546 CM
0·22500 CM
0·19553 CM
0·16820 CM
dynes/cm²
10
100
1000
10
100
1000
2<U>/r_H or 2[<U> - Uw]/r_H SEC⁻¹

FIG 13

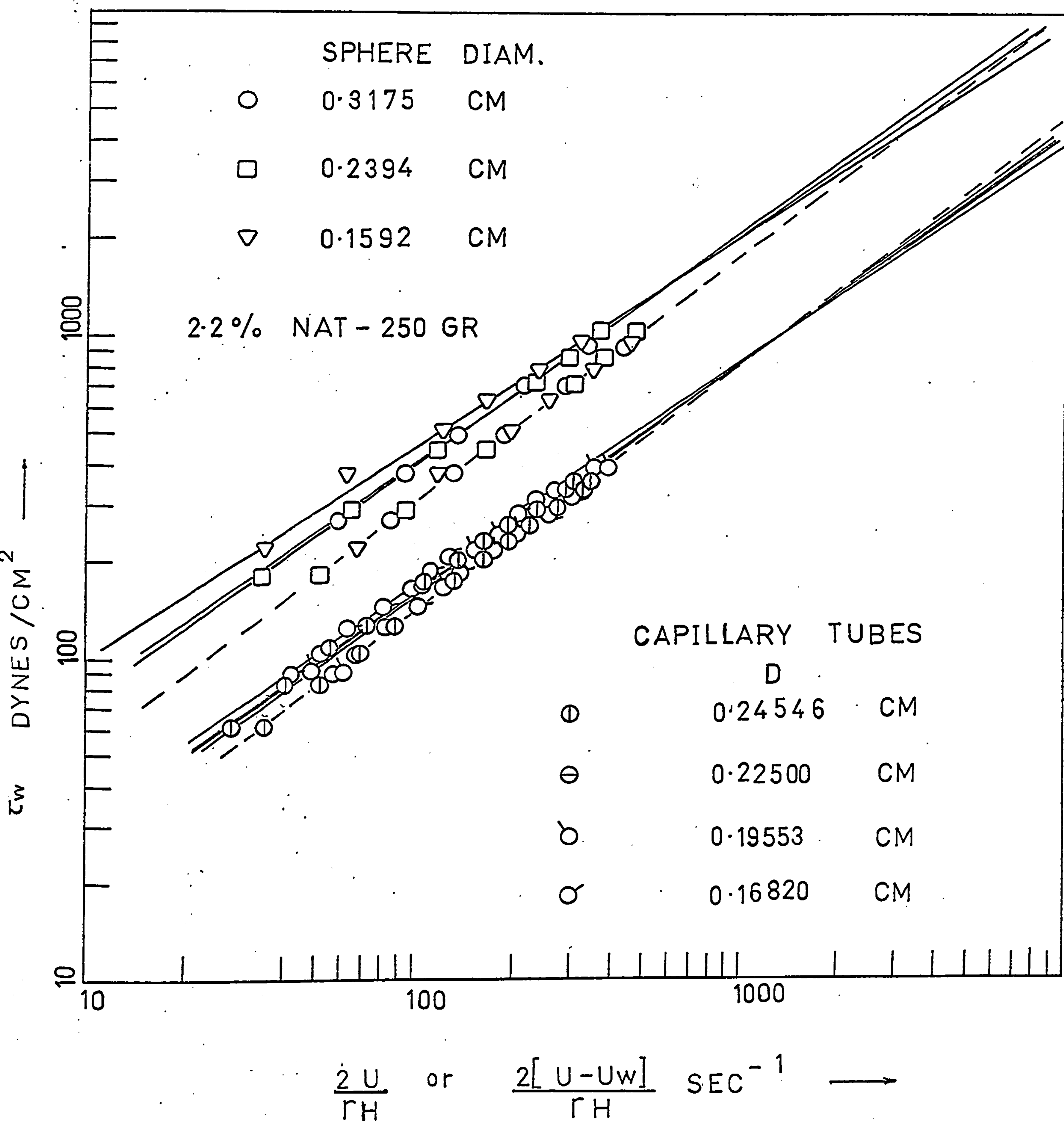
SPHERE DIAM.
0·3175 CM
0·2394 CM
0·1592 CM
2·2 % NAT - 250 GR
CAPILLARY TUBES
D
0·24546 CM
0·22500 CM
0·19553 CM
0·16820 CM
τw DYNES/CM2
10
100
1000
2U/rH or 2[U-Uw]/rH SEC-1

FIG 14

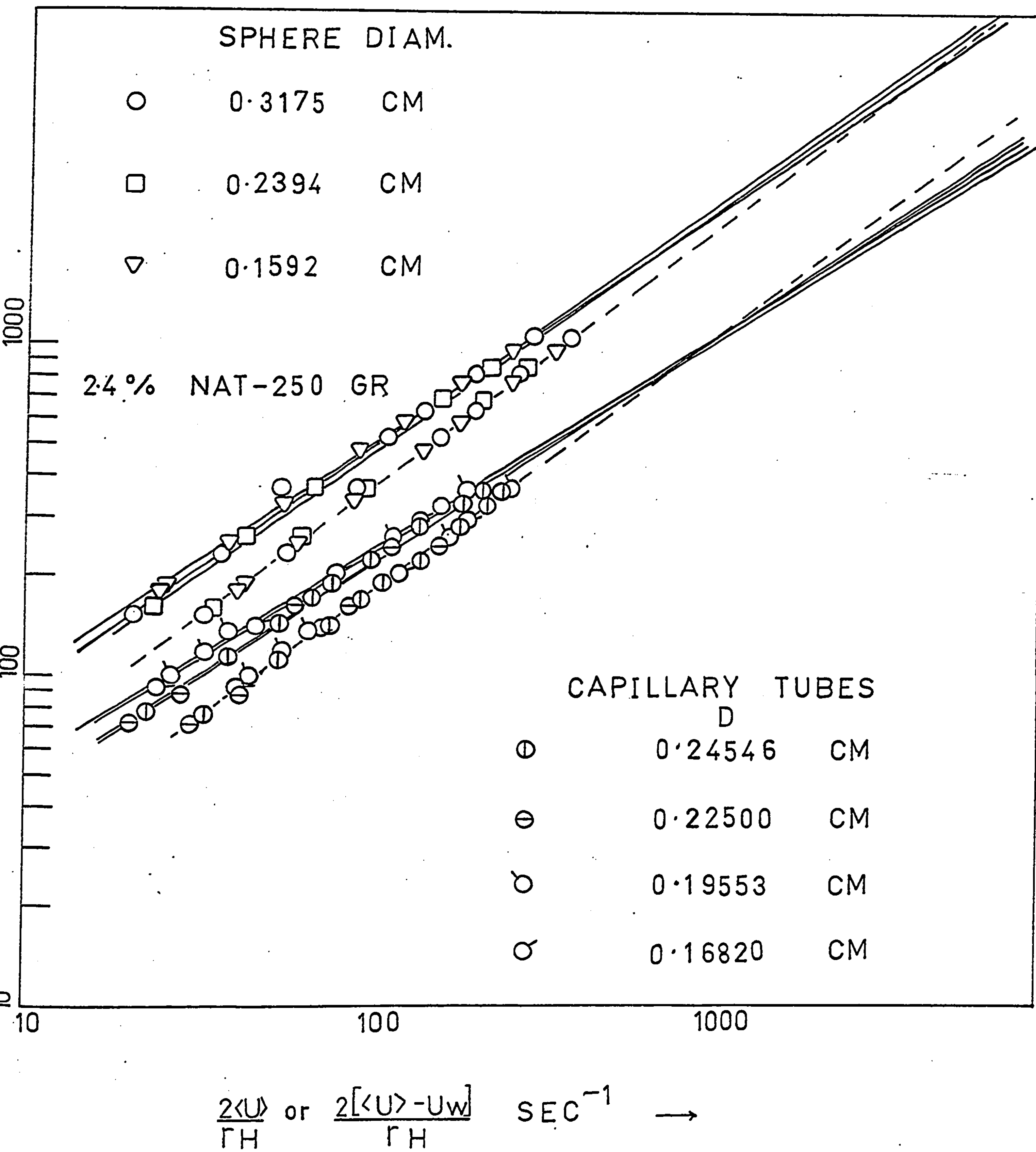
SPHERE DIAM.
○ 0·3175 CM
□ 0·2394 CM
▽ 0·1592 CM
2·4 % NAT-250 GR
CAPILLARY TUBES
D
0·24546 CM
0·22500 CM
0·19553 CM
0·16820 CM
1000
100
10
10
100
1000
τw DYNES/CM 2 ⟶
2⟨U⟩ / ΓH or 2[⟨U⟩-Uw] / ΓH SEC⁻¹ ⟶

is similar to that of Pasari for the capillary tubes, however he obtained a linear plot, instead of a curve. This might be explained by the fact that his range of concentration was limited so he was unable to obtain extra points.

An attempt was made to relate the critical shear stress to the hydraulic radius with the solution concentration as a parameter, as shown in fig. 17 & 18. The plot of τ_c^2 versus D or 4rH is linear for some capillary tubes, but not for different sized packed beds. In both figures the separate curves all intersect at an intercept when the shear stress is zero. The intercept is the critical diameter equal to 0.09 cm and 0.036 cm for capillary tubes and packed beds respectively. This suggests that when the tube diameter D or 4rH is smaller than the critical diameter the effective velocity at the surface is always positive.

The modified slip coefficient, ξ''', was obtained from the slope of the final plot of $\frac{2\langle u\rangle}{rH}$ vs $8(\tau_w - \tau c)/D^2$ as shown in figures 19 to 26 for the capillary viscometer, but for the packed beds the slope has to be multiplied by a constant 0.042056 to take the porosity term into account. Those points and lines which are located to the left of the origin lie in the region of gel formation, that is negative slip velocity, whereas those at the right lie in the region of positive effective velocity (separation phenomenon). The slip coefficient was found to vary linearly with the shear stress, except for the case of the capillary tubes at high concentra-

FIG 15

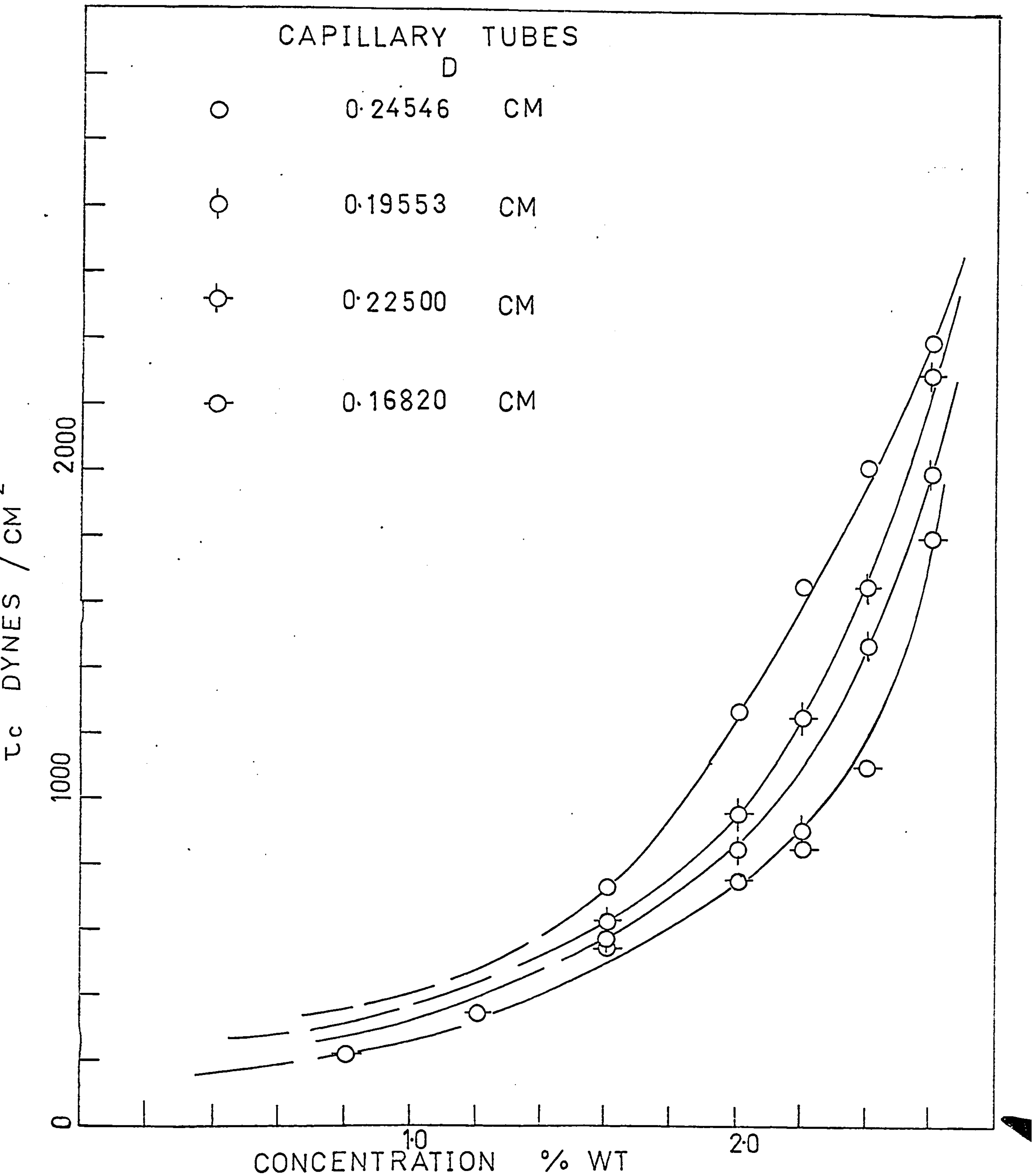
CAPILLARY TUBES
D
0·24546 CM
0·19553 CM
0·22500 CM
0·16820 CM
τc DYNES / CM 2
2000
1000
0
1·0
2·0
CONCENTRATION % WT

FIG 16

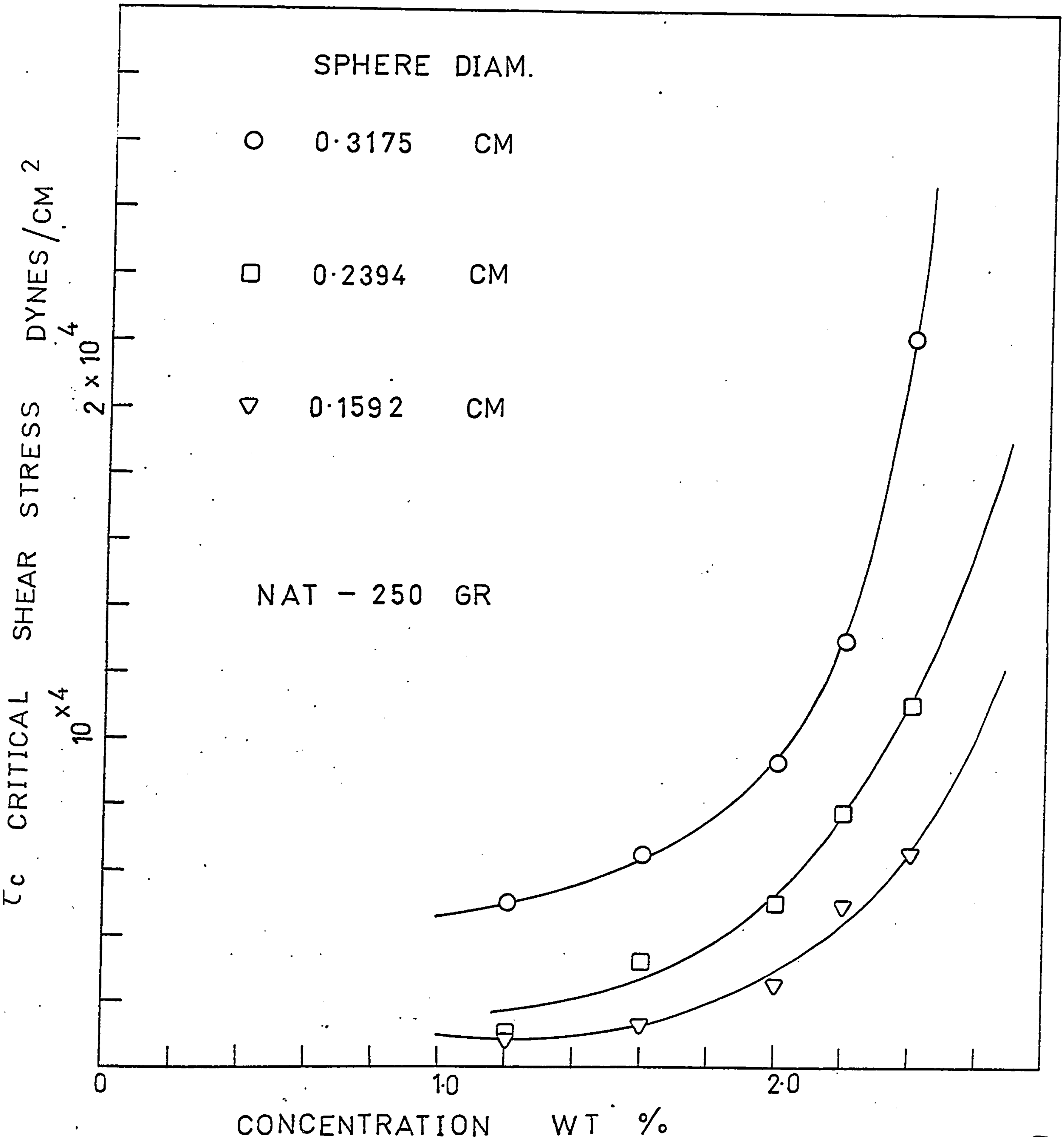
SPHERE DIAM.
○ 0·3175 CM
□ 0·2394 CM
▽ 0·1592 CM
NAT - 250 GR
τc CRITICAL SHEAR STRESS DYNES/CM 2
2 x 10 4
10 x4
0
1·0
2·0
CONCENTRATION WT %

FIG 17

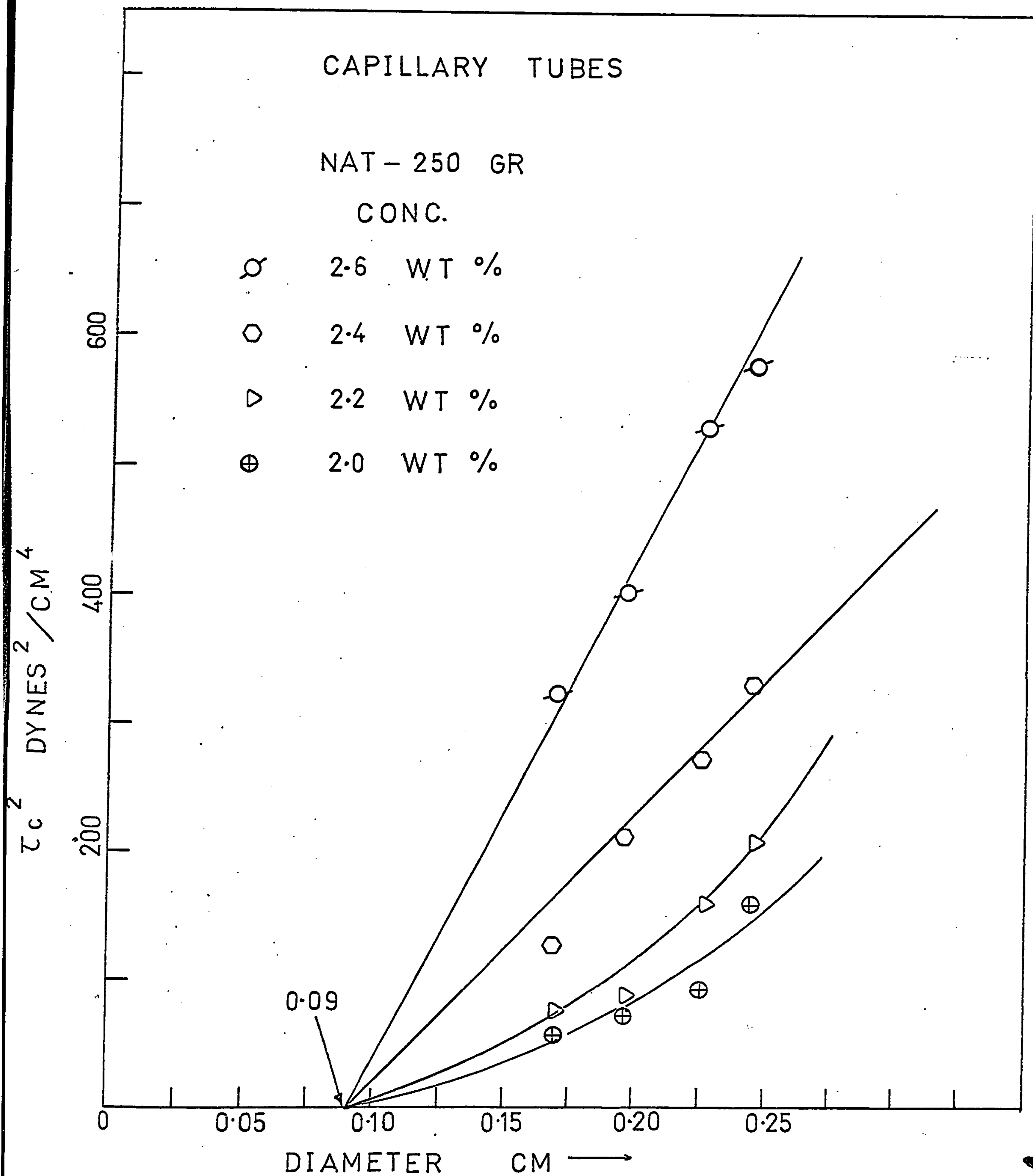
CAPILLARY TUBES
NAT - 250 GR
CONC.
2·6 WT %
2·4 WT %
2·2 WT %
2·0 WT %
0·09
600
400
200
0
0·05
0·10
0·15
0·20
0·25
τ_c^2 DYNES^2/CM^4
DIAMETER CM

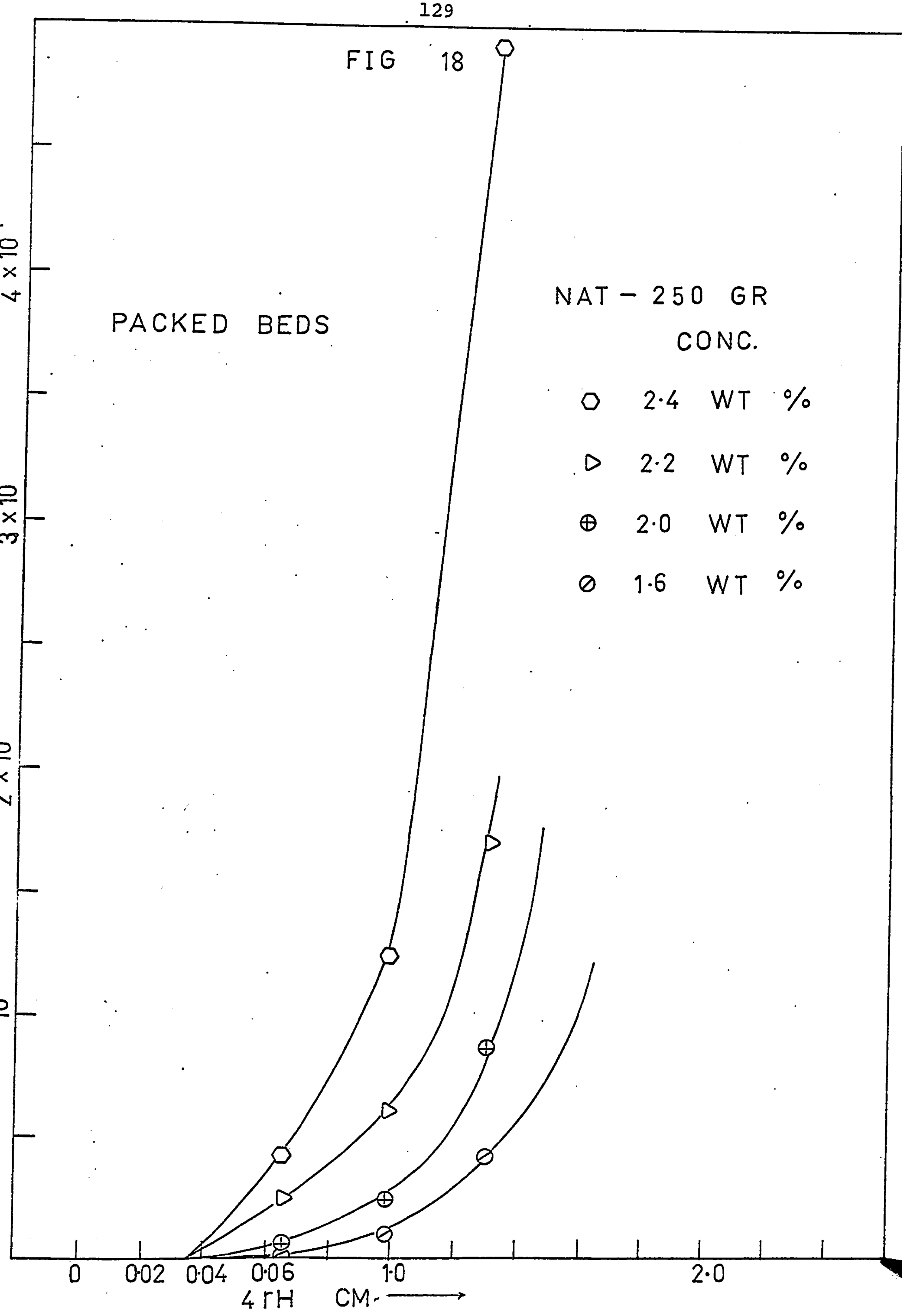
FIG 18
PACKED BEDS
NAT - 250 GR
CONC.
2·4 WT %
2·2 WT %
2·0 WT %
1·6 WT %
τ_c^2 DYNES^2/CM^4 →
10^4
2×10^4
3×10^4
4×10^4
0
0·02
0·04
0·06
1·0
2·0
4 rH CM →

FIG 19

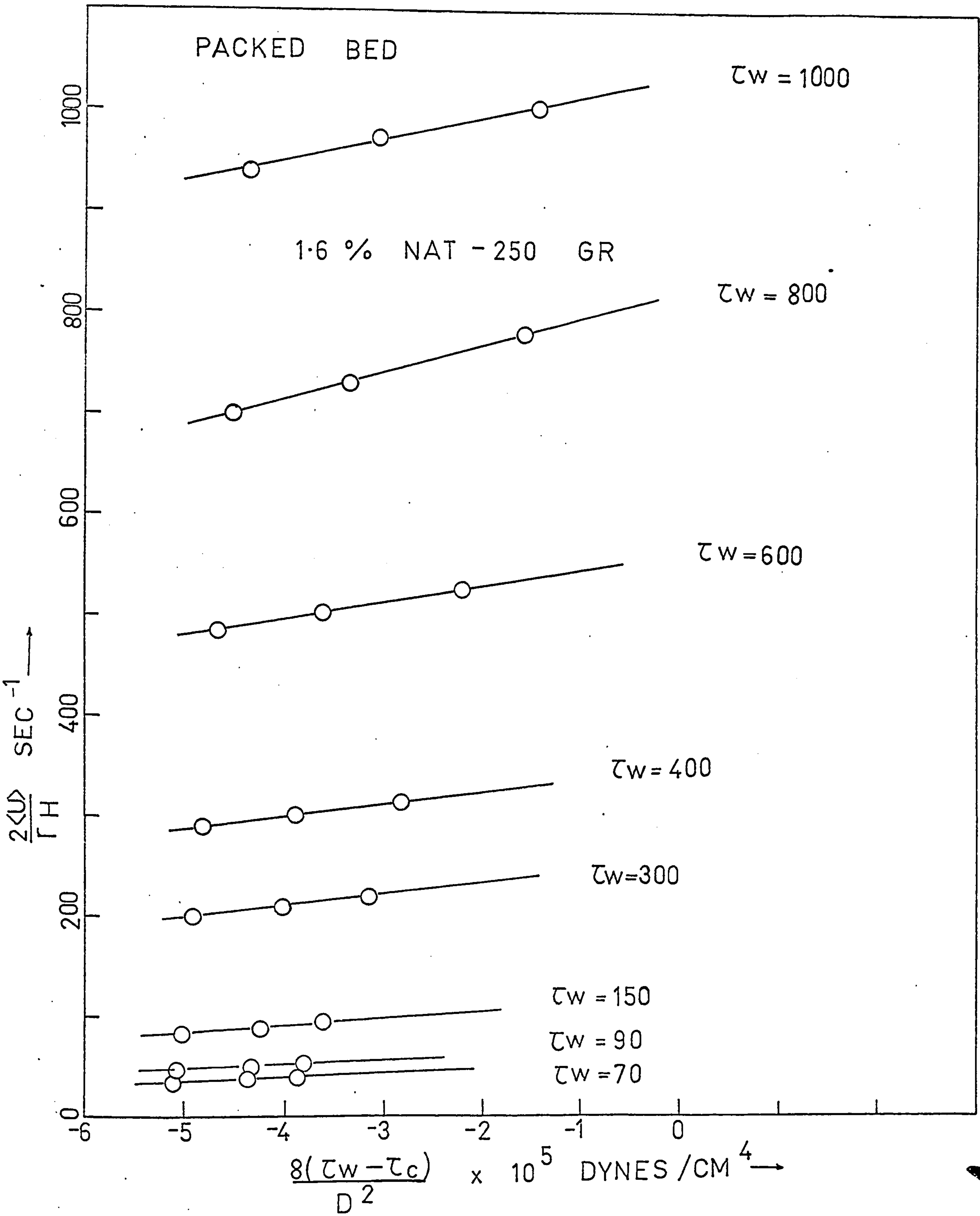
PACKED BED
1·6 % NAT - 250 GR
τw = 1000
τw = 800
τw = 600
τw = 400
τw = 300
τw = 150
τw = 90
τw = 70
2⟨U⟩ / ΓH SEC⁻¹
1000
800
600
400
200
0
-6
-5
-4
-3
-2
-1
0
8(τw − τc) / D² x 10⁵ DYNES / CM⁴

FIG 20

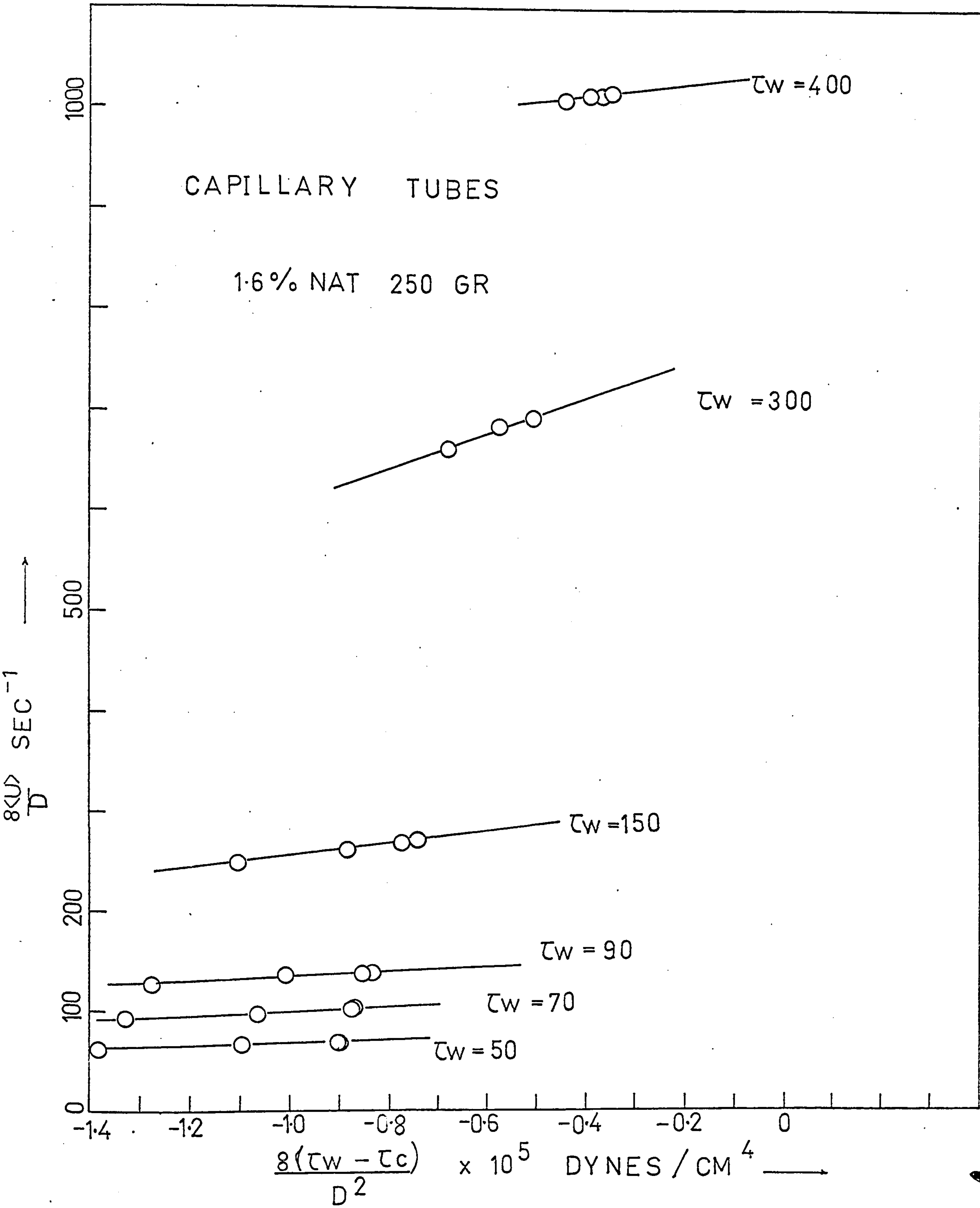
CAPILLARY TUBES
1·6% NAT 250 GR
τw = 400
τw = 300
τw = 150
τw = 90
τw = 70
τw = 50
1000
500
200
100
0
−1·4
−1·2
−1·0
−0·8
−0·6
−0·4
−0·2
0
8⟨U⟩/D SEC⁻¹
8(τw − τc)/D² x 10⁵ DYNES/CM⁴

FIG 21

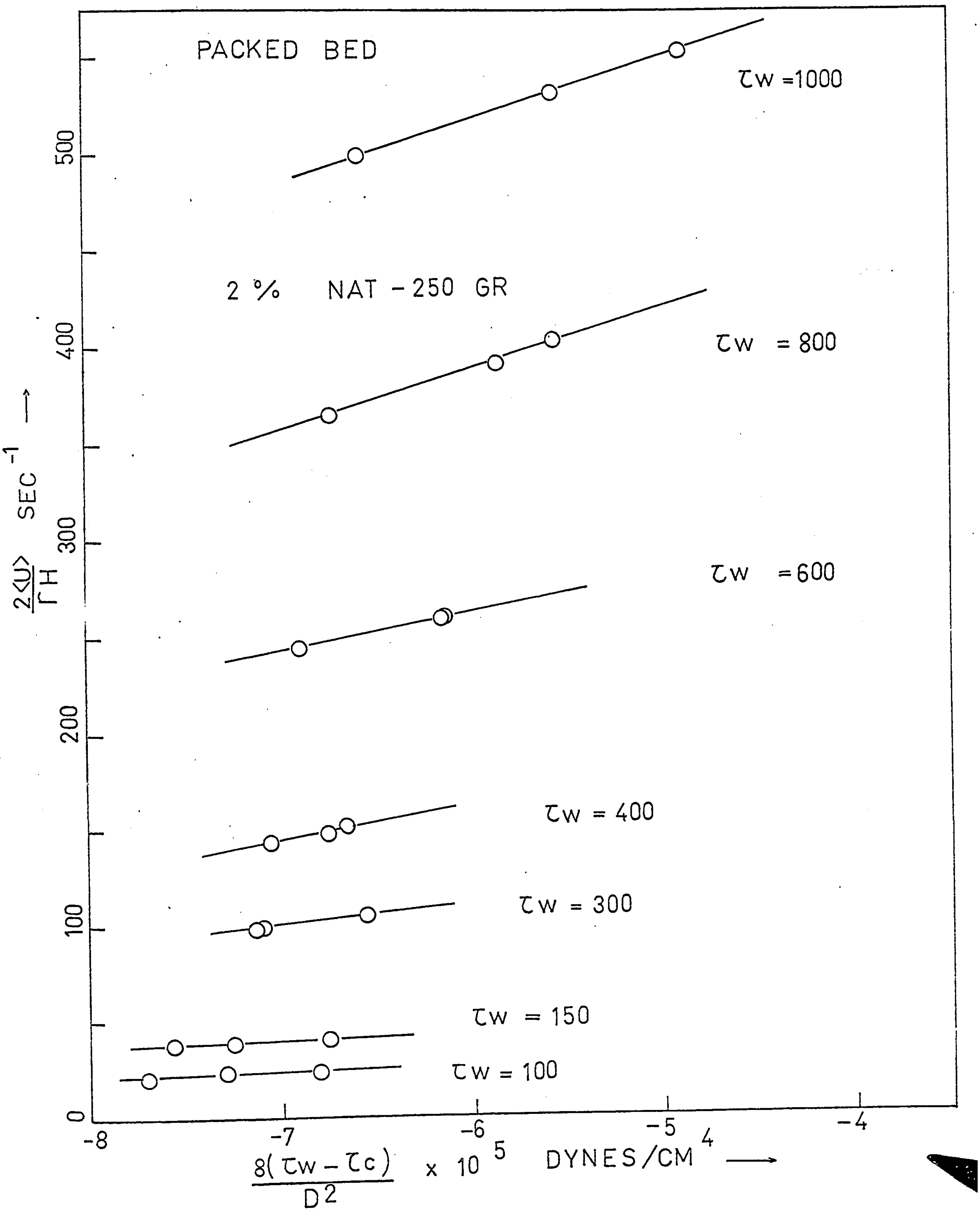
PACKED BED
2 % NAT - 250 GR
τw =1000
τw = 800
τw =600
τw = 400
τw = 300
τw = 150
τw = 100
500
400
300
200
100
0
2<U>/ΓH SEC^-1
-8
-7
-6
-5
-4
8(τw - τc)/D^2 x 10^5 DYNES/CM^4

FIG 22

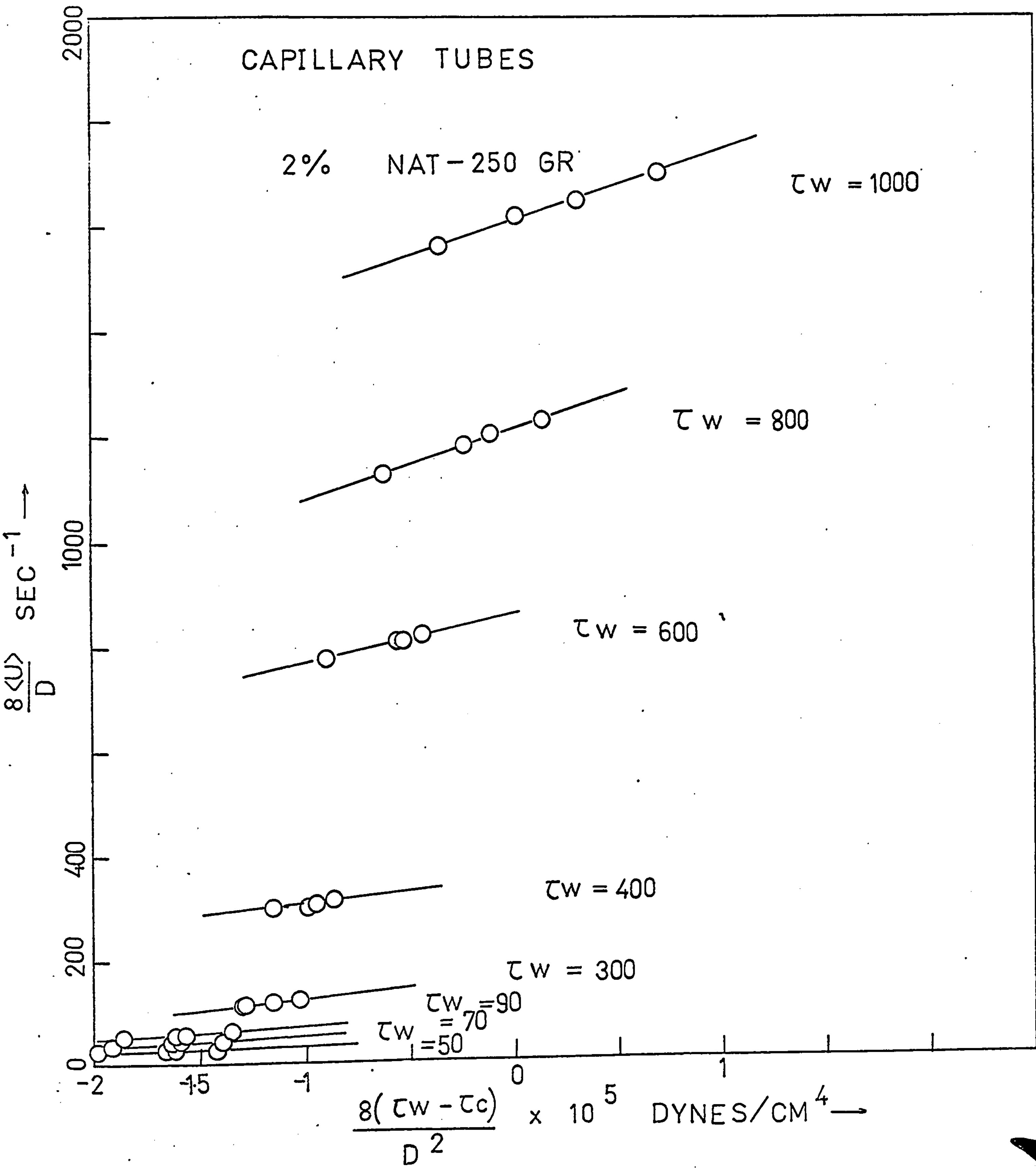
CAPILLARY TUBES
2% NAT-250 GR
τw = 1000
τw = 800
τw = 600
τw = 400
τw = 300
τw = 90
τw = 70
τw = 50
2000
1000
400
200
0
-2
-1.5
-1
0
1
8⟨U⟩/D SEC⁻¹ →
8(τw - τc)/D² x 10⁵ DYNES/CM⁴ →

FIG 23

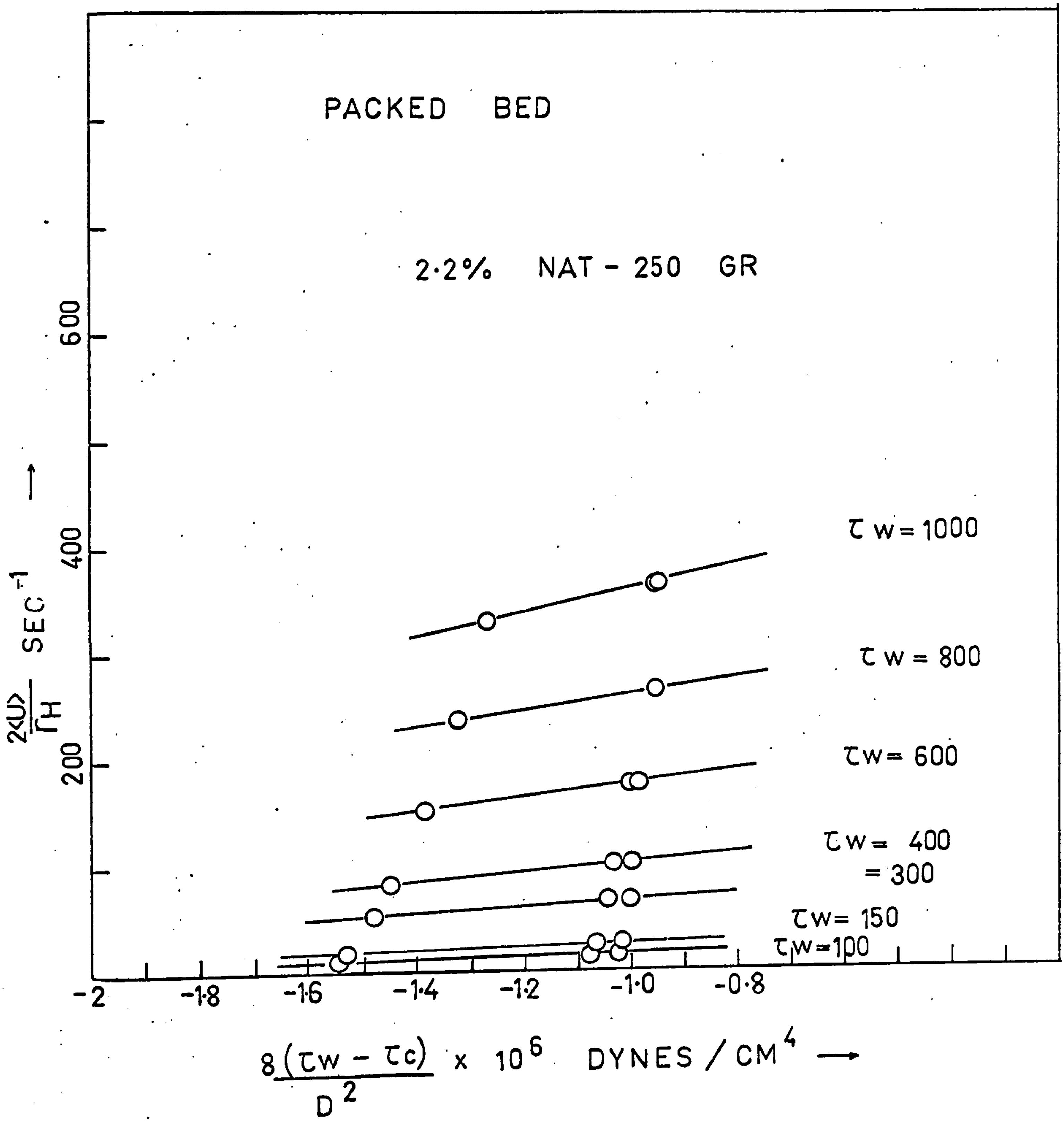
PACKED BED
2·2% NAT - 250 GR
τ w = 1000
τ w = 800
τw = 600
τw = 400
= 300
τw = 150
τw=100
600
400
200
$\frac{2\langle U\rangle}{\Gamma H}$ SEC^{-1} →
-2
-1·8
-1·6
-1·4
-1·2
-1·0
-0·8
$\frac{8(\tau w - \tau c)}{D^2}$ x 10^6 DYNES / CM^4 →

FIG 24

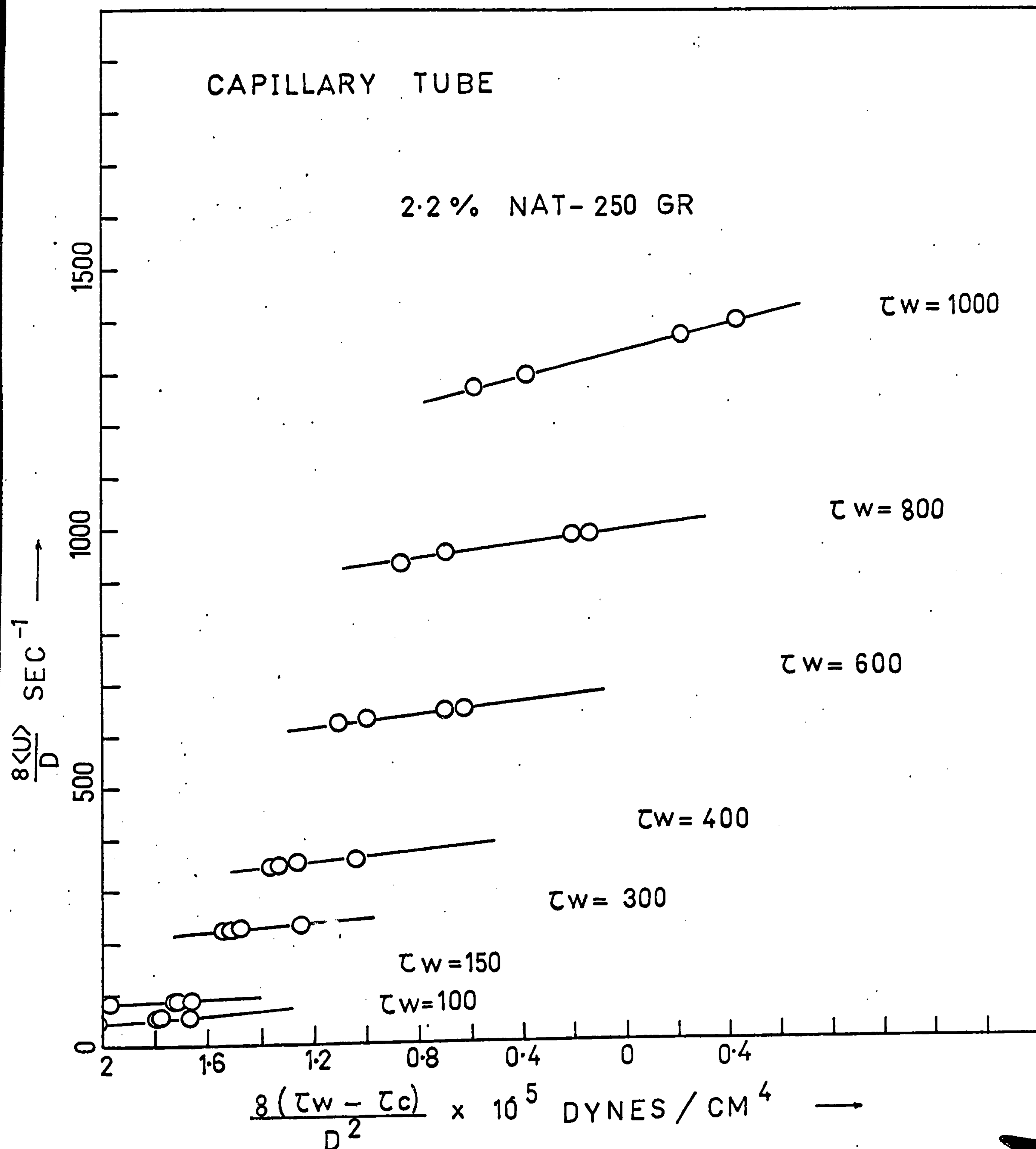

CAPILLARY TUBE
2·2 % NAT- 250 GR
τw = 1000
τw = 800
τw = 600
τw = 400
τw = 300
τw = 150
τw = 100
8⟨U⟩/D SEC⁻¹
0
500
1000
1500
2
1·6
1·2
0·8
0·4
0
0·4
8 (τw − τc)/D² x 10⁵ DYNES / CM⁴

FIG 25

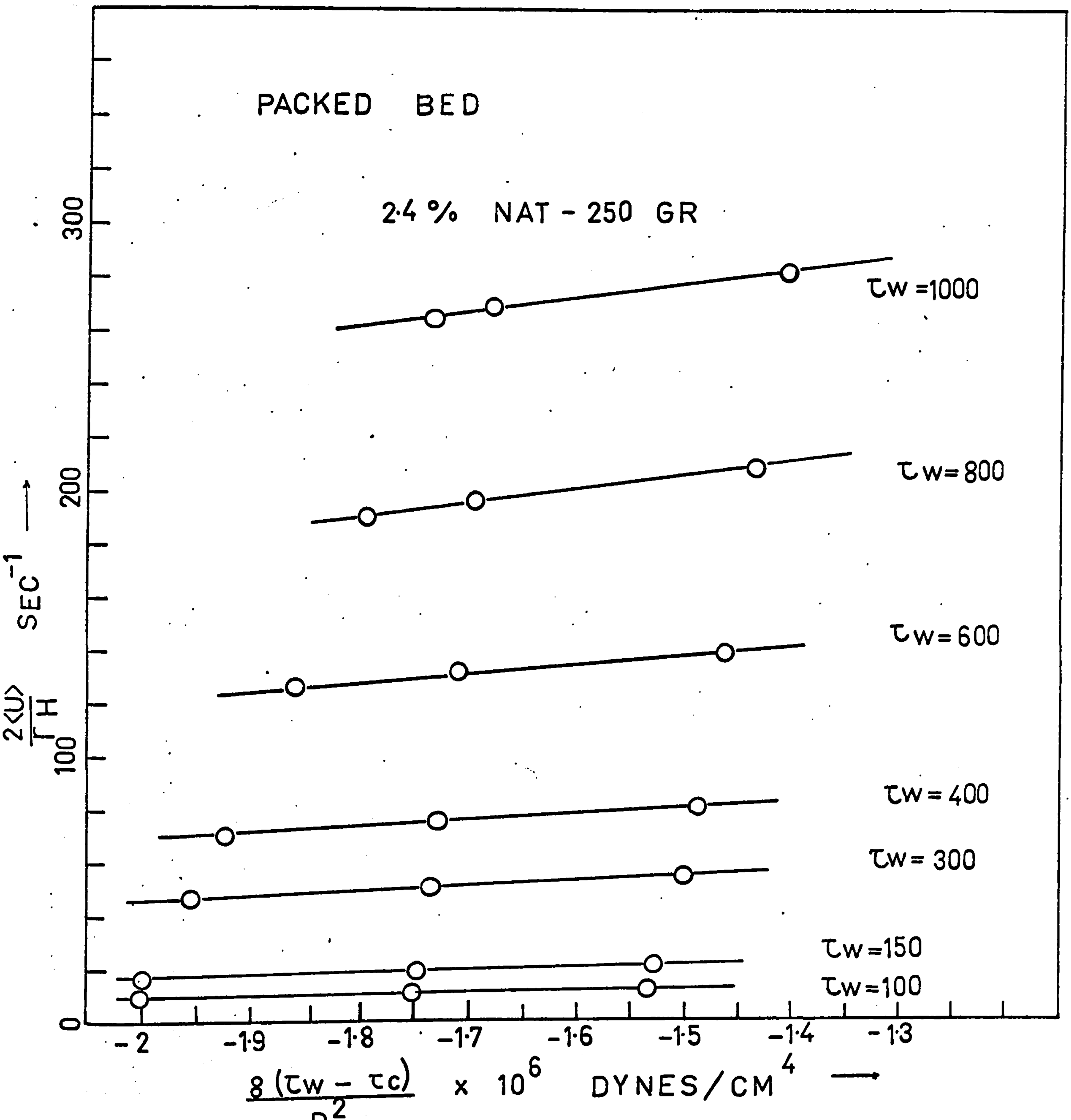

PACKED BED
2·4 % NAT - 250 GR
τw =1000
τw= 800
τw= 600
τw= 400
τw= 300
τw=150
τw=100
2⟨U⟩ / Γ H SEC⁻¹ →
0
100
200
300
- 2
-1·9
-1·8
-1·7
-1·6
-1·5
-1·4
-1·3
8 (τw − τc) / D² x 10⁶ DYNES/CM⁴ →

FIG 26

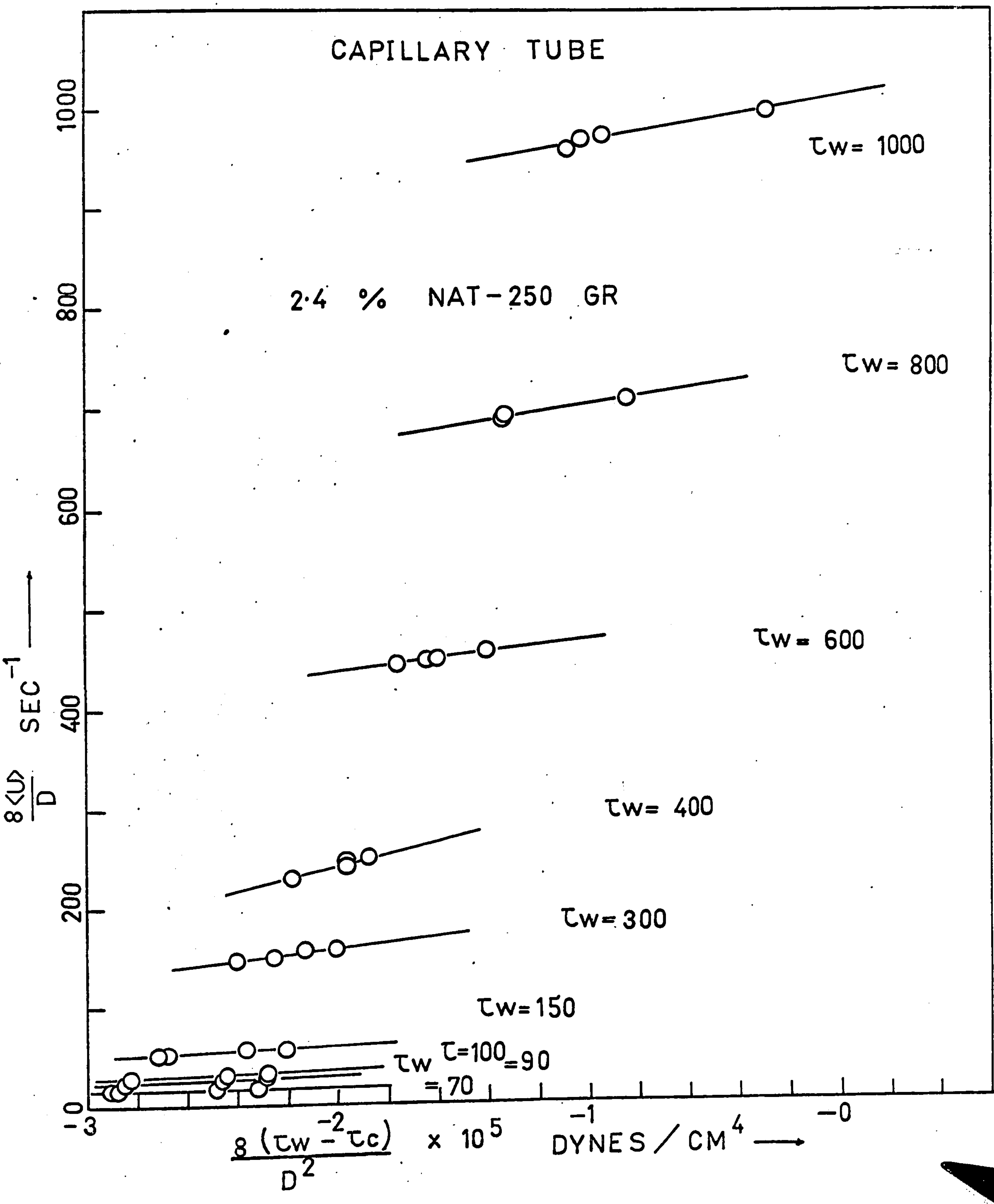
CAPILLARY TUBE
2·4 % NAT-250 GR
τw= 1000
τw= 800
τw= 600
τw= 400
τw= 300
τw=150
τw τ=100 =90
=70
1000
800
600
400
200
0
-3
-2
-1
-0
8⟨U⟩/D SEC⁻¹
8(τw - τc)/D² × 10⁵ DYNES / CM⁴

FIG 27

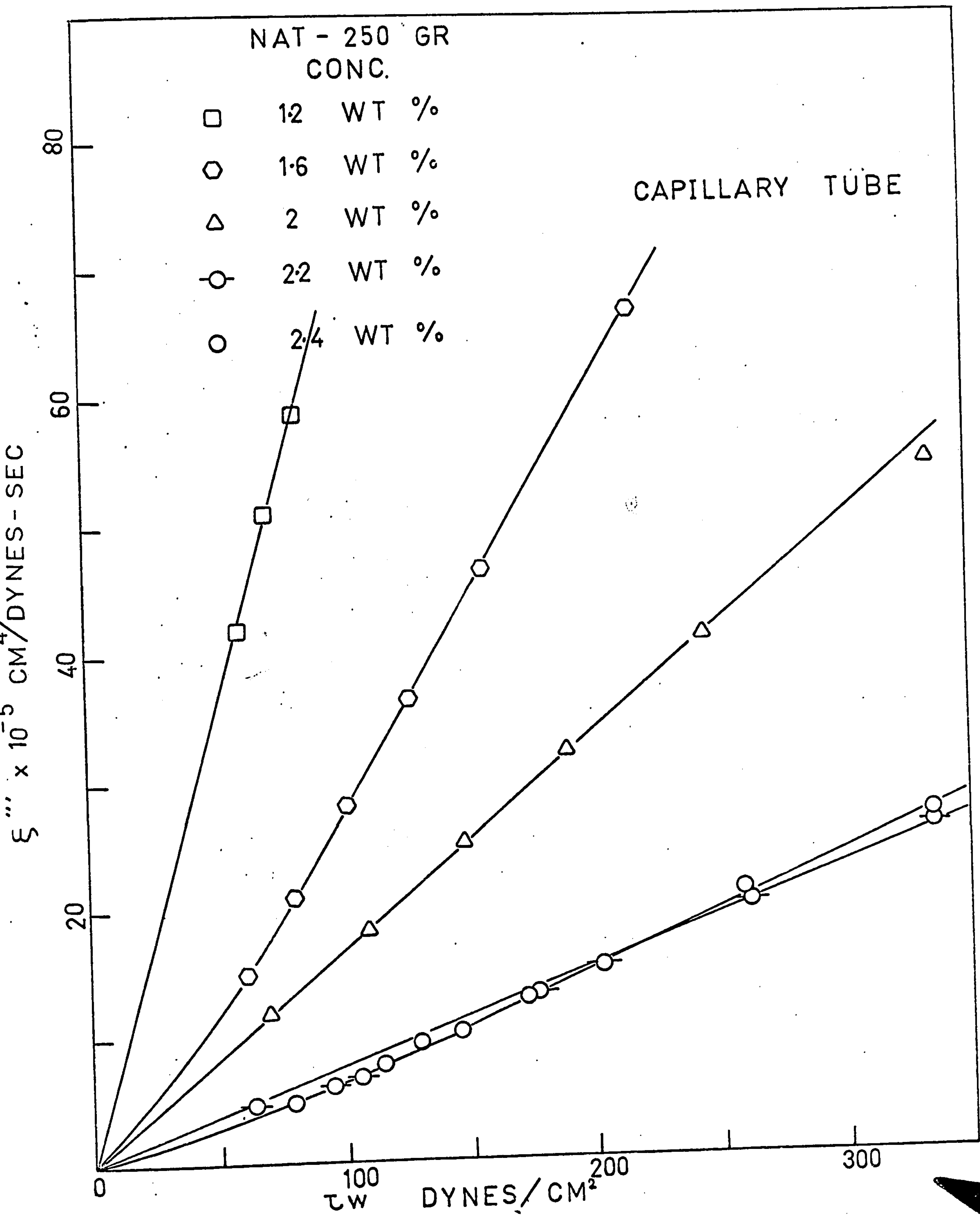
NAT - 250 GR
CONC.
1·2 WT %
1·6 WT %
2 WT %
2·2 WT %
2·4 WT %
CAPILLARY TUBE
ξ''' x 10⁻⁵ CM⁴/DYNES-SEC
80
60
40
20
0
100
200
300
τw DYNES/CM²

FIG 28

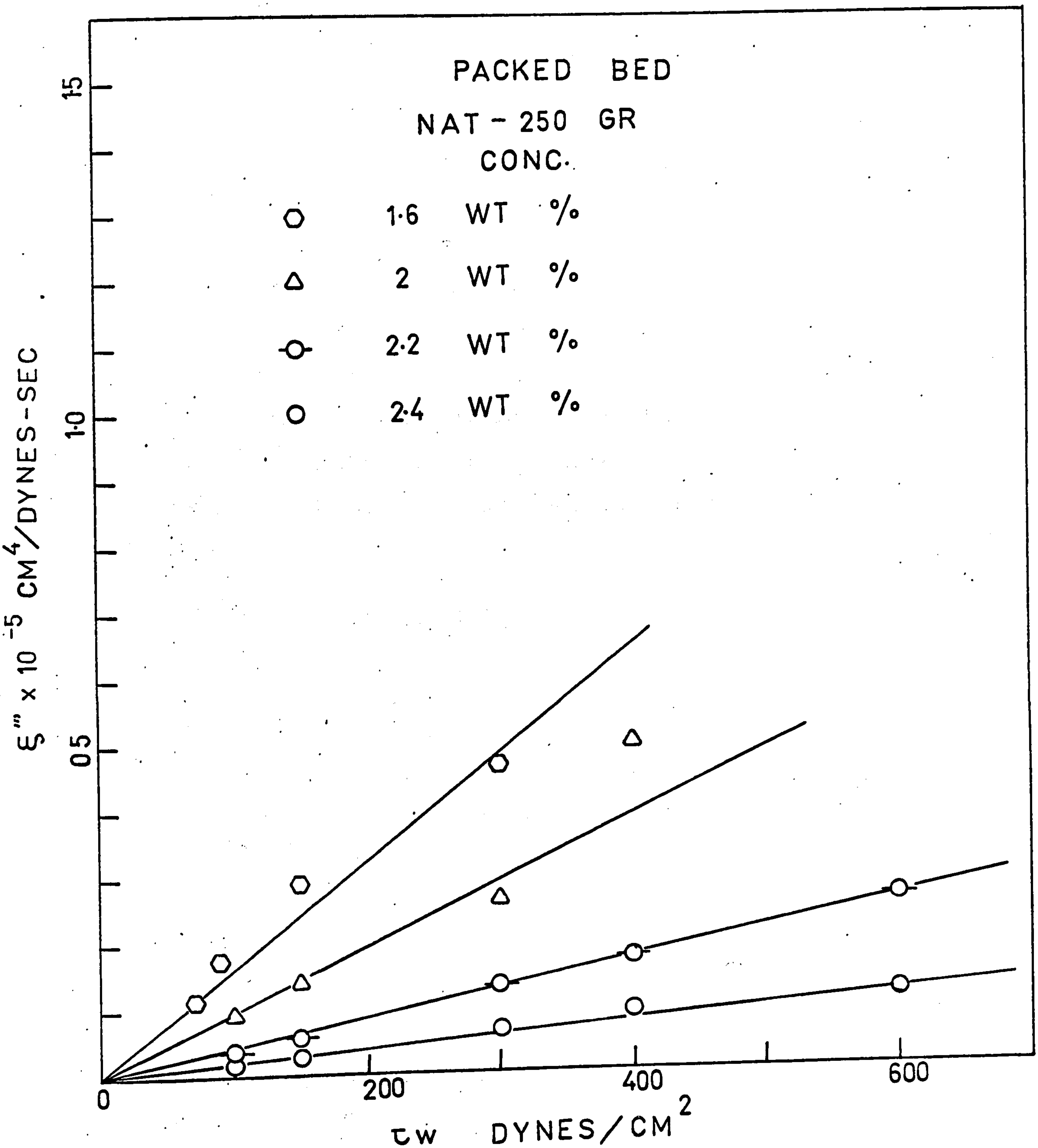
PACKED BED
NAT - 250 GR
CONC.
1·6 WT %
2 WT %
2·2 WT %
2·4 WT %
ξ''' x 10^-5 CM^4/DYNES-SEC
15
1·0
0·5
0
200
400
600
τw DYNES/CM^2

tion 2.4% as shown in fig. 27 & 28. This is probably due to greater surface effect at higher concentration.

The Power-Law parameters for the various concentrations were obtained from the final curves of the capillary viscometer. These values are tabulated in table 21. The flow behaviour index n' calculated according to equation (67) decreases as the concentration increases this indicates the increase of Non-Newtonian behaviour of the fluid. The range of n' varies from 0.6445 to 0.9989 for all the concentrations. Knowing these values of n', the flow behaviour index n, and the fluid consistency index K of the Power-Law fluid were determined from the plot of $f(\tau)$ vs τ in fig. 29 where

$$f(\tau) = \frac{(1+3n')}{4n'} \; \frac{2(\langle u\rangle - uw)}{rH} \qquad \ldots \quad (89)$$

$$\tau = K(f(\tau))^n \qquad \ldots \quad (90)$$

These values of n and K were then applied to the packed bed data to calculate the dimensionless group $(\tau/K)^s/w$. The results are shown in Tables 29 - 33 and in fig. 30 solid line. The broken line represents the theoretical value calculated for the parametric equation with only the first two geometric coefficients ε_o and ε_1. The value of $\frac{(\frac{\tau}{K})^s}{w}$ when n=0.5 or s=2 was determined by extrapolation and then used to evaluate the third geometric coefficient ε_2 according to equation (40). This was found to be $\varepsilon_2=0.375$.

The anomalous layer thickness δ was calculated according to equations (61) and (62). Fig. (31-36) shows the plot of δ versus τw, where it can be observed that polymer adsorption increases as the shear stress decreases and that maximum adsorption occurs when the shear stress at the wall is zero. In the case of the capillary tubes the anomalous layer thickness is extrapolated to $\tau w = 0$ to obtain δ max. This information of δ max, provide a method of determining the zero shear stress viscosity ηo according to the following equation

$$\eta o = \frac{\delta \text{ max } D}{\xi'''_o \ \tau_c} \qquad \ldots\ldots\ldots\ldots \ (93)$$

where ξ'''_o is the slope of ξ''' vs τw at zero wall shear stress shown in fig. (37).

Fig. (38) shows the plot of the viscosity η vs τ for the Ellis fluid model for the various concentrations. The solid line represents the experimental values whereas the broken one, the theoretical values for the Ellis fluid. It may be seen that the Non-Newtonian fluid is well represented by the Ellis fluid. The flow curves were extrapolated to low shear stress in order to compare the values obtained for the calculated zero shear viscosity. The results agreed well with those calculated.

The parameter α for the Ellis fluid model for the various concentrations was obtained from the slope of $\frac{(\eta o}{\eta}-1)$

FIG 29

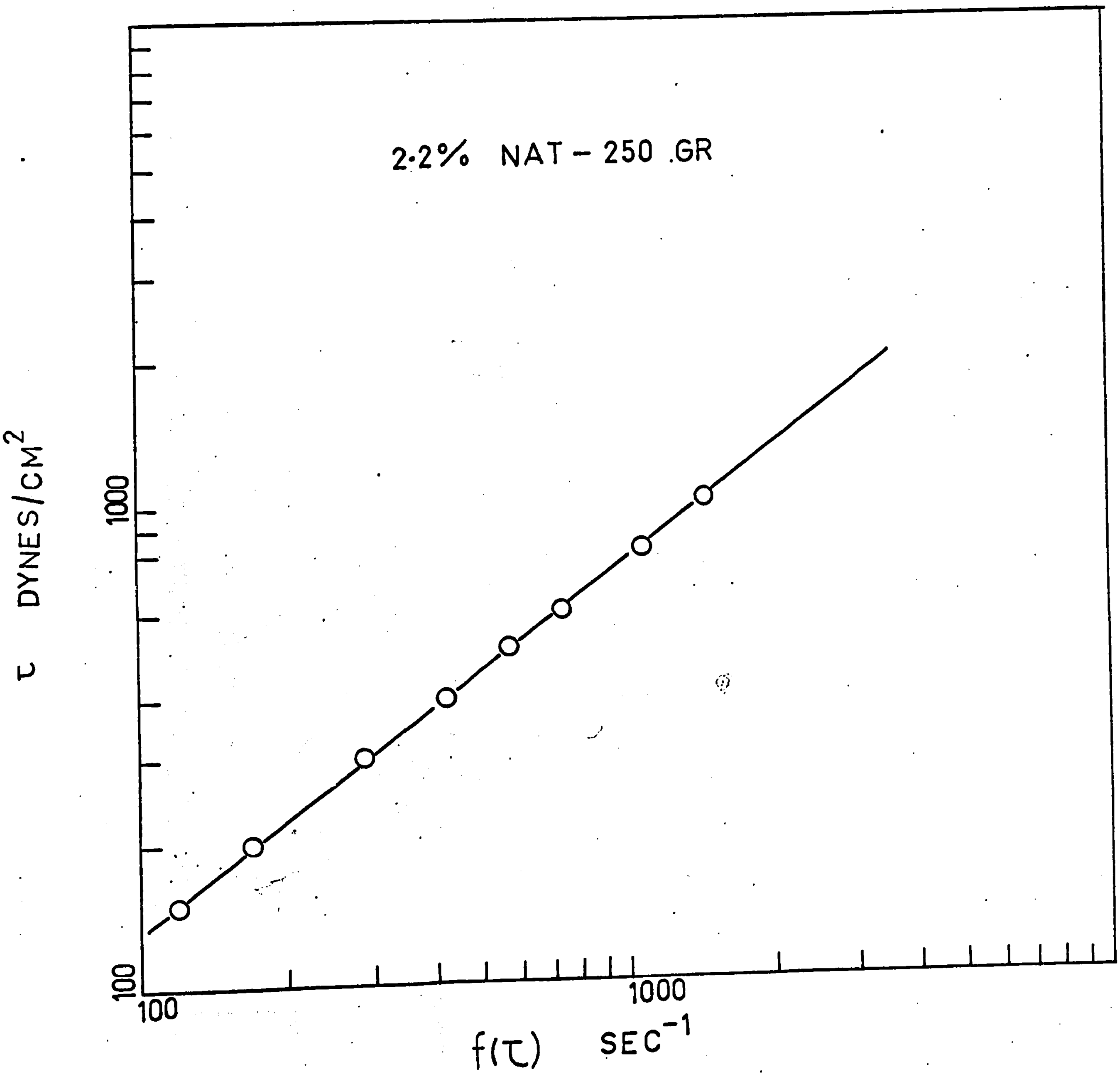

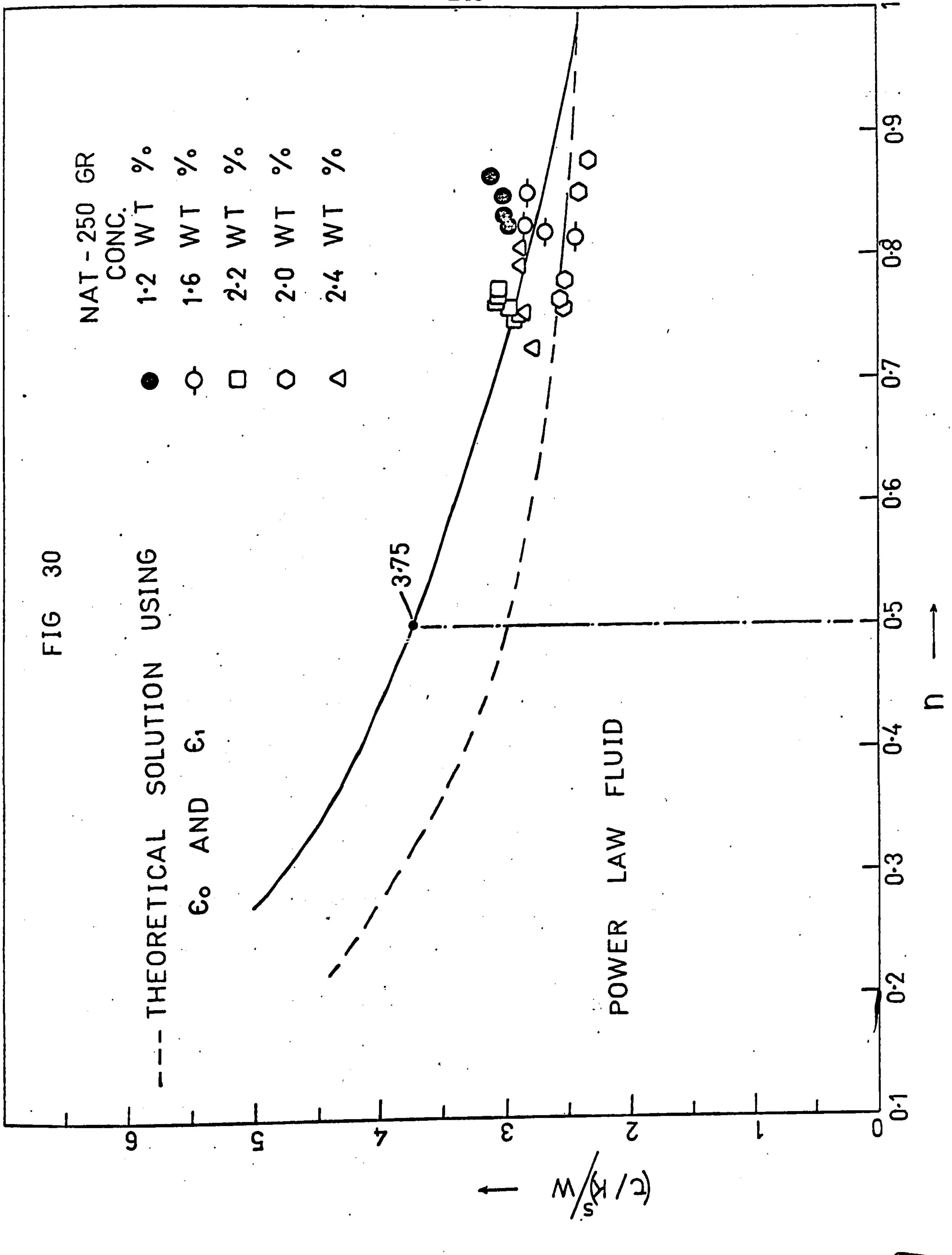
FIG 30
--- THEORETICAL SOLUTION USING
ε₀ AND ε₁
POWER LAW FLUID
NAT - 250 GR
CONC.
1·2 WT %
1·6 WT %
2·2 WT %
2·0 WT %
2·4 WT %
3·75
n
0·1
0·2
0·3
0·4
0·5
0·6
0·7
0·8
0·9
1
0
1
2
3
4
5
6

vs $\frac{\tau}{\tau_{\frac{1}{2}}}$ as shown in fig. 39 . The shear stress $\tau_{\frac{1}{2}}$, when the viscosity is $\eta = \frac{\eta o}{2}$ was obtained from fig. 38 . When obtained these parameters were utilized to make the plot of $w\eta o/\tau$ vs $(\tau/\tau_{\frac{1}{2}})^{\alpha - 1}$ for the different concentrations of Nat-250GR as shown in fig. 41 . According to equation (48) the slope of the lines is equivalent to $\frac{1}{\epsilon_o + \alpha\epsilon_1 + \alpha(\alpha - 1)\epsilon_2 \ldots}$ and the curves should have a common intercept equal to $\frac{1}{\epsilon_o + \epsilon_1}$ 0.417.

Fig. 40 shows the plot of the slopes versus the Ellis fluid parameter (solid line). The broken line is the theoretical value calculated using only two geometric parameters when $\alpha = 2$ the slope is equal to 0.265 by extrapolation. This was used to evaluate $\epsilon_2 = 0.3868$ from equation (49) which agreed very well with the value calculated for the Power-Law fluid.

The datas for Natrosol-250HR solution are presented in appendices A, B for both packed beds and capillary viscometer respectively. These are not analyzed since they are viscoelastic in behaviour. However, the same theory could be extended to explain the flow behaviour of these solutions.

FIG 31

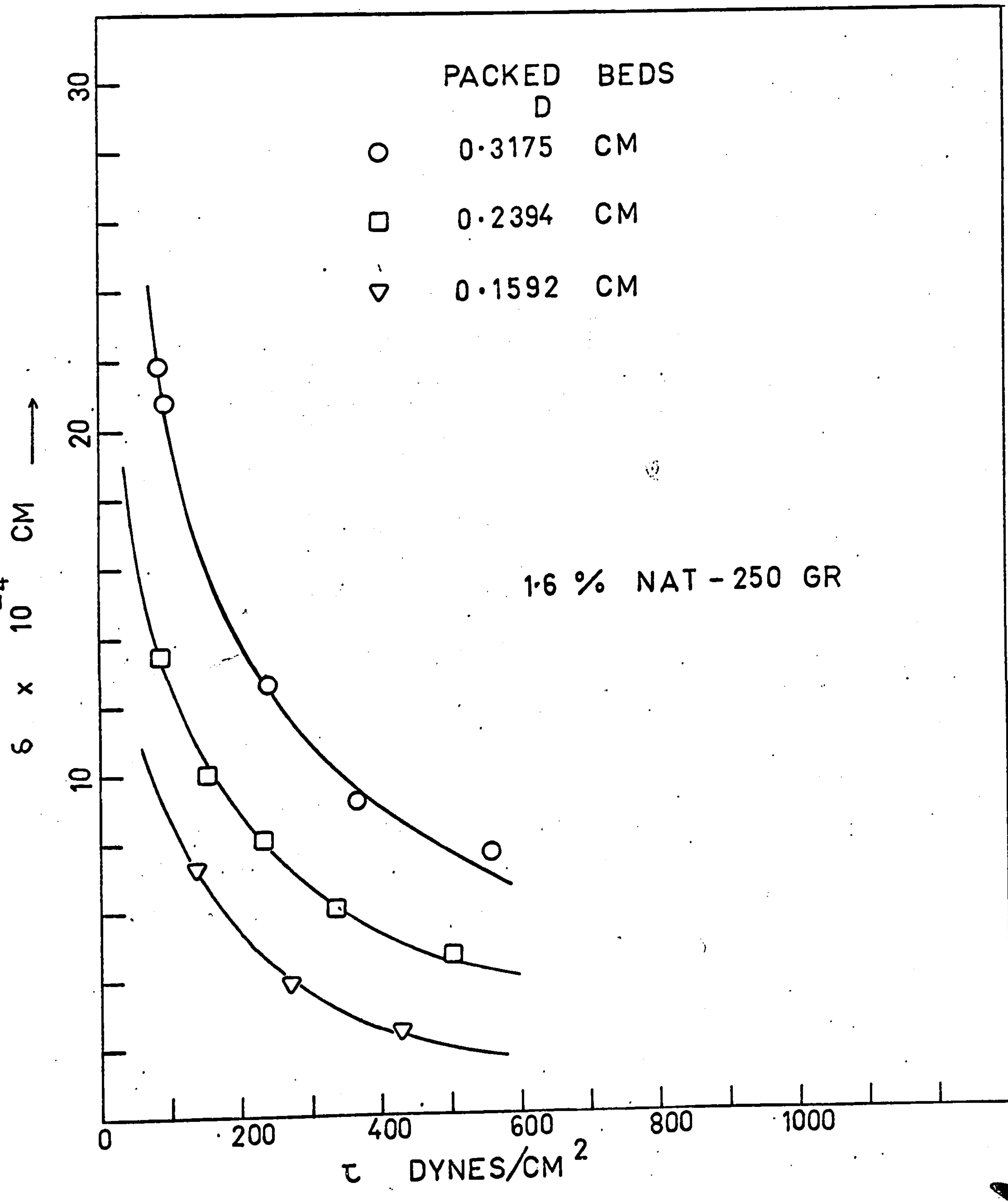
PACKED BEDS
D
0·3175 CM
0·2394 CM
0·1592 CM
1·6 % NAT - 250 GR
δ × 10⁻⁴ CM
30
20
10
0
200
400
600
800
1000
τ DYNES/CM 2

FIG 32

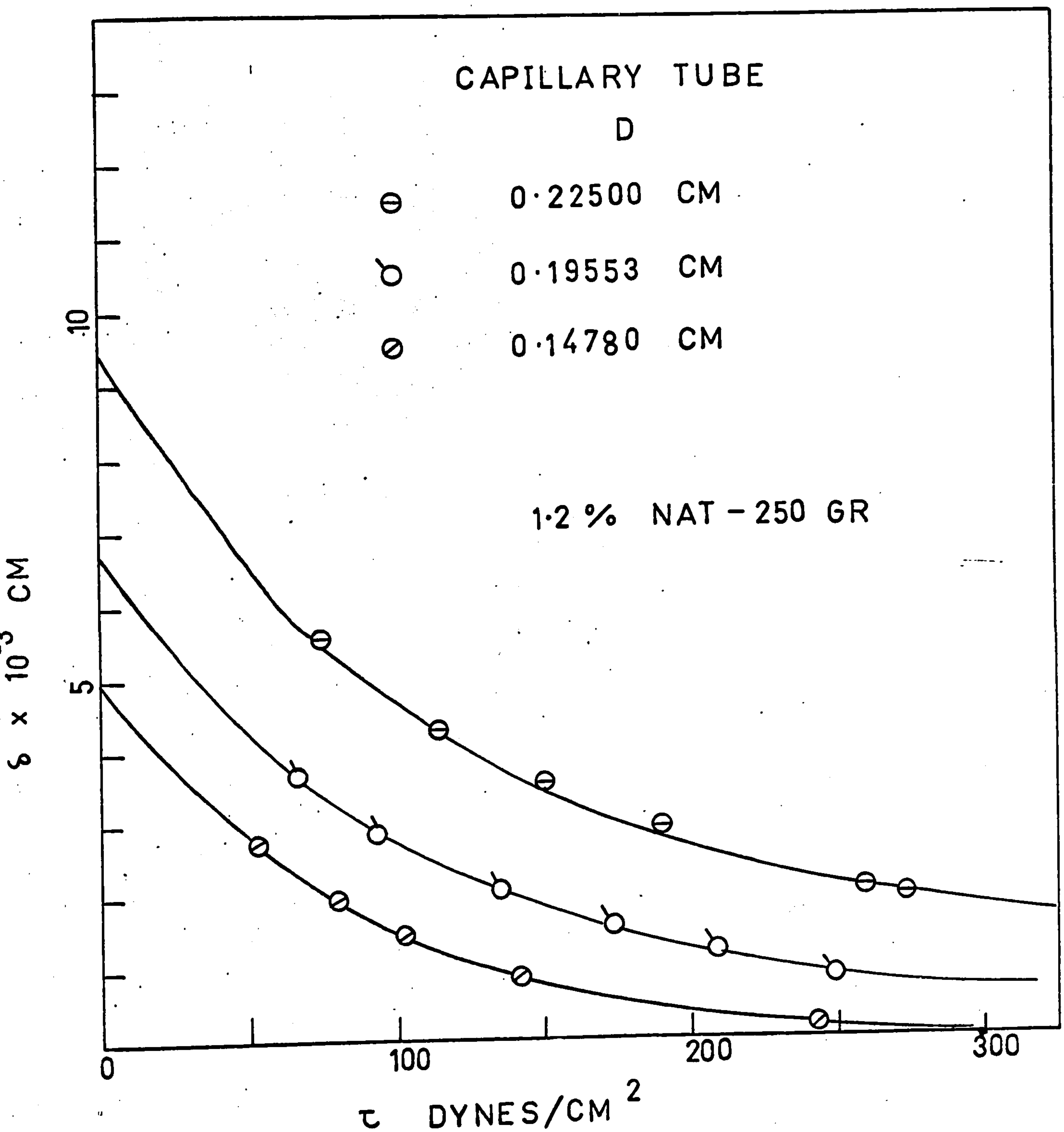
CAPILLARY TUBE
D
0·22500 CM
0·19553 CM
0·14780 CM
1·2 % NAT - 250 GR
δ x 10^-3 CM
τ DYNES/CM 2
0
100
200
300
5
10

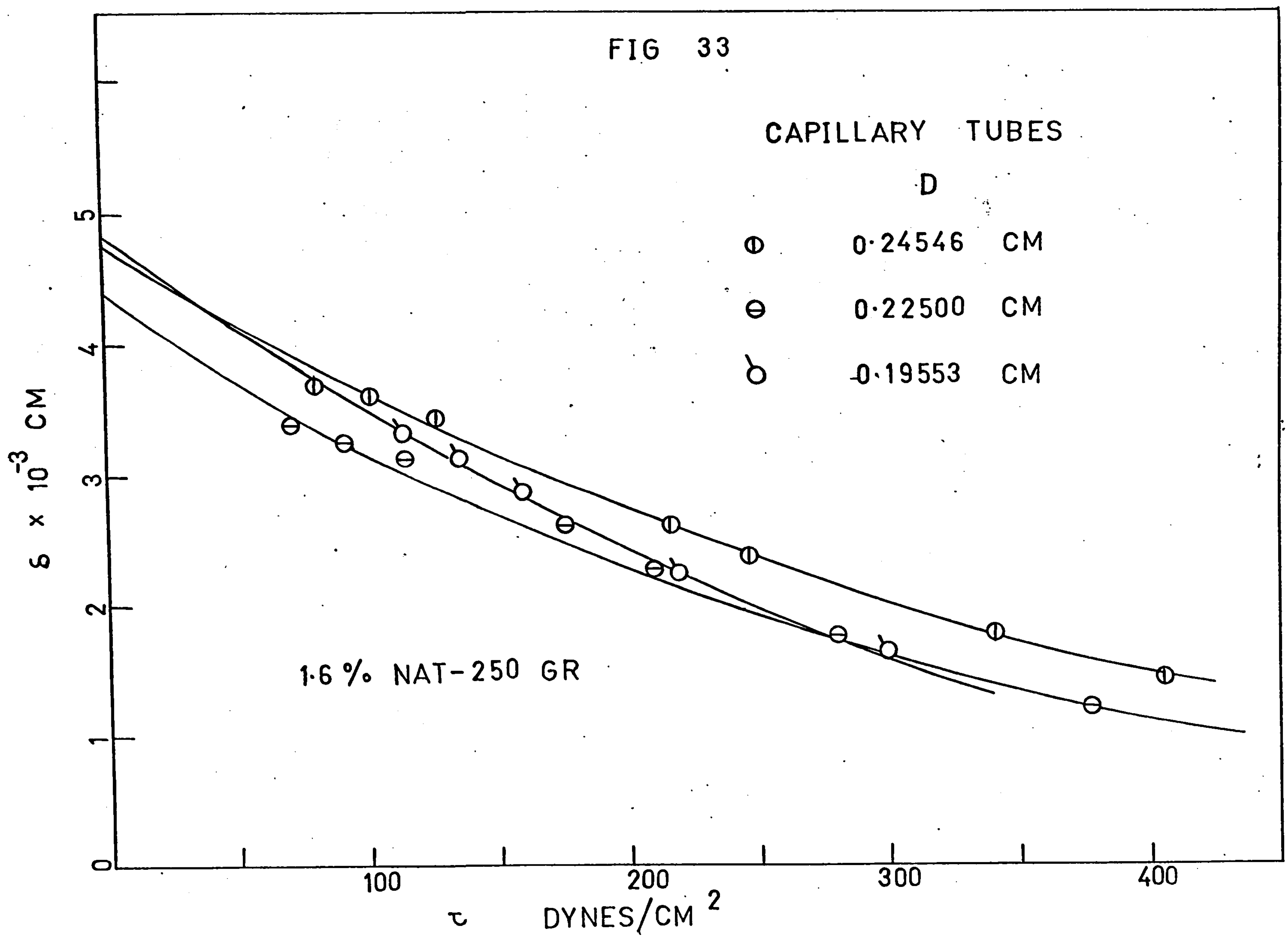

FIG 33
CAPILLARY TUBES
D
0·24546 CM
0·22500 CM
0·19553 CM
1·6 % NAT-250 GR
δ x 10^-3 CM
τ DYNES/CM 2
0
1
2
3
4
5
100
200
300
400

FIG 34

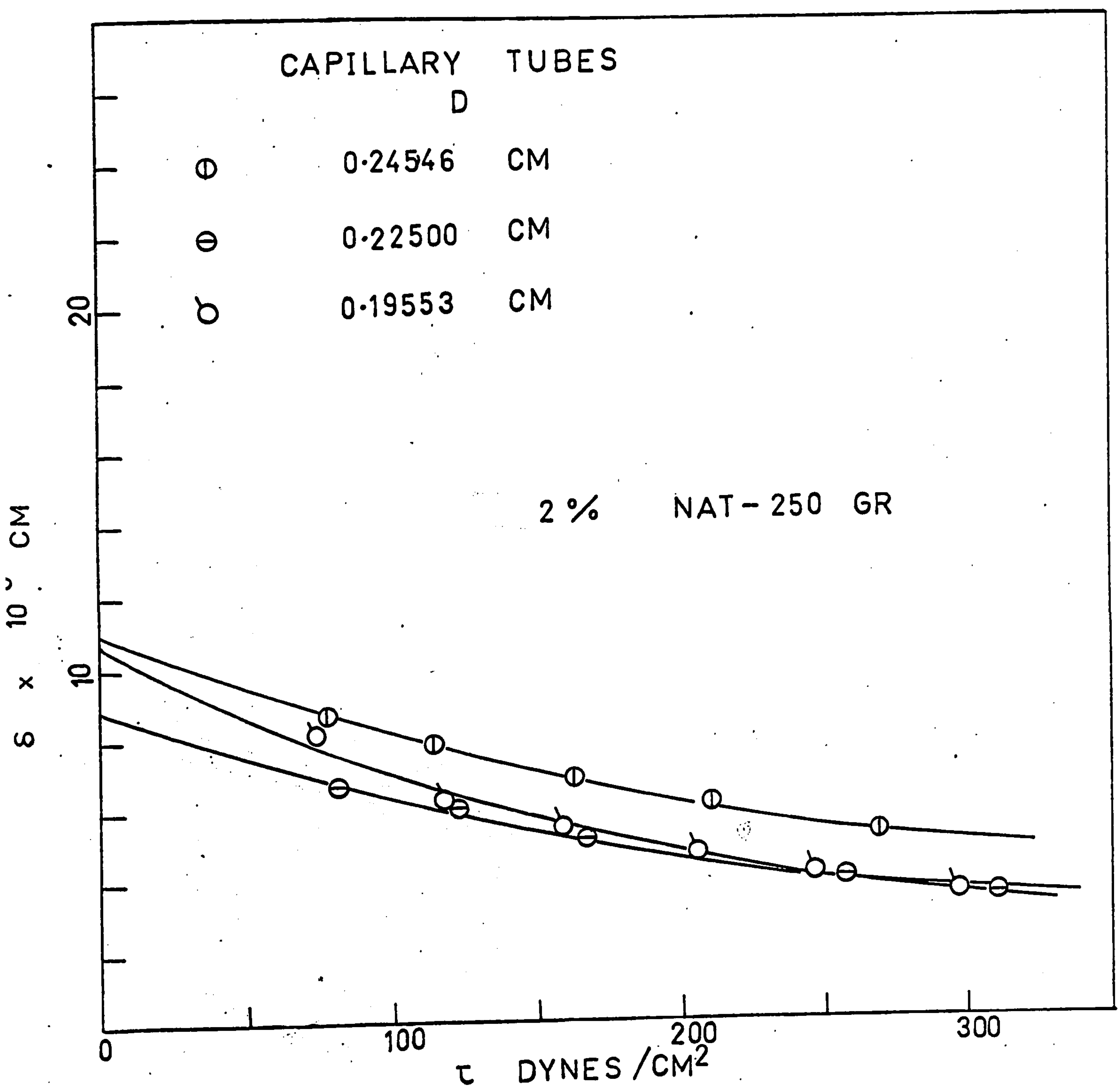

CAPILLARY TUBES
D
0·24546 CM
0·22500 CM
0·19553 CM
2 % NAT - 250 GR
δ x 10 CM
20
10
0
100
200
300
τ DYNES /CM2

FIG 35

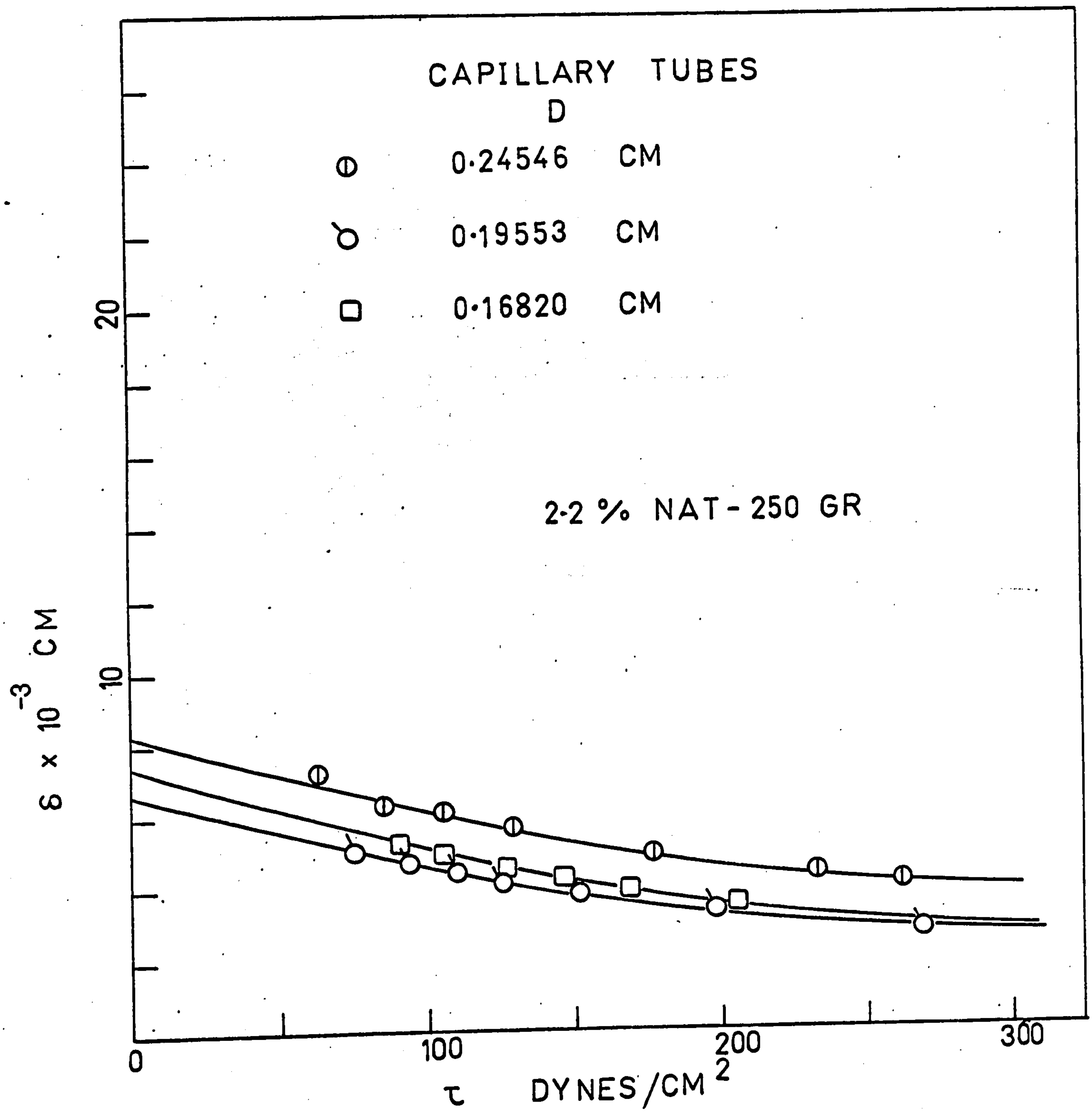

CAPILLARY TUBES
D
0·24546 CM
0·19553 CM
0·16820 CM
2·2 % NAT-250 GR
δ × 10⁻³ CM
20
10
0
100
200
300
τ DYNES/CM 2

FIG . 36

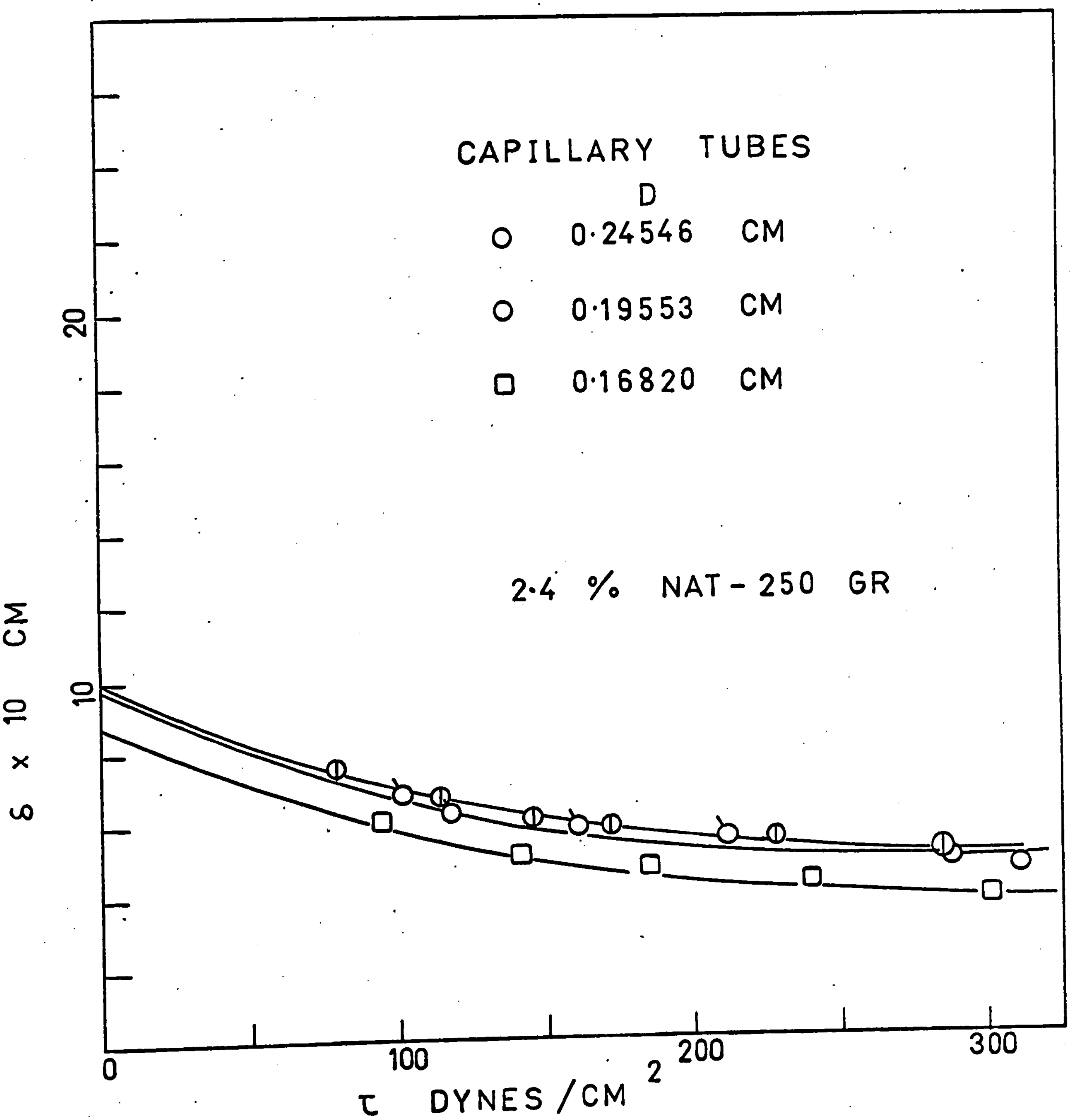
CAPILLARY TUBES
D
0·24546 CM
0·19553 CM
0·16820 CM
2·4 % NAT - 250 GR
δ x 10^-3 CM
τ DYNES / CM 2
0
100
200
300
10
20

FIG 37

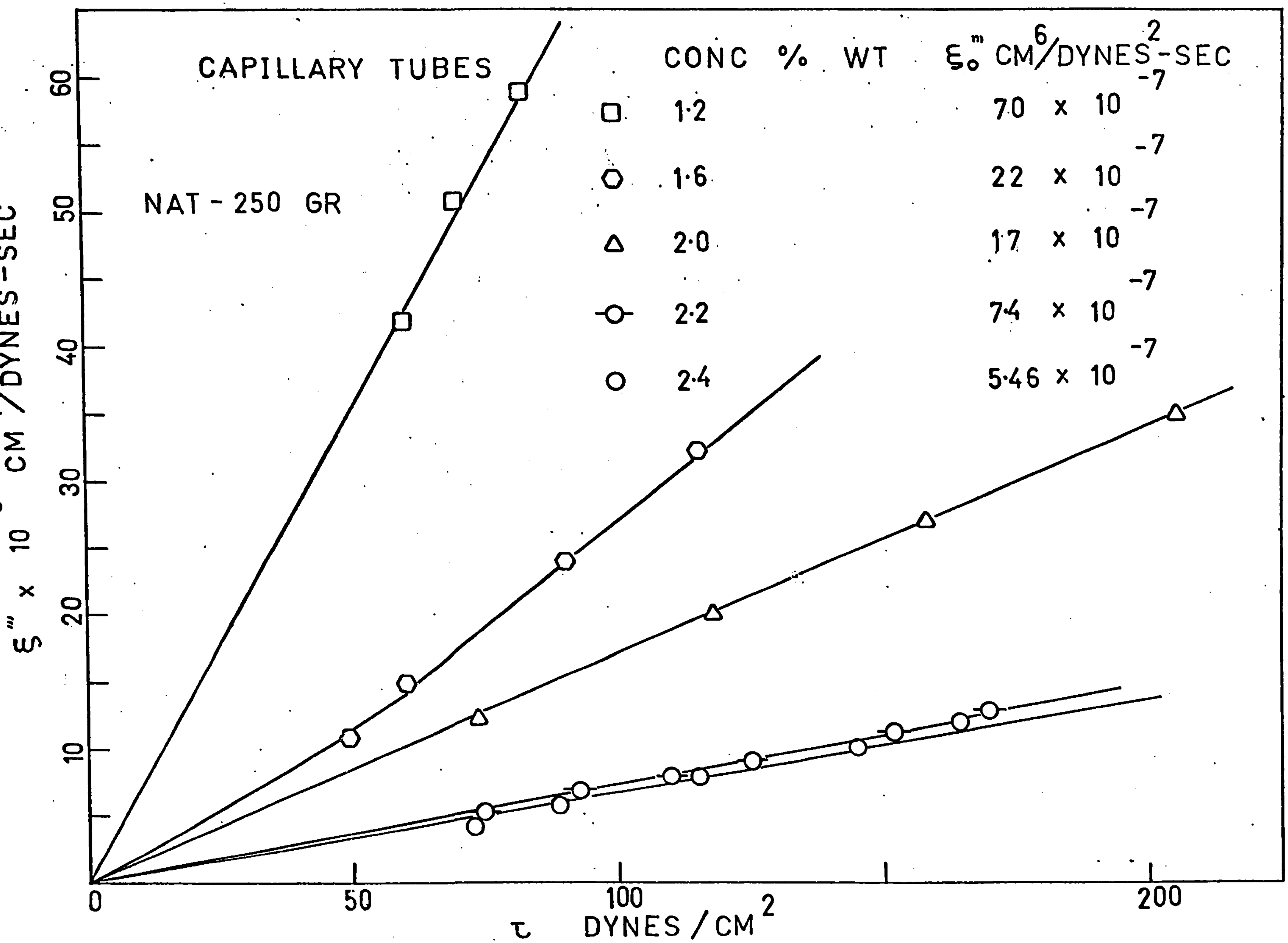

CAPILLARY TUBES
NAT - 250 GR
CONC % WT
ξ₀''' CM⁶/DYNES²-SEC
1·2 70 x 10⁻⁷
1·6 22 x 10⁻⁷
2·0 17 x 10⁻⁷
2·2 7·4 x 10⁻⁷
2·4 5·46 x 10⁻⁷
ξ''' x 10⁻⁵ CM⁴/DYNES-SEC
τ DYNES / CM²
0
50
100
200
10
20
30
40
50
60

FIG 38

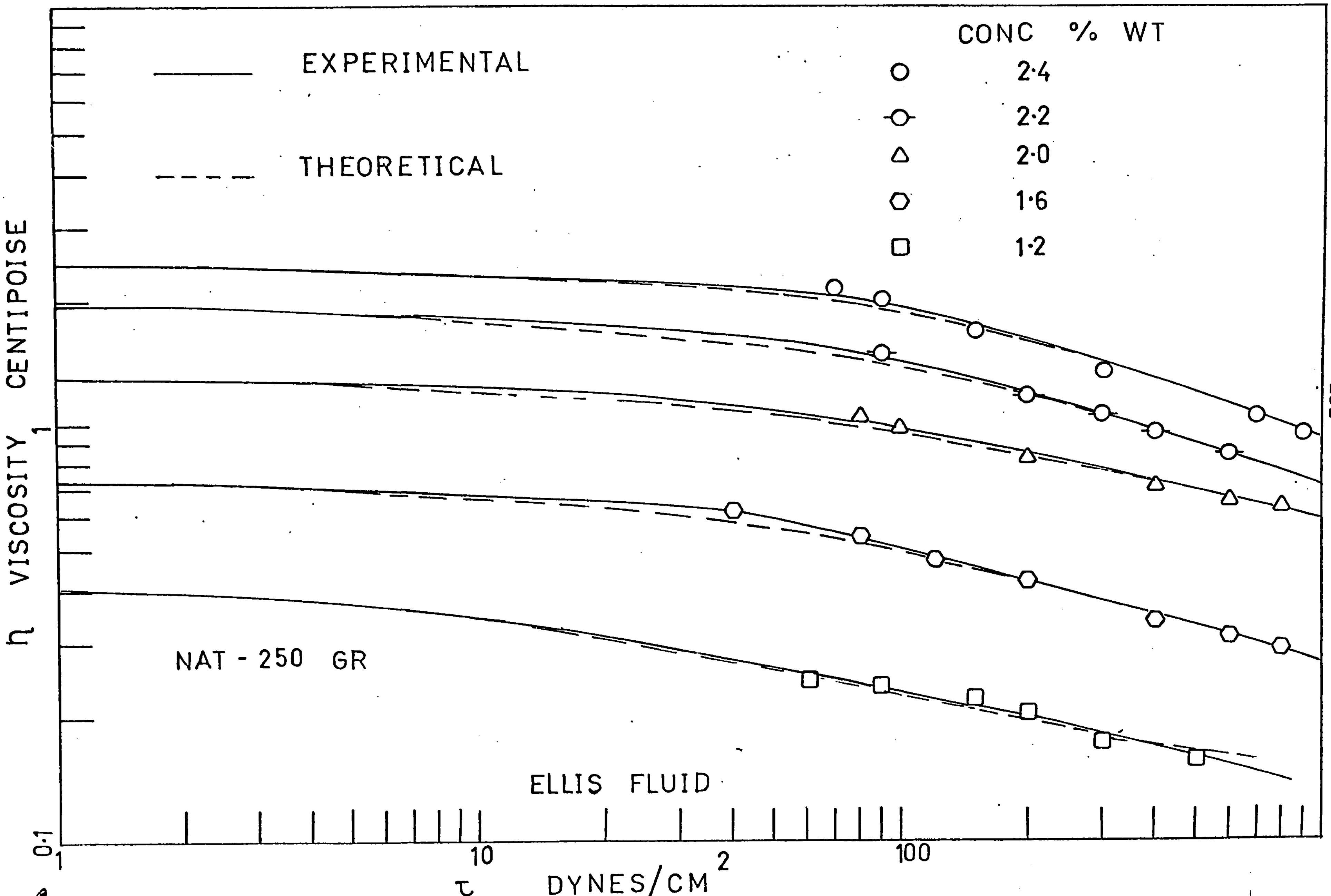

EXPERIMENTAL
THEORETICAL
CONC % WT
2·4
2·2
2·0
1·6
1·2
NAT - 250 GR
ELLIS FLUID
η VISCOSITY CENTIPOISE
0·1
1
10
100
τ DYNES/CM2

FIG 39

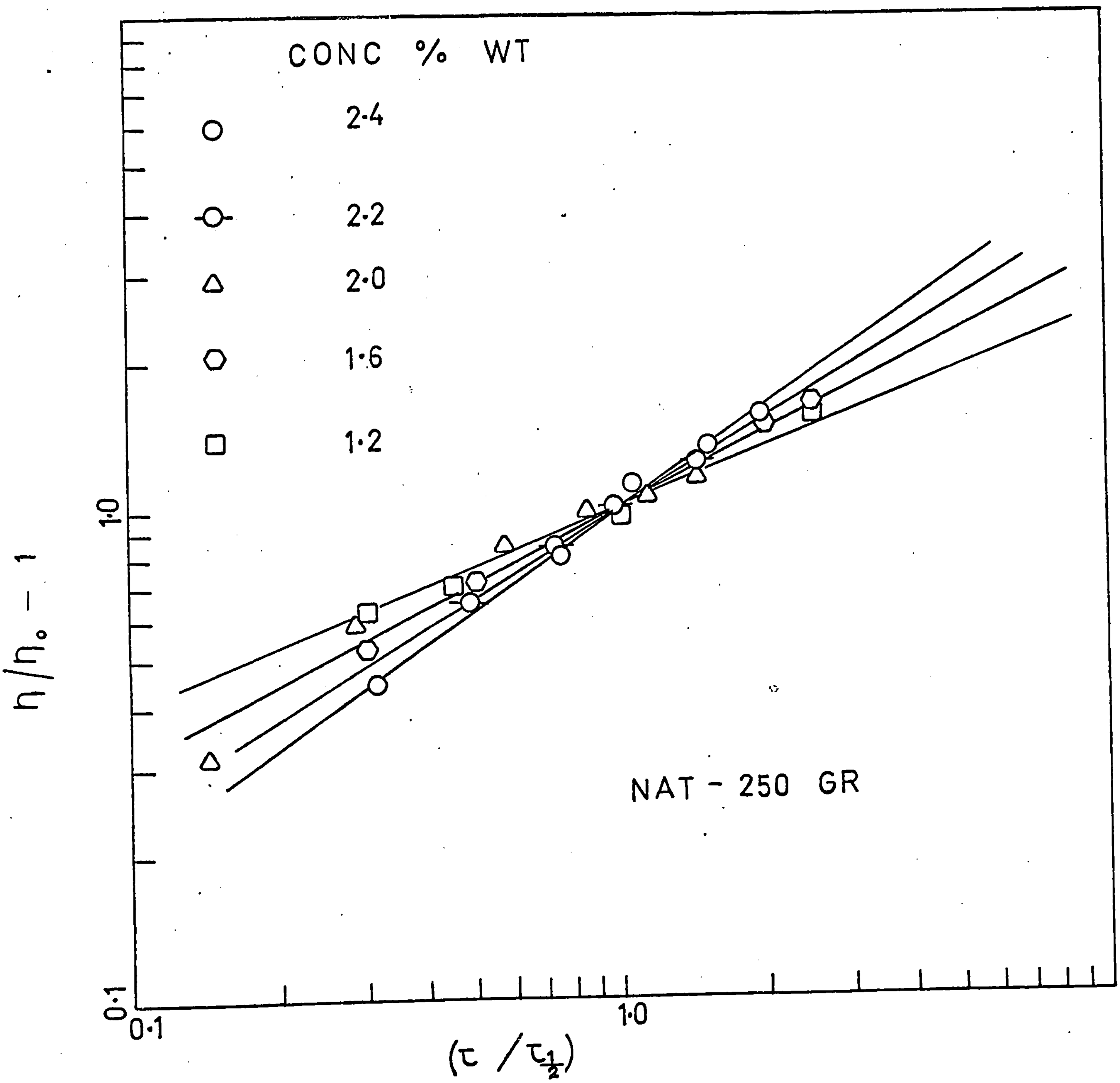

FIG 40

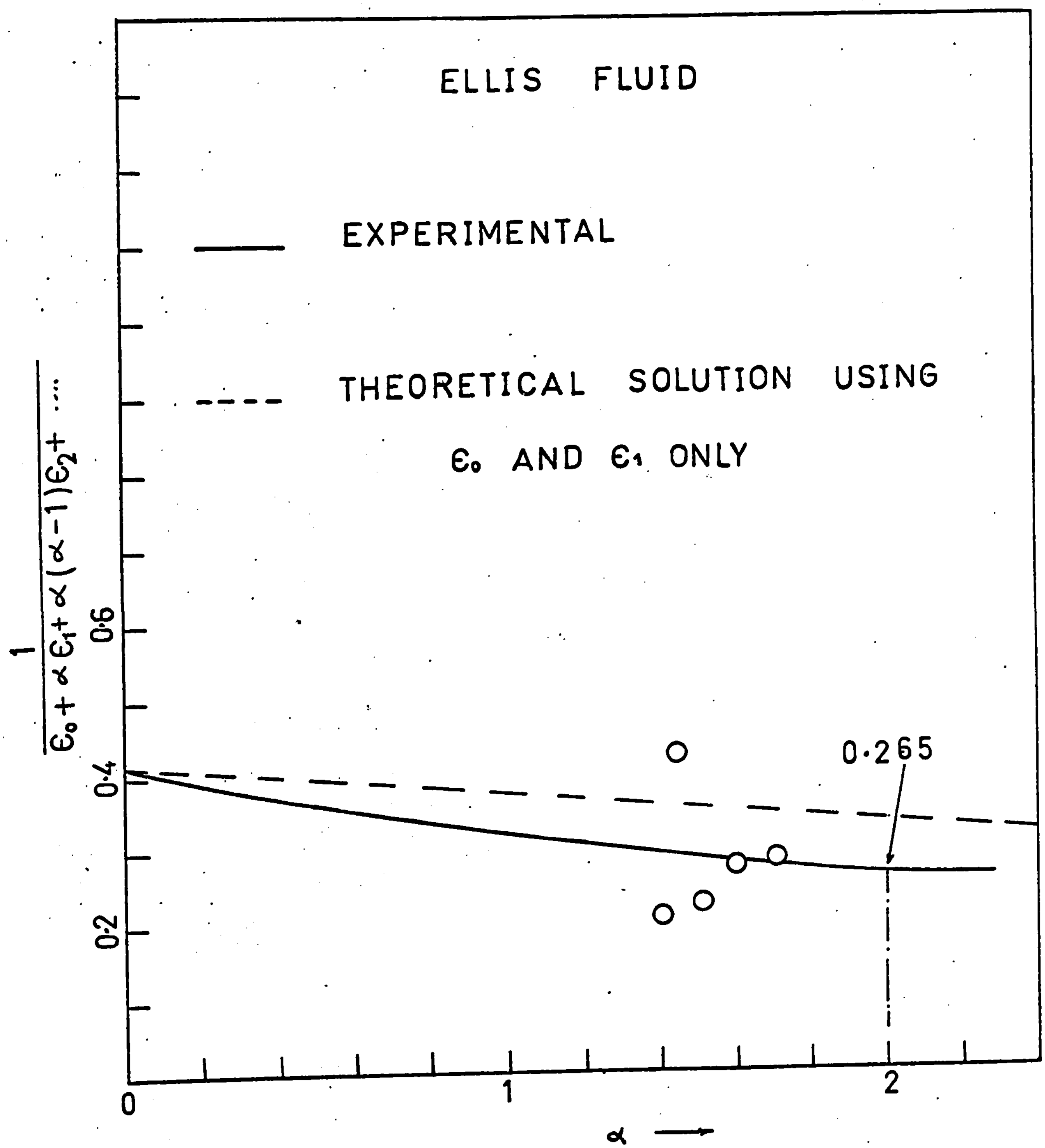
ELLIS FLUID
EXPERIMENTAL
THEORETICAL SOLUTION USING
ε₀ AND ε₁ ONLY
$\frac{1}{\epsilon_0+\alpha\epsilon_1+\alpha(\alpha-1)\epsilon_2+\cdots}$
0·6
0·4
0·2
0·265
0
1
2
α →

FIG 41

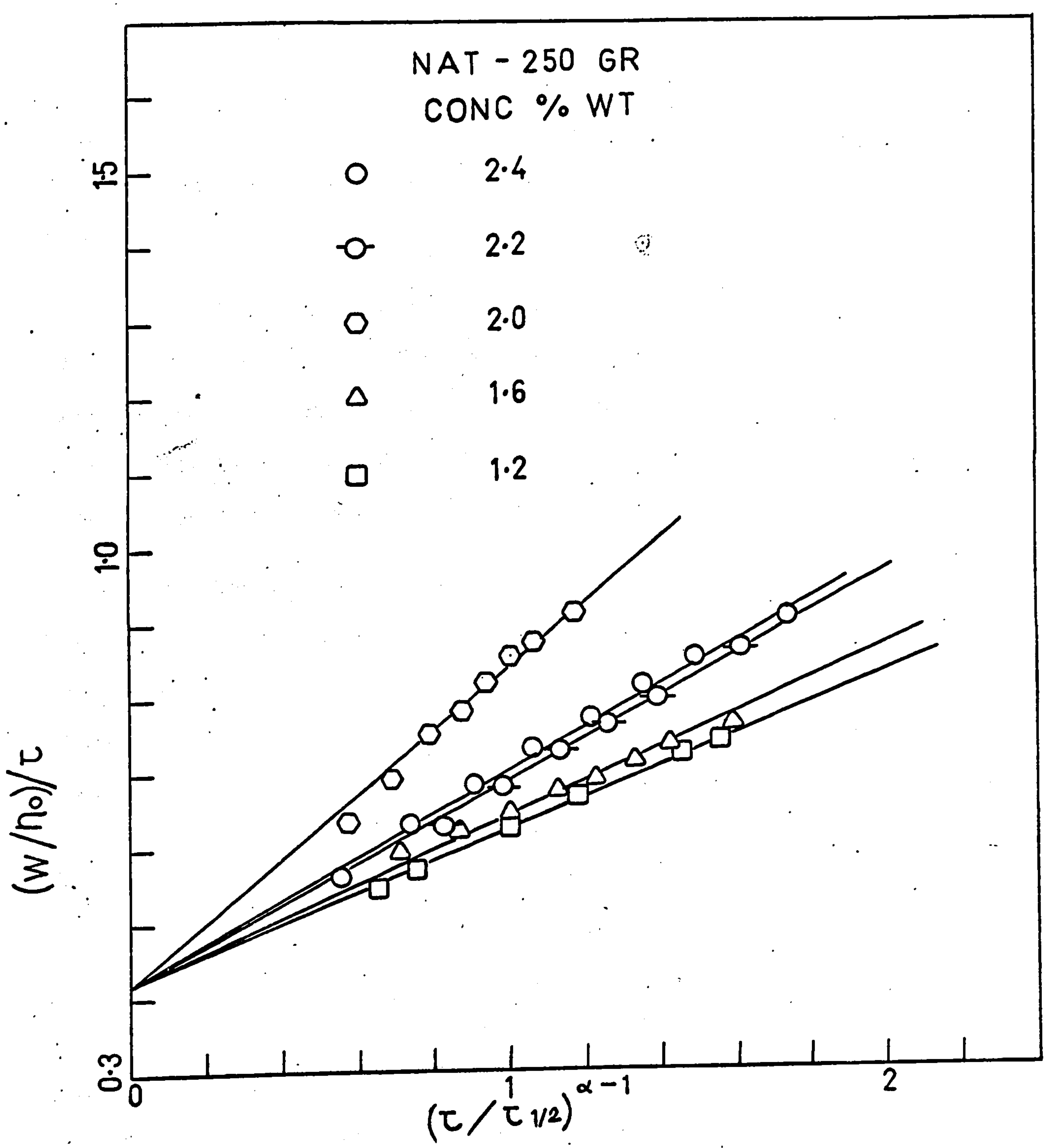

Chapter VII

Discussion:

The present work and analysis provide us significant information concerning the prediction of flow of any fluids through any channels whether it is open, closed or porous. It also provides deeper knowledge of Non-Newtonian fluids that exhibit anomalous surface behaviour.

Much effort has been devoted to present a method of predicting the flow of fluids accurately through an arbitrary flow geometry. However none has been as successful in presenting as general and accurate a method as that which is presently proposed.

Among the many researchers who explored the field of Non-Newtonian flow, are Fredrickson and Bird (6) who presented an analytical solution for the flow of Power-Law fluids through concentric annuli. Schechter (30) used the variational principle to obtain a solution for the flow of Power-Law fluids through rectangular ducts. Wheeler and Wissler (35) employed a numerical technique to solve the same problem. McEachern (23) obtained the solution for the flow of Ellis fluids through annular ducts, also Rotem presented the solution for the Rabinowitsch fluid through concentric annuli. Although there is so much literature, none is available to compare with the present results for the flow through packed beds. Fortunately, the analytical results calculated by Dr. Kozicki and Carlos Tiu (to be published in C. J. of Chem. Eng. Vol. 49, Oct. 1971) using the improved parametric equation for different fluids through concentric annuli and rectangular ducts were compared with the available literature and show excellent agreement.

The explanation of the surface effects behaviour of Natrosol-250GR solutions was based on Olroyd's theory. The theory proposed is applicable to any fluid model and to all possible polymer behaviours in low shear rate region as was evidenced by its successful use.

The present experimental work shows conclusively the anomalous surface effects exhibited by Non-Newtonian fluids. It is seen that for a particular capillary diameter a critical shear stress exists which indicates the transition from polymer adsorption to separation phenomenon. Many theories have been proposed to explain the polymer behaviour. Sadowski (28) and many others suggested that the polymer adsorption-gel formation on the tube wall is due to multiple points of attachment. Statistical mechanical approaches have been developed to explain the phenomenon theoretically. Lodge and Goodeve (37, 39) theories predict a lower Newtonian regime and suggest the network association of macromolecules predominating over the hydrodynamic effects of individual macromolecules Merrill (22) does not predict the first Newtonian regime instead he postulated a random coil model to explain the behaviour of macromolecules, non-electrolytic in solution, under low shear rates.

All these above effects could be accounted for by calculating the effective slip velocities. The present results obtained for different capillary tubes may be compared with those of Pasari (26). He evaluated the slip velocities at much higher shear rates, using smaller diameter tubes which are less than an order of 10 if compared to the present capillary tubes. The general trend of the present results agrees well with his, since a single curve is obtained after applying the correction of the effective slip velocities. There is a critical shear stress which marks the transition from polymer adsorption to separation phenomenon and the critical shear stress decreases when the tube diameter decreases. Greater wall effect is obtained for smaller tube diameters due to the proportionally larger amount of fluid under the influence of the wall. This effect was also observed by Pasari (26), Harper and Morrison (24). Jastrezebski (13) noticed that for concentrated suspensions the discrepancies between the flow curves are greater in the region of low shear rate than at high shear rates. This was evidenced in the present analysis. The presence of a critical tube diameter below which only polymer adsorption occurs, has also been observed. The results obtained for the packed bed datas are analogous since the porous media is pictured as a bundle of capillary tubes.

Chapter VIII

Summary and Conclusion:

An improved parametric equation of infinite order was proposed by Dr. Kozicki to predict Non-Newtonian flow in open and closed conduits of arbitrary cross-section and inelastic flow in packed beds and porous media, in replacement for the previous generalized Rabinowitsch-Mooney equation. The infinite order differential equation was solved by the perturbation technique. The solutions for the Ostwald-de-Waele fluid and the Ellis fluid have been presented, which have interesting and useful properties that allow one to obtain the geometric parameters easily.

The second geometric parameter ε_2 has been evaluated experimentally for both the Ostwald-de-Waele and the Ellis fluid model. The maximum deviation of ε_2 from one fluid to the other is less than 5%.

Anomalous surface effects exhibited by Nat-250GR solutions through both packed beds and capillary tubes have been examined. The theory developed which was based on Oldroyd's analysis was seen to be quite successful when applied experimentally. An additional information obtained was that the zero shear viscosity η_0 may be evaluated by the knowledge of the anomalous layer thickness δ max at zero shear stress, utilizing the relationship given earlier.

$$\eta o = \frac{\delta \max D}{\xi'''_o \tau_c} \qquad \text{............ (93)}$$

It may be concluded, from the present work, that the goal has been successfully achieved.

Chapter IX

Suggestions:

The present work may be extended further to investigate

(a) flow of viscoelastic fluids through packed beds or porous media.

(b) flow through different flow geometries such as rectangular ducts, triangular ducts etc.

(c) flow through flow geometries using different kinds of materials such as glass, plastics, wool etc.

NOMENCLATURE

a, b	previous geometric coefficients, dimensionless
D	diameter of the capillary tube, cm
Dp	sphere diameter, cm
f	fanning friction factor
K	fluid consistency index for Ostwald-de-Waele fluid, dynes-sec^n/cm^2
K'	$(8\langle u\rangle/D)^{-n'}$ fluid consistency index for circular conduits, dynes-sec$^{n'}$/cm^2
K*	function defined by equation (75)
k	aspect ratio, ratio of inner to outer radius of annulus
ki	impermeability factor
n	flow behaviour index for Ostwald-de-Waele fluid, dimensionless
n'	flow behaviour index for circular conduits, dimensionless
n*	generalized index, dimensionless
p	contour perimeter, cm
P	pressure dynes/cm^2
P'	P - αh, potential function, dynes/cm^2
rH	hydraulic radius, cm
R	radius of the outer tube of annulus
Re	Reynolds number

$s=\frac{1}{n}$	reciprocal of the flow behaviour index
S'	specific surface per unit volume of particle, cm^2/cm^3
T	tortuosity, dimensionless
u	local point velocity in axial direction, cm/sec
u_m	maximum velocity, cm/sec
u_w	slip velocity at the wall, cm/sec
u_w	average slip velocity at the wall, cm/sec
u	average velocity, cm/sec
u_s	superficial velocity, cm/sec
u_{ws}	superficial slip velocity, cm/sec
r,y	radial distance from the wall, cm
p* =	$R(-dP'/dx)/2\tau_{1/2}$, dimensionless pressure drop
Q* =	$Q\eta o/\tau_{1/2}''R^3$, dimensionless flow rate

<u>Greek</u>

α, ηo, $\tau_{1/2}$	fluid parameters in Ellis fluid model
γ	rate of deformation tensor, sec^{-1}
δ = δ (s,k)	function defined by Fredrickson and Bird ( )
δ	anomalous layer thickness, cm
εi	geometric parameters, = 0,1, 2...
ε	porosity, dimensionless
η	Non-Newtonian viscosity, $gm/sec/cm^2$
ηap	apparent viscosity
μ	Newtonian viscosity, $gm/sec/cm^2$

μs	solvent viscosity, gm sec/cm^2
$\xi = \frac{\varepsilon o}{\varepsilon_1}$	aspect factor, dimensionless
ξ'	Oldroyd's slip coefficient cm^4/dynes/sec
ξ''	New slip coefficient defined by equation (56)
ξ'''	modified slip coefficient defined by equation (57)
ξ'''_o	modified slip coefficient at zero shear stress
τ	stress tensor, dynes/cm^2
λc	stability parameter, dimensionless
$\tau^* = \tau/\tau_{1/2}$	dimensionless shear stress
τc	critical shear stress, dynes/cm^2
τw	shear stress at the wall, dynes/cm^2
$\tau_w = rH\left(\frac{-dP'}{dx}\right)$	average shear stress at the wall, dynes/cm^2
$w = \frac{2(\langle u\rangle - u_w)}{rH}$	sec^{-1}
$w^* = \frac{w\eta o}{\tau}$	dimensionless
ρ	density of solution
ρHg	density of Mercury

BIBLIOGRAPHY

1. Bird R.B., Can. J. Chem. Eng., 43, 161, 1965.

2. Breeche F., J. Chem. Phys., 22, 1570, 1954.

3. Chu J.C., Burridge K.G.S., Brown F. Chem. Eng. Sci., 3, 63, 229, 1954.

4. Christopher R.H., Jr., M.Sc. Thesis, Dept. of Chem. Eng., University of Rochester, 1965.

5. Christopher R.H., Jr., and Middleman S., I.E.C. Fundamentals, 4, 422, 1965.

6. Fredrickson, A.G., Bird, R.B., Ind. Eng. Chem., 50, 347 (1958).

7. Gaitonde N.Y., M.Sc. Thesis, Dept. of Chem. Eng., University of Rochester, 1966.

8. Gaitonde N.Y., and Middleman S., I.E.C. Fundamentals, 6, 1, 145, 1967.

9. Goodeve C.F., Trans. Faraday Soc., 35, 342, 1935.

10. Hsu, C.J., M.Sc. Thesis, University of Ottawa, 1965.

11. Hershey D., and Cho S.J., Preprint No. 7A, 58th. A.J. Ch. E. meeting Phil., Pa., Dec. 5-9, 1965.

12. Hassel H.L. and Bondi A., A.I.Ch.E. Jnl., 11, 23, 217, 1965.

13. Jastrezebski F.D., Ind. Eng. Chem. Fundls., 6, 445, 1967.

14. Kozicki W., Hsu C.J. and Tiu C., Chem. Eng. Sci., 22, 487, 1967.

15. Kozicki, W., Pasari S. N., Rao A.R.K. and Tiu C., Chem. Eng. Sci., 25, 41-52, 1970.

16. Kozicki W. and Tiu C., Can., Jnl. of Chem. Eng., 45, 127, 1967.

17. Kozicki W., Chou, C.H., Tiu C., Chem. Eng. Sci., 21, 665 (1966).

18. Mooney M., Jrnl. Rheology, 2, 20, 1931.

19. Marshal R.J. and Metzner A. B., I.E.C. Fundamentals, 6, 393, 1967.

20. McKinley R.M., Jahns H.O., Hams W.W. and Greenkom R.A., A. I. Ch. E. Jrnl., 12, 13, 17, 1966.

21. Metzner A.B., and Reed J.C., A. I. Ch. E. Jrnl., 1, 434, 1955.

22. Merrill E. W., Ind. S. Eng. Chem., 51, 868, 1959.

23. McEachern, D.W., A. I. Ch. E. J., 12, 328 (1966).

24. Morrison, S.R., and Harper J.C., I. S. E. C. Fundamentals, 4, 176, (1965).

25. Oldroyd J.G., Jrnl. Colloid Sci., 4, 333, 1949.

26. Pasari N.P. M. A. Sc. Thesis University of Ottawa 1969.

27. Rowland F.W. and Eirich F.R., Jrnl. Poly. Sci., part A1, 4, 2033, 1966.

28. Sadowski T.J., Ph. D. Thesis, University of Wisconsin 1963.

-Sadowski T.J. and Bird R.B., Trans. Soc. Rheol. 1965, 9.

-Sadowski T.J., ibid. 1965.

29. Scott - Blair G.W., Rheo. Acta, 1, 123, 1958.

30. Schechter, R.S., A. I. Ch. E. Jrnl., 7, 445 (1961).

31. Slattery J.C., A. I. Ch. E. Jrnl., 13, 63, 1066, 1967.

32. Savins J.G., Non-Newtonian Flow through Porous Media Mobil Research and Dev. Corp., Dallas, Texas.

33. Toms B.A., Jrnl. Colloid Sci., 4, 511, 1949.

34. Winding C.C., Bauman G.P., and Kranick W.L., Chem. Eng. Prog., 43, 11, 613, 1947.

35. Wheeler J.A., Wissler, E.H., A. I. Ch. E. Jrnl., 11, 207 (1965).

36. Foust, A.S., et al, "Principles of Unit operations", John Wiley and Sons, New York, 1960.

37. Lodge, A.S., Trans. Faraday Soc., 52, 120 (1956).

38. Goring, D. A., and Sitaramiah, G., Polymer, 4, 7, 1963.

39. Scheidegger, A. E., The Physics of Flow through Porous Media, Rev. Ed., MacMillan, New York.

APPENDIX A

SUMMARY OF PACKED BED RESULTS*

FOR NATROSOL - 250 GR AND HR SOLUTIONS

(* All measurements were taken at 25^{o}C)

TABLE 46

PACKED BEDS SPECIFICATIONS

Packed Bed No	I	II	III
Length, L, cm	30.73	25.78	16.915
Diameter D, cm	4.85	3.81	2.65
Diameter of Spheres Dp, cm	0.3175	0.2394	0.1592
H Height Between Pressure Taps	19.80	14.70	9.70
$\frac{L}{D}$ Ratio	6.33608	6.7664	6.3830
Density of Spheres	7.6195 gm/^{3}cm		

TABLE 47

Solutions: 0.8% (by wt) Natrosol-250GR

Data for Packed Bed I

ε : 0.3811

rH : 0.032585

H cm, Hg	Q cm³/sec	$\frac{2\langle u\rangle}{rH}$ sec^{-1}	τw dynes/cm²
1.66	12.6479	110.3145	33.7332
2.47	19.7528	172.2834	50.1934
5.40	42.6980	372.4108	109.7346
9.19	70.1172	611.5600	186.7521
13.64	102.1778	891.1922	277.1813
18.427	134.8315	1175.9597	374.4593
19.820	141.7602	1236.4283	402.7667
21.385	153.9622	1342.8540	434.5695

Packed Bed II

ε : 0.3807

rH : 0.0245286

H cm, Hg	Q cm³/sec	$\frac{2\langle u\rangle}{rH}$ sec^{-1}	τw dynes/cm²
2.690	10.1738	191.2164	55.4248
4.675	17.8017	334.5842	96.3238
7.470	29.7917	559.9357	153.9120
12.642	48.7738	916.7065	260.4864
17.930	67.2810	1264.5497	369.4301
23.390	85.6512	1609.8173	481.9281
29.825	106.6860	2005.1689	614.5150
32.080	115.3846	2168.6588	660.9771
36.660	127.1831	2390.1831	755.3435

TABLE 47

Packed Bed III

ε : 0.3808

rH : 0.01632

H cm, Hg	Q cm^3/sec	$\frac{2\langle u\rangle}{r_H}$ sec^{-1}	τ_w $dynes/cm^2$
1.815	2.0588	120.1677	37.7093
2.600	3.0414	177.5214	54.0188
3.490	4.0689	237.4934	72.5099
6.810	8.3427	486.9431	141.4879
10.750	13.6619	797.4048	223.3473
16.510	21.2544	1240.5592	343.0198
23.390	30.3770	1772.0227	485.9621
32.070	41.3288	2412.2472	666.3020
44.230	56.0896	3273.7944	918.9442
57.960	71.2257	4157.2422	1204.2054
69.210	83.2558	4859.4071	1437.9409

TABLE 48

Solution: 1.2% (by wt) Natrosol-250GR

Data for Packed Bed I

ε : 0.38108

rH : 0.03258216

H, cm Hg	Q cm^3/sec	$\frac{2\langle u\rangle}{r_H} sec^{-1}$	τw $dynes/cm^2$
2.700	7.5600	65.9476	54.8624
3.425	9.7957	85.4505	69.5940
6.148	19.0681	166.3352	124.9238
11.330	38.3468	334.5082	230.2190
17.580	63.3106	552.2724	357.2154
25.660	97.3958	849.6058	521.3963
36.640	141.8753	1237.6101	744.5035

Packed Bed II

ε : 0.3807

rH : 0.02453134

H cm, Hg	Q cm^3/sec	$\frac{2\langle u\rangle}{r_H} sec^{-1}$	τw $dynes/cm^2$
2.345	3.1297	58.8126	48.32
3.270	4.6841	88.0214	67.38
5.575	8.2735	155.4728	114.88
11.085	18.4739	347.1549	228.40
19.960	36.7498	690.5852	411.30
28.185	55.1431	1036.2297	580.79
37.600	76.5532	1438.5606	774.79
50.98	105.7034	1986.3415	1050.51
62.63	130.8273	2458.4612	1290.57

TABLE 48 (cont'd)

Packed Bed III

ε : 0.380865

rH : 0.016322

H cm, Hg	Q cm^3/sec	$\frac{2\langle u\rangle}{rH}$ sec^{-1}	τw dynes/cm^2
3.140	1.4225	83.0157	65.2429
4.560	2.1259	124.0731	94.7477
6.585	3.2234	188.1167	136.8232
12.610	6.8584	400.2586	262.0106
21.340	12.7839	746.0741	443.4026
30.885	19.7210	1150.9251	641.7287
42.300	28.8372	1682.9480	878.9096
53.500	37.7589	2203.6188	1111.6233
75.75	55.9517	3265.3554	1573.9339

TABLE 49

Solution: 1.6% (by wt) Natrosol-250GR

Data for Packed Bed I

ε : 0.38104

rH : 0.03247

H cm, Hg	Q cm^3/sec	$\frac{2\langle u\rangle}{rH} sec^{-1}$	τw $dynes/cm^2$
3.986	4.7131	41.1247	80.9792
4.470	5.5569	48.4875	90.8121
11.690	17.2095	150.1648	237.4929
17.910	29.2919	255.5919	363.8578
27.300	49.7832	434.3921	559.6241
35.090	69.3837	605.4192	712.8850
46.560	100.8571	880.0461	945.9084
47.060	100.8053	879.5938	956.0664
56.775	129.0909	1126.4046	1153.4353

Packed Bed II

ε : 0.3807

rH : 0.02453188

H cm, Hg	Q cm^3/sec	$\frac{2\langle u\rangle}{rH} sec^{-1}$	τw $dynes/cm^2$
4.280	2.4790	46.5838	88.1970
7.315	4.6634	87.6306	150.7386
11.185	7.9034	148.5134	230.4868
16.130	12.2326	229.8629	332.3870
24.360	20.7773	390.4250	501.9811
35.840	34.2214	643.0533	738.5469
52.760	56.2874	1057.6958	1087.2137

TABLE 49 (cont'd)

Packed Bed III

ε : 0.3809

rH : 0.01632725

H cm, Hg	Q cm^3/sec	$\frac{2\langle u\rangle}{rH}$ sec^{-1}	τw $dynes/cm^2$
6.44	1.4458	84.3375	133.8549
12.96	3.2753	191.0503	269.3361
20.50	5.7385	334.7332	426.0806
31.97	9.9289	579.1633	664.4779
45.54	15.8020	921.7514	946.3225
60.49	22.9389	1338.0567	1257.2496

TABLE 50

Solution: 2% (by wt) Natrosol 250GR

Packed Bed I

ε : 0.38105

rH : 0.03257819

H cm, Hg	Q cm^3/sec	$\frac{2<u>}{rH} sec^{-1}$	τw $dynes/cm^2$
8.80	5.806016	50.6048	178.7891
16.41	13.0575	113.9260	333.4010
27.03	25.5719	223.1133	549.1669
44.81	51.5351	449.6413	910.4022
63.50	84.0363	733.2127	1290.1259

Packed Bed II

ε : 0.38069

rH : 0.02452685

H cm, Hg	Q cm^3/sec	$\frac{2<u>}{rH} sec^{-1}$	τw $dynes/cm^2$
6.010	1.7647	33.1720	123.8213
10.005	3.3815	63.5638	206.1285
14.510	5.5501	104.4775	298.9430
20.615	8.7800	165.0402	424.7216
28.030	13.2948	249.9051	577.4890
36.740	19.1870	360.6630	756.9378
46.940	27.0852	509.1264	967.0838
62.740	40.8602	768.0581	1292.6042

TABLE 50 (cont'd)

Packed Bed III

ε : 0.38093

rH : 0.0163273

H cm, Hg	Q cm^3/sec	$\frac{2\langle u\rangle}{rH}$ sec^{-1}	τw dynes/cm^2
10.82	1.1584	67.5715	224.8881
19.30	2.4623	143.6302	401.1405
32.58	4.9838	290.7124	677.1585
44.29	7.6042	443.5614	920.5448
54.11	9.9785	582.0567	1124.6484
76.00	16.3895	956.0175	1579.6208

TABLE 51

Solution: 2.2% (by wt) Natrosol-250GR

Packed Bed I

ε : 0.3800

rH : 0.032568

H cm, Hg	Q cm^3/sec	$\frac{2\langle u\rangle}{rH}$ sec^{-1}	τw $dynes/cm^2$
8.85	3.78906	33.0719	179.7626
13.43	6.7201	58.6550	272.7923
18.78	10.6323	92.8015	381.4624
24.63	15.4994	135.2827	500.2885
34.61	24.6986	215.5764	703.0039
46.56	38.6169	337.0591	945.7342

Packed Bed II

ε : 0.3806

rH : 0.0245214

H cm, Hg	Q cm^3/sec	$\frac{2\langle u\rangle}{rH}$ sec^{-1}	τw $dynes/cm^2$
8.98	1.8042	33.9265	184.9700
14.28	3.4291	64.4803	294.1394
21.70	6.2100	116.7726	446.9766
35.29	12.4160	233.4703	726.9034
41.73	15.5630	292.7635	859.5545
48.78	19.6735	369.9394	1004.7704

TABLE 51 (cont'd)

Packed Bed III

ε : 0.380

rH : 0.01626236

H cm, Hg	Q cm^3/sec	$\frac{2\langle u\rangle}{rH} sec^{-1}$	τw $dynes/cm^2$
10.890	0.5874	34.4861	225.4429
18.395	1.2941	61.4917	380.8100
25.025	2.0580	120.8235	518.0631
30.510	2.7833	163.4045	631.6126
38.531	3.9841	233.8986	797.6619
47.225	5.4332	318.9785	977.6436

TABLE 52

Solution: 2.4% (by wt) Natrosol-250GR

Packed Bed I

ε : 0.3811

rH : 0.032585

H cm, Hg	Q cm^3/sec	$\frac{2\langle u \rangle}{rH} sec^{-1}$	τw dynes/cm^2
7.530	2.3573	20.5602	153.0199
11.680	4.2152	36.7648	237.3536
15.580	6.3398	55.2955	376.6069
26.195	12.7492	111.1965	532.3183
31.390	16.4912	143.8343	637.8878
40.100	23.3980	204.0748	814.8869
52.320	34.5709	301.5228	1063.2214

Packed Bed II

ε : 0.3806

rH : 0.0245216

H cm, Hg	Q cm^3/sec	$\frac{2\langle u \rangle}{rH} sec^{-1}$	τw dynes/cm^2
7.890	1.2451	23.4124	162.5195
12.690	2.2832	42.9325	261.3907
17.970	3.6822	69.2384	370.1491
27.675	6.5811	123.7486	570.0543
33.620	8.6237	162.1573	692.5104
41.720	12.1197	227.8952	859.3556
52.095	16.2963	306.4306	1073.0616

TABLE 52 (cont'd)

Packed Bed III

ε : 0.38119

rH : 0.01634487

H cm, Hg	Q cm^3/sec	$\frac{2<u>}{rH}$ sec^{-1}	τw $dynes/cm^2$
8.831	0.41477	24.15164	183.7453
9.227	0.43685	25.43755	191.9848
12.440	0.66576	38.76681	258.8372
16.205	0.95986	55.8920	337.1750
23.190	1.57487	91.70369	482.5109
28.456	2.14912	125.14199	592.0797
37.653	3.18760	185.61264	783.44036
47.210	4.48000	260.86743	982.2914

TABLE 53

Solution: 0.2% (by wt) Natrosol-250GR

Packed Bed I

ε : 0.3813

rH : 0.032615

H cm, Hg	Q cm^3/sec	$\frac{2\langle u\rangle}{rH}$ sec^{-1}	τw $dynes/cm^2$
1.54	19.8099	172.5183	31.3242
1.915	25.1990	219.4503	38.9518
2.610	34.3985	299.5658	53.0883
3.445	45.3277	394.7447	70.0726
4.320	57.1620	497.8067	87.8704
5.575	71.7660	624.9879	113.3975
7.450	90.7962	790.7161	151.5357
9.325	108.0477	940.9537	189.6739
12.790	138.8861	1209.5158	260.1533

Packed Bed II

: 0.3807

rH : 0.024534

H cm, Hg	Q cm^3/sec	$\frac{2\langle u\rangle}{rH}$ sec^{-1}	τw $dynes/cm^2$
1.110	7.2240	135.5593	22.8755
1.805	11.9243	223.7612	37.1986
2.755	18.1390	340.3814	56.7768
3.330	22.0509	413.7876	68.6268
4.660	30.5359	573.0097	96.0363
5.375	34.9321	655.5056	110.7715
7.195	46.0319	863.7947	148.2792
9.405	58.1989	1092.1087	193.8243
12.150	72.2018	1354.8751	250.3850
13.655	78.9957	1482.3639	281.4110

TABLE 53 (cont'd)

Packed Bed III

ε : 0.38325

rH : 0.016488

H cm, Hg	Q cm^3/sec	$\frac{2\langle u\rangle}{rH}$ sec^{-1}	τw dynes/cm^2
2.363	5.5830	320.5356	49.5978
2.830	6.7552	387.8341	59.3999
3.540	8.3622	480.0935	74.3623
5.491	10.1335	581.7881	115.2526
7.073	14.3623	824.5773	148.4577
11.858	25.2688	1450.7449	248.8918
12.790	26.9726	1548.5627	268.4539
15.810	32.7286	1879.0309	331.8418
19.585	39.9472	2293.4677	411.0766
23.0425	46.3929	2663.5353	483.6473

TABLE 54

Solution: 0.3% (by wt) Natrosol-250GR

Packed Bed I

ε : 0.38127

rH : 0.0325909

H cm, Hg	Q cm^3/sec	$\frac{2\langle u\rangle}{rH} sec^{-1}$	τw dynes/cm^2
0.755	3.4341	29.9333	15.3453
2.400	14.1872	123.6642	48.7798
3.080	17.9557	156.5126	62.6008
4.100	26.3835	229.9733	83.3322
5.180	34.1159	297.3735	105.2831
7.940	56.3656	491.3098	161.3799
10.955	79.9359	696.7669	222.6596
17.100	124.7494	1087.3874	347.5562
22.020	155.0210	1351.2516	447.5548

Packed Bed II

ε : 0.38071

rH : 0.0245286

H cm, Hg	Q cm^3/ sec	$\frac{2\langle u\rangle}{rH} sec^{-1}$	τw dynes/cm^2
1.07	2.7668	52.0015	22.0403
4.65	15.6143	293.4714	95.8088
6.27	22.0589	414.5968	129.1873
8.09	30.0335	564.4814	166.6867
10.40	39.5209	742.7975	214.2820
13.08	49.8933	937.7463	269.5008
15.62	59.6617	1121.3433	321.8351
19.44	75.0444	1410.4613	406.5425
22.43	85.6757	1610.2762	462.1486
26.70	100.0776	1880.9604	550.1279

TABLE 54 (cont'd)

Packed Bed III

ε : 0.3815

rH : 0.0163665

H cm, Hg	Q cm^3/sec	$\frac{2\langle u\rangle}{rH}$ sec^{-1}	τw dynes/cm^2
1.79	1.6064	93.3280	37.2937
2.80	2.7278	158.4836	58.3364
4.70	5.0917	295.8192	97.9219
7.29	8.7406	507.8167	151.8831
10.99	14.2847	829.9213	228.9706
15.39	21.0488	1222.9107	320.6422
20.24	28.2496	1641.2646	421.6892
25.38	35.1643	2043.0026	528.7783
30.655	42.5466	2471.5529	638.6800
37.20	50.4417	2936.5967	775.0415
44.58	59.6000	3466.5559	928.7997
49.31	64.6583	3756.5647	1027.0000

TABLE 55

Solution: 0.4% (by Wt) Natrosol-250GR

Packed Bed I

ε : 0.3813

rH : 0.0326107

H cm, Hg	Q cm^3/sec	$\frac{2\langle u\rangle}{rH}$ sec^{-1}	τw dynes/cm^2
1.54	3.4288	29.8679	31.3193
3.86	11.4409	99.6607	78.5017
5.24	17.3153	150.4868	106.5671
6.87	25.0548	218.2499	139.7167
8.95	36.1440	314.8471	182.0182
12.022	54.0936	471.2038	244.4942
13.955	65.0519	566.6608	283.806
15.93	77.3109	673.4479	323.9721
20.305	103.1977	898.9453	412.9475

Packed Bed II

ε : 0.3807

rH : 0.0245278

H cm, Hg	Q cm^3/ sec	$\frac{2\langle u\rangle}{rH}$ sec^{-1}	τw dynes/cm^2
2.39	3.0873	58.0292	49.2421
3.00	4.0622	76.3532	61.8101
3.55	5.0091	94.1502	73.1420
4.50	6.9042	129.7707	92.7152
5.88	9.8387	184.9294	121.1479
8.50	16.2758	305.9210	175.1288
10.575	21.7471	408.7590	217.8808
13.90	31.48.3	591.7218	286.3871
16.55	39.9571	751.0331	340.9860
21.57	55.3000	1039.4185	444.4150

TABLE 55 (cont'd)

Packed Bed III

ε : 0.3813

rH : 0.01641

H cm, Hg	Q cm^3/sec	$\frac{2\langle u\rangle}{rH}$ sec^{-1}	τw dynes/cm^2
5.130	3.3695	194.9407	107.1673
2.600	1.3664	79.0512	54.3148
2.010	0.9561	55.3159	41.9895
4.975	3.0200	174.7172	103.9293
6.000	3.7982	219.7412	125.3418
8.210	5.7408	332.1277	171.5094
9.775	7.2831	421.3521	204.2027
12.465	10.3292	597.5815	260.3977
17.005	15.4592	894.3659	355.2397
21.830	22.0280	1274.39663	436.0354

TABLE 56

Solution: 0.5% (by wt) Natrosol-250GR

Packed Bed I

ε : 0.3813

rH : 0.032607

H cm, Hg	Q cm^3/sec	$\frac{2\langle u\rangle}{rH}$ sec^{-1}	τw dynes/cm^2
4.64	7.25598	63.2161	94.3553
5.83	10.3837	90.4659	118.5542
8.14	16.4919	143.6818	165.5285
10.09	23.3974	203.8942	205.1822
13.665	36.4087	317.2023	277.8805
16.550	49.9226	434.9395	336.5476
19.860	66.1592	576.3536	403.8571
27.955	105.8366	922.0774	568.4706
34.87	138.9392	1210.4765	709.0885

Packed Bed II

ε : 0.3811

rH : 0.024577

H cm, Hg	Q cm^3/sec	$\frac{2\langle u\rangle}{rH}$ sec^{-1}	τw dynes/cm^2
3.98	3.3731	63.3237	82.1655
6.22	6.2896	117.8381	128.4095
8.29	9.3881	175.8879	171.1438
11.36	14.8939	279.0910	234.5228
15.62	23.7918	445.7456	322.4688
19.09	32.1128	601.6422	394.1056
21.93	39.4849	739.7610	452.7363
25.565	48.5168	908.9755	527.7795
30.240	61.3273	1148.9824	624.2930
33.60	69.6894	1305.6481	693.6589
36.46	76.1912	1427.4619	752.7026

TABLE 56 (cont'd)

Packed Bed III

ε : 0.3821

rH : 0.016409

H cm, Hg	Q cm^3/sec	$\frac{2\langle u\rangle}{rH}$ sec^{-1}	τw dynes/cm^2
5.660	1.6597	96.03083	118.2298
10.775	4.2445	245.5914	225.0752
14.300	6.53303	378.0058	298.7077
17.680	8.9509	517.9104	369.3114
21.070	11.5884	670.5135	440.1239
24.450	14.4233	834.5463	510.7276
27.520	17.2875	1000.2700	574.8557
31.565	20.8743	1207.8059	659.3503
36.260	25.0968	1452.1209	757.4225
44.105	32.5838	1885.3211	921.2940
50.950	39.3660	2277.7464	1064.2769

TABLE 57

Solution: 0.6% (by wt) Natrosol-250GR

Packed Bed I

ε : 0.38126

rH : 0.032607

H cm, Hg	Q cm^3/sec	$\frac{2\langle u\rangle}{rH}$ sec^{-1}	τw dynes/cm^2
3.98	2.6879	23.4184	80.9158
4.72	3.3363	29.0675	95.9605
6.47	5.4470	47.4568	131.5390
8.44	8.4087	73.2598	171.5903
10.97	12.7234	110.8508	223.0268
16.86	26.8049	233.5341	342.7741
22.065	42.4481	369.8240	440.5949
28.645	67.1842	585.1808	582.3703
37.58	103.4501	901.2969	764.0243
46.27	138.3290	1205.1753	940.6973

TABLE 57 (cont'd)

Solution: 0.6% (by wt) Natrosol-250GR

Packed Bed II

ε : 0.38059

rH : 0.024517

H cm, Hg	Q cm^3/sec	$\frac{2\langle u\rangle}{rH} sec^{-1}$	τw $dynes/cm^2$
5.86	2.6550	49.9603	120.6557
8.30	4.5856	86.2541	170.8946
10.73	6.8750	129.3159	220.9276
14.185	11.0740	208.2980	292.0650
17.27	15.4232	290.1045	355.5843
21.04	21.1136	397.1397	433.2075
25.005	28.6640	539.1587	514.8457
30.420	39.8087	748.7851	626.3389
34.820	49.6554	933.9984	716.9337
42.075	65.9758	1240.9784	866.3120
46.680	75.9090	1427.8121	961.1276

TABLE 57 (cont'd)

Packed Bed II

ε : 0.3815

rH : 0.0163718

H cm, Hg	Q cm^3/sec	$\frac{2\langle u\rangle}{rH} sec^{-1}$	τw $dynes/cm^2$
7.83	1.2457	72.3374	163.1508
11.25	2.2902	132.9995	234.4120
13.40	3.0288	175.8982	279.2108
18.97	5.4585	316.9987	395.2708
22.71	7.2852	423.0810	473.1998
27.415	9.9371	577.0874	571.2362
33.590	14.2427	827.1340	699.9023
40.100	19.0258	1104.9122	835.8696
46.780	23.9134	1388.7550	974.7375
58.965	33.8241	1955.7553	1228.6318

TABLE 58

Solution: 0.7% (by wt) Natrosol-250GR

Packed Bed I

ε : 0.3806

rH : 0.03252

H cm, Hg	Q cm^3/sec	$\frac{2\langle u \rangle}{rH}$ sec^{-1}	τw dynes/cm^2
6.80	2.8836	25.2280	137.9237
8.07	3.8077	33.3120	163.6829
8.98	4.4952	39.3269	182.1404
11.565	7.0345	61.5426	234.5717
14.540	10.5365	92.1806	294.9133
18.440	16.3359	142.9178	374.0167
23.195	25.4605	222.7453	470.4618
31.185	44.9335	393.1025	632.5222
41.430	77.5000	673.6477	840.3205

Packed Bed II

ε : 0.3807

rH : 0.02453066

H cm, Hg	Q cm^3/sec	$\frac{2\langle u \rangle}{rH}$ sec^{-1}	τw dynes/cm^2
5.52	1.1117	20.8926	113.7438
8.52	2.1875	41.1084	175.5610
11.09	3.4755	65.3139	228.5178
15.87	6.7139	126.1704	327.0133
13.05	4.6875	88.0898	268.9051
18.65	8.8572	166.4483	384.2973
22.40	12.6416	237.5679	461.5685
28.55	20.1131	377.9751	588.2943
38.630	35.8745	674.1708	796.0003
48.98	54.4545	1023.3366	1009.2698

TABLE 58 (cont'd)

Packed Bed III

ε : 0.3815

rH : 0.01637

H cm, Hg	Q cm^3/sec	$\frac{2\langle u\rangle}{rH}$ sec^{-1}	τw $dynes/cm^2$
9.355	1.6618	96.5268	194.9517
12.940	1.4838	86.187	269.6607
16.925	2.4127	140.1393	352.7053
18.860	2.9310	170.2411	393.030
26.300	5.5285	321.1100	548.0739
34.580	9.2183	535.4225	720.6234
39.875	11.9363	693.2923	830.9675
45.170	15.1565	880.3299	941.3117
61.65	25.9397	1506.6447	1284.7436

APPENDIX B

SUMMARY OF VISCOMETRIC RESULTS *

FOR NATROSOL - 250GR AND HR SOLUTIONS

(*All measurements were taken at 25^{o}C)

TABLE 59

CAPILLARY TUBE SPECIFICATIONS

CAPILLARY	LENGTH IN: CM	CALI. DIAM.D, IN: CM	L/D
1	79.80	0.24546	325.10388
2	80.74	0.19553	412.9289
3	83.95	0.1290	677.0161
6	81.90	0.2250	364.000
7	83.88	0.16820	498.692
8	84.25	0.1478	570.027
9	84.6	0.1014	834.3195
10	84.6	0.0890	950.5617

TABLE 60

Solution: 0.8% (by wt) Natrosol-250GR

Density of Solution: 1.001706 gm/cm³ at 25°C

DATA FOR CAPILLARY 3

H cm, Hg	Q cm^3/sec	$\frac{8\langle u \rangle}{D}$ sec^{-1}	τw $dynes/cm^2$
1.84	0.06479	345.9942	40.8591
6.07	0.10363	553.4092	61.6729
10.22	0.14581	778.6605	82.0816
14.18	0.18405	982.8713	101.5485
21.27	0.26432	1411.5325	136.3641
26.07	0.31915	1704.3379	159.9129
30.10	0.35874	1915.7580	179.6843
35.87	0.42918	2291.9246	207.9436
40.87	0.49917	2665.6880	232.3838

DATA FOR CAPILLARY 7

H cm, Hg	Q cm^3/sec	$\frac{8\langle u \rangle}{D}$ sec^{-1}	τw $dynes/cm^2$
1.48	0.21544	460.9715	53.4389
6.05	0.32787	701.5352	77.2611
9.20	0.47619	1018.8917	104.8987
14.40	0.6768	1445.7355	139.4373
19.88	0.88757	1899.1111	175.7343
25.79	1.15016	2460.9684	214.6767
34.03	1.48410	3175.4914	268.8197
39.13	1.6800	3597.9200	301.2604

TABLE 60 (cont'd)

DATA FOR CAPILLARY 9 — Ho = 5.48cm

H cm, Hg	Q cm^3/sec	$\frac{8\langle u\rangle}{D}$ sec^{-1}	τw $dynes/cm^2$
0.870	0.02726	266.228085	29.9917
3.080	0.035955	351.1327	38.8175
5.640	0.04561	445.4225	49.0442
10.230	0.066335	647.8207	67.3756
16.720	0.09604	937.9166	93.2873
23.420	0.130081	1270.3575	120.0234
30.120	0.15957	1558.3439	146.7551
38.260	0.19640	1918.0219	175.2218
47.640	0.25641	2504.07334	216.5642

DATA FOR CAPILLARY 10 — Ho = 2.020 cm

H cm, Hg	Q cm^3/sec	$\frac{8\langle u\rangle}{D}$ sec^{-1}	τw $dynes/cm^2$
2.23	0.019299	277.5440	30.2151
6.400	0.030511	439.9265	44.8461
10.090	0.039683	572.1741	57.7918
13.980	0.05022	724.1031	71.4371
16.90	0.05596	806.8660	81.6806
26.53	0.08531	1230.0525	115.4469
39.87	0.12076	1827.70435	162.1987
48.65	0.15544	2241.2304	192.95188

TABLE 61

Solution: 1.2% (by wt) Natrosol-250GR

Density of Solution: 1.00280 gm/cm^3 at 25^{o}C

DATA FOR CAPILLARY 2 — Ho = 5.970 cm

H cm, Hg	Q cm^3/sec	$\frac{8\langle u\rangle}{D}$ sec^{-1}	τw dynes/cm^2
1.85	0.16304	222.0646	66.5953
5.16	0.25316	344.8104	93.3073
10.45	0.39301	535.2896	135.9753
15.24	0.53691	731.2851	174.5711
20.57	0.63559	865.6898	209.4644
24.45	0.8547	1164.1232	248.6418
29.63	1.03090	1404.1121	290.2386
34.32	1.23711	1684.9753	327.7747
38.87	1.34185	1827.6339	364.3287
46.05	1.7500	2383.5446	421.3813

DATA FOR CAPILLARY 6 — Ho = 5.085 cm

H cm, Hg	Q cm^3/sec	$\frac{8\langle u\rangle}{D}$ sec^{-1}	τw dynes/cm^2
1.77	0.27273	243.7872	74.9762
6.09	0.45889	410.1915	114.4811
10.03	0.65359	584.2295	150.4661
14.35	0.87591	782.9563	189.8716
18.25	1.03448	924.6985	216.2879
22.05	1.32353	1183.0738	259.9236
23.45	1.40288	1254.0030	272.6421
28.69	1.70455	1523.6591	311.0234

TABLE 61 (cont'd)

DATA FOR CAPILLARY 7 Ho = 4.520 cm

H cm, Hg	Q cm^3/sec	$\frac{8\langle u\rangle}{D}$ sec^{-1}	τ_w $dynes/cm^2$
2.220	0.08772	187.69227	58.4667
5.410	0.12739	272.5732	79.8057
10.280	0.18692	399.9480	105.6839
13.370	0.24540	525.0762	133.0269
17.270	0.30822	659.4906	159.0875
20.850	0.36530	781.6232	183.0024
26.370	0.44860	959.8581	213.1746
30.140	0.54645	1169.2253	244.9862

DATA FOR CAPILLARY 8 Ho = 3.600 cm

H cm, Hg	Q cm^3/sec	$\frac{8\langle u\rangle}{D}$ sec^{-1}	τ_w $dynes/cm^2$
2.430	0.052724	166.2688	52.1297
7.210	0.084151	265.3760	80.0821
11.030	0.11917	375.8109	102.4145
17.77	0.17266	544.4953	141.8127
24.00	0.23747	748.8781	178.2094
28.39	0.28436	896.7989	203.8468
34.97	0.35191	1109.7726	242.2633
39.61	0.41150	1297.6938	269.3279
46.37	0.48232	1521.0296	302.9139

TABLE 62

Solution: 1.6% (by wt) Natrosol-250GR

Density of Solution: 1.004078 gm/cm^3 at 25^{o}C

DATA FOR CAPILLARY 1 Ho = 1.88 cm

H cm, Hg	Q cm^3/ sec	$\frac{8 \langle u \rangle}{D}$ sec^{-1}	τw dynes/cm^2
0	0.12652	87.0995	61.8420
1.85	0.16735	115.2148	80.8118
3.88	0.23292	160.3480	101.6218
6.33	0.31390	216.0966	126.7325
9.23	0.41612	286.4670	156.4465
11.72	0.49813	342.9250	181.9555
15.09	0.62241	428.4820	216.4650
18.0	0.74377	512.0300	246.2460
21.14	0.89552	616.4980	278.3550
23.62	1.01078	695.8460	303.7057
27.20	1.18624	816.6370	340.2740
29.06	1.25918	866.8500	359.2810
33.55	1.49254	1027.5020	405.0840
37.59	1.71149	1178.2329	446.2480

TABLE 62 (cont'd)

DATA FOR CAPILLARY 2 — Ho = 2.88 cm

H cm, Hg	Q cm^3/sec	$\frac{8\langle u\rangle}{D}$ sec^{-1}	τ_w dynes/cm^2
.0	0.04819	65.6360	49.8488
1.89	0.06615	90.0979	65.1159
4.95	0.10169	138.5043	89.8320
7.90	0.13825	188.3000	113.6570
10.63	0.17254	235.0038	135.7040
13.49	0.21254	289.4840	158.7970
15.64	0.23885	325.3197	176.1577
18.08	0.28257	384.8670	195.8520
20.92	0.32720	445.6547	218.7753
24.45	0.38647	526.3819	247.2610
26.62	0.42520	579.1332	264.7680
30.80	0.50042	681.5847	298.4840
33.60	0.54545	742.9160	321.0689
36.55	0.59721	813.4150	344.8560
40.54	0.68755	936.4606	377.0026

TABLE 62 (cont'd)

DATA FOR CAPILLARY 6 Ho = 2.69 cm

H cm, Hg	Q cm^3/ sec	$\frac{8\langle u\rangle}{D}$ sec^{-1}	τw dynes/cm^2
0.00	0.09063	81.0121	57.2025
1.49	0.11285	100.8740	70.8487
3.75	0.15686	140.2136	91.5447
6.21	0.20888	186.7130	114.06916
9.50	0.28470	254.4860	144.1870
12.94	0.37037	331.0650	175.6706
14.72	0.41344	369.5640	191.9590
16.65	0.41537	371.2890	209.6370
20.88	0.58442	522.3990	248.3010
24.35	0.68441	611.7787	280.0250
27.44	0.79734	712.7240	308.2480
30.95	0.91954	821.9560	340.2970
34.42	1.03520	925.3420	371.9720
37.45	1.15207	1029.8090	399.6026

TABLE 62 (cont'd)

DATA FOR CAPILLARY 7 Ho = 2.32 cm.

H cm, Hg	Q cm^3/sec	$\frac{8\langle u\rangle}{D}$ sec^{1}	τw $dynes/cm^2$
2.78	0.03630	77.6702	61.1547
4.90	0.05440	116.3983	75.3407
8.48	0.06700	143.3580	49.2977
10.85	0.08287	177.3148	115.1560
13.48	0.09615	205.7297	132.7540
16.50	0.11650	249.2721	152.9600
20.26	0.014229	304.4540	178.1160
23.85	0.17167	367.3179	202.1310
25.70	0.18519	396.2460	235.9107
28.9	0.21112	451.7280	262.9960
32.95	0.24540	525.0760	293.4227
37.50	0.28601	611.9680	293.4227

TABLE 63 (cont'd)

DATA FOR CAPILLARY 2

H cm, Hg	Q cm^3/sec	$\frac{8\langle u\rangle}{D}$ sec^{-1}	τw dynes/cm^2
2.99	0.03264	44.4565	73.7358
5.19	0.04357	59.3434	91.5082
8.39	0.05938	80.8770	117.3587
11.30	0.07403	100.8307	140.8662
13.51	0.09195	125.2382	158.7177
15.96	0.10702	145.7639	178.5082
19.31	0.13100	178.4253	205.5674
22.10	0.14652	199.9726	228.1035
24.32	0.16371	222.9772	246.0342
27.10	0.18957	258.1992	268.4859
30.62	0.22075	300.6671	296.9131
34.27	0.24896	339.0898	326.3902
37.45	0.27815	378.8479	352.0687

TABLE 63 (cont'd)

DATA FOR CAPILLARY 6 $\qquad$ Ho = 2.05 cm

H cm, Hg	Q cm^3/sec	$\frac{8\langle u\rangle}{D}$ sec^{-1}	τw dynes/cm^2
2.65	0.05772	51.5946	81.2441
4.55	0.08125	72.6275	98.6466
7.19	0.09938	88.8335	122.8276
9.18	0.11984	107.1223	141.0539
11.92	0.14901	133.1967	166.1486
14.39	0.18161	162.3371	188.7686
16.51	0.20053	179.2493	208.1844
19.64	0.24732	221.0738	236.8451
21.89	0.28070	250.9114	257.4466
24.71	0.31623	283.1179	283.2674
27.70	0.36810	329.0363	310.6387
30.30	0.40107	358.5075	334.4425
34.55	0.47198	421.8924	373.3424

TABLE 63 (cont'd)

DATA FOR CAPILLARY 7 Ho = 2.10 cm

H cm, Hg	Q cm^3/sec	$\frac{8\langle u\rangle}{D}$ sec^{-1}	τw dynes/cm^2
4.01	0.01756	37.5727	69.4268
6.81	0.02538	54.3049	88.1651
9.80	0.03393	72.5992	108.1748
12.78	0.04292	91.8398	128.1173
15.75	0.05291	113.2102	147.9926
19.20	0.06380	136.5112	171.0799
21.95	0.07394	158.2075	189.4824
25.11	0.08658	185.2530	210.6280
27.75	0.09585	205.0878	228.2940
30.12	0.10204	218.3324	244.1535
34.25	0.1200	256.7609	271.7886

B-11 (A)

TABLE 64

Solution: 2.2% (by wt) Natrosol-250GR

Density of solution: 1.005602 gm/cm³ at 25°C

DATA FOR CAPILLARY 1 Ho = 2.99 cm

H cm, Hg	Q cm³/sec	$\frac{8\langle u\rangle}{D}$ sec⁻¹	τw dynes/cm²
0.0	0.04036	27.81409	62.70197
2.1	0.05874	40.47547	84.21924
4.2	0.079760	54.96264	105.73650
6.41	0.104621	72.09353	128.38196
11.10	0.15789	108.80423	176.43799
13.65	0.197530	136.11723	202.56602
16.55	0.23753	163.68108	232.28066
19.45	0.280114	193.02489	261.99590
22.47	0.342859	236.26255	292.93975
26.60	0.42553	293.23397	335.25805
28.55	0.44499	306.6428	358.84706

TABLE 64 (cont'd)

DATA FOR CAPILLARY 2 Ho = 2.61 cm

H cm, Hg	Q cm^3/sec	$\frac{8\langle u\rangle}{D}$ sec^{-1}	τw $dynes/cm^2$
3.05	0.02572	35.06792	74.33875
5.35	0.03636	49.57325	92.90044
7.35	0.04362	59.46635	109.03910
9.35	0.05194	70.81941	125.17729
12.62	0.06890	93.93742	151.56376
14.89	0.07714	105.16997	169.88066
18.35	0.09662	131.71714	197.80008
21.15	0.11157	152.10791	220.39393
24.37	0.130086	178.39906	246.37656
27.05	0.14563	198.53489	268.00177
29.30	0.16194	220.177198	286.15770
33.50	0.18801	256.31330	320.04799
37.50	0.21739	296.36404	352.32484
43.30	0.26316	358.75382	399.12596

TABLE 64 (cont'd)

DATA FOR CAPILLARY 6 Ho = 2.45 cm

H cm, Hg	Q cm^3/sec	$\frac{8\langle u\rangle}{D}$ sec^{-1}	τw $dynes/cm^2$
0.00	0.02607	23.3296	57.09186
3.00	0.04504	40.3014	84.55348
5.00	0.05714	51.1252	102.86104
7.87	0.07663	68.5586	129.13251
12.66	0.11645	104.1854	172.97949
14.60	0.13072	116.9529	190.73801
17.59	0.165289	147.8827	218.10813
20.55	0.19950	178.4918	245.20316
23.20	0.22889	204.7936	269.46092
25.95	0.25806	230.8882	294.63430
30.07	0.3967	277.0658	332.34807
34.0	0.34913	312.36268	368.32265

DATA FOR CAPILLARY 7

H cm, Hg	Q cm^3/sec	$\frac{8\langle u\rangle}{D}$ sec^{-1}	τw $dynes/cm^2$
7.20	0.01963	42.03379	90.6729
9.47	0.02464	52.78177	105.8399
12.60	0.02941	62.98895	126.7531
15.60	0.03759	80.51202	146.7976
18.80	0.04656	99.72631	168.1780
21.60	0.05242	111.83412	186.8865
24.40	0.05997	128.43325	205.6205
28.50	0.07086	151.75351	232.9887
33.30	0.08918	191.00311	265.0595
36.45	0.09744	208.68432	286.1062
39.95	0.10944	234.37742	309.5991
44.13	0.12539	268.5419	337.4201

B-13 (A)

TABLE 65

Solution: 2.4% (by wt) Natrosol 250-GR

Density of Solution: 1.006392 gm/cm^3 at 25^{0}C

DATA FOR CAPILLARY 1 Ho = 1.79 cm

H cm, Hg	Q cm^3/sec	$\frac{8\langle u\rangle}{D}$ sec^{-1}	τw dynes/cm^2
1.60	0.032706	22.53645	78.2797
5.00	0.055866	38.49452	113.1271
8.20	0.080483	55.45689	145.92470
10.80	0.099132	68.30749	172.57273
12.60	0.114123	78.63645	191.02136
16.20	0.149068	102.71581	227.91863
19.20	0.180995	124.71528	258.66635
21.70	0.204342	140.80243	284.28945
24.50	0.25126	173.12862	312.98733
26.65	0.272479	187.7256	335.02319
29.30	0.316623	218.16947	362.18367

TABLE 65 (cont'd)

DATA FOR CAPILLARY 2 Ho = 2.08 cm

H cm, Hg	Q cm^3/sec	$\frac{8\langle u\rangle}{D} sec^{-1}$	τw $dynes/cm^2$
6.46	0.01957	26.67837	101.26589
8.79	0.02478	33.78599	120.06709
11.01	0.02900	39.54357	137.98068
13.77	0.03853	52.53428	160.25163
17.44	0.05006	68.24855	189.86554
20.26	0.06097	83.12589	212.62059
22.90	0.07011	95.58385	233.92328
26.99	0.08753	119.32295	266.92625
29.50	0.09685	132.03532	287.17990
32.51	0.11019	150.22200	311.46815
35.66	0.12565	171.30028	336.88608
39.09	0.14354	195.68393	364.56338

TABLE 65 (cont'd)

DATA FOR CAPILLARY 6 $\qquad$ Ho = 2.35 cm

H cm, Hg	Q cm^3/sec	$\frac{8\langle u\rangle}{D}\ sec^{-1}$	τw dynes/cm^2
1.65	0.02252	20.152177	72.17305
3.57	0.031348	28.046724	89.74843
6.41	0.044297	39.631915	115.74535
9.60	0.060150	53.815969	144.94612
11.60	0.067854	60.708431	163.25381
14.7	0.090497	80.9674664	191.63077
17.63	0.106524	95.3065578	218.45151
20.76	0.133333	119.29207	247.10304
24.08	0.172662	154.47893	277.49382
28.10	0.186263	166.64782	314.29227
30.93	0.205761	184.09269	340.19767
34.30	0.235294	210.515309	371.04612

TABLE 65 (cont'd)

DATA FOR CAPILLARY 7 $H_o = 2.35$ cm

H cm, Hg	Q cm^3/sec	$\frac{8\langle u\rangle}{D}$ sec^{-1}	τ_w dynes/cm^2
7.66	0.01129	24.18087	93.81443
11.20	0.01487	31.84560	117.46686
14.87	0.02178	46.65838	141.98789
18.01	0.02670	57.22985	162.96773
21.20	0.033167	71.03216	184.28164
24.80	0.038511	82.47573	208.33497
29.41	0.047733	102.22528	239.13658
33.18	0.05358	114.75524	264.32576
36.07	0.061068	130.78595	283.63523
38.57	0.066006	141.36104	300.33892
42.91	0.07597	162.70615	329.3354

TABLE 66

Solution: 2.6% (by wt) Natrosol-250GR

Density of solution: 1.00790 gm/cm^3 at 25 C

DATA FOR CAPILLARY 1 — Ho = 3.68 cm

H cm, Hg	Q cm^3/sec	$\frac{8\langle u\rangle}{D}$ sec^{-1}	τw dynes/cm^2
2.32	0.024096	16.60366	87.18749
4.48	0.034014	23.43714	109.32585
6.70	0.045558	31.39188	132.07916
10.30	0.064620	44.52678	168.97643
12.83	0.081383	56.07747	194.907009
15.70	0.103627	71.40434	224.32232
18.25	0.123456	85.06814	250.45789
21.10	0.145454	100.22573	279.66823
24.07	0.169312	116.66487	310.10847
26.78	0.191387	131.87596	337.88391
28.78	0.208695	143.80214	358.38239

TABLE 66 (cont'd)

DATA FOR CAPILLARY 2 — Ho = 2.35 cm

H cm, Hg	Q cm^3/sec	$\frac{8\langle u\rangle}{D}$ sec^{-1}	τ_w dynes/cm^2
4.65	0.0104438	14.23775	87.21033
7.36	0.0160192	21.83844	109.07793
11.15	0.021645	29.50789	139.66003
13.89	0.0274536	37.42662	161.76960
16.47	0.0329489	44.91811	182.58809
19.39	0.0421941	57.52172	206.15011
22.40	0.0479616	65.38440	230.43835
26.14	0.0596125	81.26764	260.61710
29.45	0.0667779	91.03604	287.32610
32.36	0.0786627	107.23813	310.80743
35.74	0.0913242	124.49906	338.0813
39.50	0.10165184	138.57837	368.42141

TABLE 66

DATA FOR CAPILLARY 6 — Ho = 2.00 cm

H cm, Hg	Q cm^3/sec	$\frac{8\langle u\rangle}{D}$ sec^{-1}	τw $dynes/cm^2$
3.66	0.0773	15.8633	90.9202
5.72	0.02448	21.9018	109.2773
8.18	0.03200	28.6300	131.7957
11.18	0.04338	38.8152	159.2573
14.30	0.056258	50.3342	187.8173
17.10	0.06768	60.5543	213.4480
19.50	0.084388	75.5013	235.4173
22.02	0.09356	83.7137	258.4849
24.22	0.105263	94.1779	278.6234
26.62	0.121089	108.3370	300.5927
28.94	0.130152	116.4445	321.8296
31.28	0.144230	129.0419	343.2996

DATA FOR CAPILLARY 7 — Ho = 2 cm

H cm, Hg	Q cm^3/sec	$\frac{8\langle u\rangle}{D}$ sec^{-1}	τw $dynes/cm^2$
14.84	0.02285	26.3098	141.6780
18.45	0.016326	34.9652	165.7981
22.55	0.021141	45.2774	193.1922
26.05	0.02442	52.2984	216.5774
29.33	0.02974	63.6913	238.4926
33.21	0.34042	72.9062	264.4168
36.07	0.037843	81.0452	283.5258
38.70	0.044297	94.86687	301.0980
41.15	0.045871	98.2399	317.4677
49.44	0.061967	111.10867	344.1936
49.44	0.061967	132.7107	372.8572

TABLE 67

Solution: 0.2% (by wt) Natrosol-250HR

Density of solution: 1.00083 gm/cm^3 at 25°C

DATA FOR CAPILLARY 3 Ho = 3.44 cm

H cm, Hg	Q cm^3/sec	$\frac{8\langle u\rangle}{D}$ sec^{-1}	τw dynes/cm^2
17.90	0.473934	2533.2194	119.7214
15.42	0.414957	2217.8809	107.5159
13.72	0.384246	2053.8320	99.1492
11.80	0.338984	1811.9011	89.9971
10.42	0.306000	1635.5985	82.9079
8.15	0.254460	1360.1156	71.7359
5.80	0.199711	1067.4759	60.1701
3.60	0.1516301	810.4770	49.3426
1.60	0.115830	619.1227	39.4994

DATA FOR CAPILLARY 9 Ho = 2.50 cm

H cm, Hg	Q cm^3/sec	$\frac{8\langle u\rangle}{D}$ sec^{-1}	τw dynes/cm^2
13.21	0.149477	1461.1029	78.3335
11.40	0.129089	1261.8175	71.1050
10.375	0.119130	1164.4779	67.0115
8.64	0.112081	1095.5703	60.0825
6.90	0.088954	869.5137	53.1335
5.80	0.082835	809.6941	48.7404
4.25	0.0695696	680.0274	42.5502
3.10	0.058608	572.8810	37.9575
1.29	0.045558	445.3201	30.7289

TABLE 67 (cont'd)

DATA FOR CAPILLARY 10 Ho = 1.67 cm

H cm, Hg	Q cm^3/sec	$\frac{8\langle u\rangle}{D} sec^{-1}$	τw $dynes/cm^2$
10.55	0.07619	1099.7125	59.2468
9.18	0.06999	1010.2414	54.4421
8.23	0.062927	908.2719	51.1103
6.81	0.056818	820.0997	46.1302
5.50	0.05035	726.7382	41.5359
3.70	0.043103	622.0744	35.2232
1.90	0.0331125	477.9379	28.9104
0.69	0.027777	400.9357	24.6608

DATA FOR CAPILLARY 11 Ho = 2.80 cm

H cm, Hg	Q cm^3/sec	$\frac{8\langle u\rangle}{D} sec^{-1}$	τw $dynes/cm^2$
11.00	0.038648	907.9442	52.0158
8.84	0.032787	770.2527	45.5644
7.30	0.030379	713.70386	40.9648
5.27	0.024570	577.2177	34.90167
4.00	0.021826	512.7582	31.1085
2.30	0.01839	432.0992	26.03098
1.44	0.016034	376.6875	23.4624

TABLE 67 (cont'd)

DATA FOR CAPILLARY 12 $H_o = 3.37$ cm

H cm, Hg	Q cm^3/sec	$\frac{8\langle u\rangle}{D}$ sec^{-1}	τ_w $dynes/cm^2$
11.60	0.10568	1270.4221	67.6548
10.42	0.10153	1220.4916	63.2256
8.80	0.08696	1045.3347	57.1449
6.82	0.07253	871.9027	49.7128
4.97	0.06041	726.2147	42.7688
3.76	0.05411	650.4556	38.2270
1.88	0.04438	533.5209	31.1704
0.75	0.03658	439.8077	26.9289

TABLE 68

Solution: 0.3% (by wt) Natrosol-250HR

Density of solution: 1.00180 gm/cm^3 at 25^{o}C

DATA FOR CAPILLARY 2

Ho = 2.85 cm

H cm, Hg	Q cm^3/sec	$\frac{8\langle u\rangle}{D}$ sec^{-1}	τw dynes/cm^2
0	0.23529	320.7682	49.6859
1.52	0.32128	437.9967	61.9572
3.66	0.45512	620.4502	79.2338
6.00	0.62015	845.4375	98.1256
8.10	0.772202	1052.7158	115.0787
10.40	0.96618	1317.1639	133.6470
13.10	1.23916	1689.3021	155.4446
15.40	1.49627	2039.8103	174.0129
18.28	1.767676	2409.8114	197.2637
20.78	2.09424	2855.0047	217.4467
23.70	2.42589	3307.1352	241.0204

TABLE 68 (cont'd)

DATA FOR CAPILLARY 3 Ho = 3.30 cm

H cm, Hg	Q cm^3/sec	$\frac{8\langle u\rangle}{D}$ sec^{-1}	τw $dynes/cm^2$
3.43	0.060015	320.7859	48.5121
5.85	0.08359	446.8212	60.4224
7.99	0.10281	549.5438	70.9546
9.99	0.12170	650.5184	80.7978
11.98	0.14746	788.21715	90.5918
14.18	0.17057	911.7429	101.4193
16.99	0.210305	1124.1007	115.2489
19.55	0.23833	1273.9062	127.8482
21.31	0.26548	1419.0512	136.5102
24.21	0.31215	1668.4815	150.7829
26.45	0.34653	1852.2399	161.8073

TABLE 68 (cont'd)

DATA FOR CAPILLARY 7 Ho = 2.85 cm

H cm, Hg	Q cm^3/sec	$\frac{8\langle u\rangle}{D}$ sec^{-1}	τw $dynes/cm^2$
1.77	0.16563	354.72117	54.5247
3.84	0.22421	480.18385	68.3685
5.90	0.29888	640.08667	82.1455
8.07	0.37234	797.41170	96.6582
11.14	0.48077	1029.63095	117.1899
13.20	0.60332	1292.08136	130.9669
16.15	0.74627	1598.22389	150.6960
18.30	0.85470	1830.44447	165.0749

DATA FOR CAPILLARY 8 Ho = 2.98 cm

H cm, Hg	Q cm^3/sec	$\frac{8\langle u\rangle}{D}$ sec^{1}	τw $dynes/cm^2$
1.77	0.09367	295.5344	47.9055
4.39	0.14035	442.7837	63.2203
6.77	0.18476	582.8787	77.1322
9.50	0.24814	782.8362	93.0899
11.00	0.27523	868.3064	101.8580
13.40	0.335008	1056.8945	115.8868
16.12	0.418850	1321.3962	131.7861
18.43	0.478470	1509.4919	145.2888
20.34	0.54595	1722.3836	156.4534
22.88	0.628273	1982.0943	171.3006
25.60	0.628273	2271.70638	187.1999
0	0.06914	218.1388	37.5593

TABLE 68 (cont'd)

DATA FOR CAPILLARY 9 Ho = 2.45 cm

H cm, Hg	Q cm^3/sec	$\frac{8\langle u\rangle}{D}$ sec^{-1}	τw $dynes/cm^2$
3.45	0.02546	248.8804	39.3866
5.91	0.03361	328.5639	49.2110
8.63	0.04449	434.9183	60.07385
11.37	0.05598	547.2236	71.0165
14.17	0.06950	679.3942	82.1988
16.85	0.084299	824.607479	92.9018
19.69	0.097959	957.5298	104.2439
22.85	0.11881	1161.3598	116.8639
25.33	0.133779	1307.6642	126.7682
28.15	0.1541425	1506.7096	138.03038

TABLE 69

Solution: 0.4% (by wt) Natrosol-250HR

Density of solution: 1.00190 gm/cm³ at 25°C

DATA FOR CAPILLARY 2 Ho = 2.67 cm

H cm, Hg	Q cm^3/sec	$\frac{8\langle u\rangle}{D}$ sec^{-1}	τw dynes/cm^2
1.89	0.15711	214.1815	64.8421
4.04	0.22805	310.8931	82.1995
5.45	0.27952	381.0665	93.5827
6.86	0.33755	460.1740	104.9658
8.60	0.41279	562.7518	119.0132
9.60	0.46029	627.5105	127.0864
11.00	0.53619	730.9783	138.3625
13.15	0.64308	876.6975	155.7462
15.51	0.77821	1060.91041	174.7989
18.90	1.00755	1373.5665	202.1670

DATA FOR CAPILLARY 6 Ho = 2.52 cm

H cm, Hg	Q cm^3/sec	$\frac{8\langle u\rangle}{D}$ sec^{-1}	τw dynes/cm^2
0.00	0.21459	191.8959	56.7986
1.60	0.28626	255.9865	71.2507
3.70	0.39801	355.9147	90.2190
5.20	0.51195	457.8041	103.7678
6.23	0.57472	513.9323	113.0713
7.55	0.69404	620.6401	124.9943
8.94	0.814667	728.5039	137.5995
10.61	0.941176	840.6491	152.6338
12.58	1.17994	1055.1444	170.4279
15.00	1.38409	1237.7101	192.2866

TABLE 69 (cont'd)

DATA FOR CAPILLARY 7 — Ho = 1.73 cm

H cm, Hg	Q cm^3/sec	$\frac{8\langle u\rangle}{D}$ sec^{-1}	τ_w dynes/cm^2
0.95	0.66781	143.01969	48.5177
2.29	0.085349	182.78442	57.4794
4.15	0.116050	248.53500	69.9188
6.05	0.147783	316.49662	82.6258
8.07	0.186393	399.18393	96.1353
9.85	0.224215	480.18385	108.0397
11.92	0.273224	585.14208	121.8835
13.90	0.321543	688.62380	135.1255
15.76	0.376648	806.635909	147.5649
17.64	0.447229	958.22405	160.1386

DATA FOR CAPILLARY 8 — Ho = 1.93 cm

H cm, Hg	Q cm^3/sec	$\frac{8\langle u\rangle}{D}$ sec^{-1}	τ_w dynes/cm^2
1.68	0.041494	130.9057	46.8573
2.82	0.047847	150.9488	53.5244
4.25	0.060377	190.4804	62.4677
5.80	0.073801	232.8288	70.9435
7.51	0.091117	287.4575	80.9389
8.75	0.104076	328.3433	88.1872
10.70	0.125000	394.3537	99.5856
11.96	0.140944	444.6556	106.9507
13.12	0.155527	490.6613	113.73133
15.02	0.181159	571.5272	124.8375
17.02	0.208772	658.6312	136.5281

TABLE 70

Solution: 0.5% (by wt) Natrosol-250HR

Density of solution: 1.002314 gm/cm^3 at 25^{o}C

DATA FOR CAPILLARY 1 Ho = 4.00 cm

H cm, Hg	Q cm^3/sec	$\frac{8\langle u\rangle}{D}$ sec^{-1}	τ_w dynes/cm^2
0.0	0.12207	87.0240	62.4575
1.08	0.15748	112.2632	72.9296
2.12	0.19474	138.8260	83.0138
3.55	0.25031	178.4411	96.8796
5.38	0.33116	236.0500	114.6239
7.03	0.42508	303.0274	130.6229
8.80	0.52219	372.2565	147.7855
10.68	0.63593	453.3373	166.0147
12.59	0.776119	553.2731	184.5347

DATA FOR CAPILLARY 2 Ho = 2.52 cm

H cm, Hg	Q cm^3/sec	$\frac{8\langle u\rangle}{D}$ sec^{-1}	τ_w dynes/cm^2
1.19	0.05618	76.5879	59.1222
2.81	0.07641	104.1655	72.2007
4.01	0.09434	128.6098	81.8885
5.93	0.12618	172.0209	97.3890
7.55	0.15707	214.1253	110.4676
8.44	0.17683	241.0726	117.6527
10.90	0.23697	323.0485	137.5127
12.65	0.27933	380.8002	151.6408
14.58	0.33578	457.7599	167.2221
15.965	0.37878	516.3881	178.4034
17.42	0.42598	580.7311	190.1499
18.82	0.47789	651.5014	201.4524
20.32	0.52792	719.6938	213.5622

TABLE 70 (cont'd)

DATA FOR CAPILLARY 7 Ho = 2.67 cm

H cm, Hg	Q cm^3/sec	$\frac{8\langle u\rangle}{D} sec^{-1}$	τw $dynes/cm^2$
1.58	0.03378	72.3520	53.1872
3.36	0.04376	93.7251	65.0916
5.28	0.05913	126.6295	77.9323
7.12	0.071749	153.6599	90.2379
8.69	0.087816	188.0678	100.7378
10.50	0.105448	225.8298	112.8429
11.70	0.119403	255.7161	120.8683
13.65	0.141844	303.7759	133.9096
15.65	0.171086	366.4022	147.2850
17.80	0.202839	434.4057	161.6642
19.60	0.231127	494.9856	173.7023
22.17	0.278607	596.6708	190.8901
24.51	0.324826	695.6538	206.5399
26.63	0.364881	781.4359	220.7179

DATA FOR CAPILLARY 8 Ho = 2.51 cm

H cm, Hg	Q cm^3/sec	$\frac{8\langle u\rangle}{D} sec^{-1}$	τw $dynes/cm^2$
3.13	0.029768	78.1780	55.6719
6.36	0.036969	116.6894	74.5524
9.89	0.055866	176.3373	95.1865
12.55	0.070671	223.0698	110.7351
15.52	0.087527	276.2748	128.0957
18.10	0.106007	334.6047	143.1767

TABLE 71

Solution: 0.6% (by wt) Natrosol-250HR

Density of Solution: 1.002746 gm/cm^3 at 25°C

DATA FOR CAPILLARY 1 — Ho = 3.10 cm

H cm, Hg	Q cm^3/sec	$\frac{8\langle u \rangle}{D}$ sec^{-1}	τ_w dynes/cm^2
1.08	0.08197	56.4797	73.7159
3.87	0.14423	99.3825	102.3113
7.31	0.24539	169.0925	137.5686
10.31	0.36271	249.9285	168.3164
12.32	0.43620	300.5679	188.9173
13.05	0.48134	331.6736	196.3998
15.25	0.60000	413.4311	218.947
19.00	0.80808	556.8096	257.3822

DATA FOR CAPILLARY 2 — Ho = 2.915 cm

H cm, Hg	Q cm^3/sec	$\frac{8\langle u \rangle}{D}$ sec^{-1}	τ_w dynes/cm^2
3.30	0.03992	54.4217	76.4130
6.31	0.06111	83.3164	100.7133
8.44	0.08501	115.8992	117.9092
12.23	0.13148	179.2459	148.5066
15.06	0.17045	232.3747	171.3542
16.80	0.19704	268.6236	185.4010
19.50	0.25467	347.1812	207.1986
21.70	0.30567	416.7185	224.9596
24.51	0.37470	510.8252	247.6453
27.67	0.46296	631.1411	273.1565
29.95	0.52863	720.6686	291.5639
33.70	0.65217	889.0857	321.8378

TABLE 71 (cont'd)

DATA FOR CAPILLARY 6 Ho = 3.49 cm

H cm, Hg	Q cm^3/sec	$\frac{8\langle u\rangle}{D}sec^{-1}$	τw dynes/cm^2
1.40	0.059746	53.4542	70.2462
3.47	0.086789	77.6304	88.9435
5.45	0.1016949	90.9855	106.8279
6.70	0.138568	123.9756	118.1185
9.35	0.200334	179.2368	142.0548
11.35	0.240385	215.0698	160.1198
12.92	0.297555	266.22034	174.3009
15.52	0.381471	341.2988	197.7855
16.81	0.406435	363.6337	209.4375
19.12	0.514579	460.3896	230.3026
23.45	0.705329	631.0513	269.4135
25.89	0.747524	668.8025	291.4528

TABLE 71 (cont'd)

DATA FOR CAPILLARY 7 Ho = 2.55 cm

H cm, Hg	Q cm^3/sec	$\frac{8\langle u\rangle}{D}$ sec^{-1}	τw $dynes/cm^2$
4.82	0.02333	49.9795	74.815
8.66	0.03980	85.2387	100.496
10.90	0.05347	114.5251	115.477
14.36	0.06420	137.5037	138.617
15.38	0.07481	160.2209	145.439
17.41	0.09345	200.1514	159.015
19.92	0.11194	239.7336	175.802
21.93	0.128205	274.5666	189.244
24.25	0.152964	327.5900	204.760
25.87	0.167189	358.0556	215.594
28.04	0.193553	414.5167	230.107
29.82	0.214809	458.2658	242.011
31.91	0.24213	518.5521	255.989
34.17	0.26948	577.1167	271.104
36.87	0.312500	669.2563	289.1608

TABLE 72

Solution: 0.7% (by wt) Natrosol-250HR

Density of Solution: 1.003716 gm/cm³ at 25°C

DATA FOR CAPILLARY 1 Ho = 3.57 cm

H cm, Hg	Q cm³/sec	$\frac{8\langle u\rangle}{D}$ sec⁻¹	τw dynes/cm²
7.65	0.097959	69.8323	136.41436
9.65	0.128388	91.5241	155.8071
11.14	0.148699	106.0031	170.2546
12.90	0.183346	130.7021	187.32025
14.63	0.219298	156.3314	204.0949
16.50	0.267141	190.4375	222.2271
18.50	0.327485	233.4549	241.6198
20.50	0.430686	307.02389	261.0126
1.34	0.032362	23.070256	75.2303
3.22	0.048193	34.30552	93.4595
5.68	0.072376	51.59501	117.31253

DATA FOR CAPILLARY 2 Ho = 2.96 cm

H cm, Hg	Q cm³/sec	$\frac{8\langle u\rangle}{D}$ sec⁻¹	τw dynes/cm²
7.61	0.03555	48.4716	111.2834
9.74	0.04474	60.9962	128.4793
11.52	0.05575	76.0008	142.8496
14.08	0.07396	100.8332	163.5169
16.47	0.09281	126.5211	182.8118
19.29	0.11713	159.6796	205.5782
21.95	0.14754	201.1374	227.0529
23.99	0.16438	224.0983	243.7564
27.30	0.21695	295.0789	270.2444
31.87	0.286298	390.3007	307.1389

TABLE 72 (cont'd)

DATA FOR CAPILLARY 6 — Ho = 2.86 cm

H cm, Hg	Q cm^3/sec	$\frac{8\langle u\rangle}{D}$ sec^{-1}	τ_w dynes/cm^2
5.30	0.050062	44.7905	105.1088
6.95	0.060698	54.3059	120.0125
9.14	0.085288	76.3062	139.7937
11.30	0.103004	92.1569	159.3039
13.08	0.126849	113.4739	175.3820
14.86	0.152381	136.3338	191.4598
17.75	0.207972	186.0708	217.5638
19.19	0.228833	204.7347	230.5706
21.33	0.274348	245.4569	249.9025
24.25	0.344827	308.5139	276.2752

DATA FOR CAPILLARY 8 — Ho = 2.43 cm

H cm, Hg	Q cm^3/sec	$\frac{8\langle u\rangle}{D}$ sec^{-1}	τ_w dynes/cm^2
17.72	0.024360	76.8925	140.9732
20.26	0.029600	93.4318	155.8204
22.88	0.035429	111.8313	171.1352
25.12	0.041841	132.0685	184.2287
28.71	0.0526085	166.0555	205.2135
30.90	0.059790	188.7257	218.0147
33.37	0.069649	219.8439	232.4530
35.37	0.078973	249.2747	244.1434
39.93	0.098684	311.4906	270.7981
43.80	0.118812	375.0223	293.4196

APPENDIX C

SAMPLE CALCULATION

I CAPILLARY TUBE 2

(a) The calculation of shear stress vs shear rate for the flow of 2.2% natrosol-250GR solution.

Density of mercury	$\rho_{Hg} = 13.6$ gm/cm^3
Length of capillary tube	$L = 80.74$ cm
Density of the solution	$\rho = 1.0056$ gm/cm^3
Diameter of capillary tube	$D = 0.19553$ cm
Height of solution above capillary	$H_o = 2.61$ cm
Pressure drop across the capillary tube	$\Delta h = 12.62$ cm
Flow rate of the solution	$Q = 0.068906$ cm^3/sec

$$\text{Shear rate} = \frac{8\langle u\rangle}{D} = \frac{32Q}{D_2}$$

$$= \frac{32 \times 0.068906}{(0.19553)^2}\ \text{sec}^{-1}$$

$$= 93.9374\ \text{sec}^{-1}$$

$$\text{Shear stress} = r_H \left(-\frac{dP'}{dx}\right)$$

$$\left(-\frac{dP'}{dx}\right) = \frac{\Delta h \rho_{Hg}}{L}\frac{g}{g_c} = \frac{(H_o+L)}{L}\rho\frac{g}{g_c} - \rho\frac{\langle u\rangle^2}{g_c L}\left(\frac{1}{2\alpha'} + \frac{k_c}{2}\right)$$

$$= \frac{12.62 \times 13.6}{80.74} + \frac{(2.61 + 80.74)}{80.74}\ 1.005602$$

$$- \frac{1.005602 \times (2.2959)^2}{980 \times 80.74}\left(\tfrac{1}{4} + \frac{0.23}{2}\right)$$

$$= 3.1638\ \text{gm/cm}^3$$

$$= r_H \left(\frac{-dP'}{dx}\right) = \frac{D}{4}\left(\frac{-dP'}{dx}\right)$$

$$= \frac{0.19553 \times 3.1638}{4} \times 980 \quad \text{dynes/cm}^2$$

$$= 151.5637 \quad \text{dynes/cm}^2$$

(b) Calculation of the effective slip velocity at a shear stress of 151.560 dynes/cm^2

The critical shear stress for 2.2% Natrosol-250GR from Table 1 τc = 900 dynes/cm^2.

The diameter of the tube D = 0.19553 cm.

From equations (56) & (57)

$$u_w = \frac{\xi'''}{D}(\tau w - \tau c)$$

$\xi''' = 11.5 \times 10^{-5}$ obtained from fig. (27) at τ = 151.56 dynes/cm^2

$$u_w = \frac{11.5\ (151.56 - 900) \times 10^{-5}}{0.19553} \quad \text{cm/sec}$$

$$= 0.4240 \text{ cm/sec}$$

(c) Calculation of the anomalous layer thickness for 2.2% Natrosol-250GR solution at a shear stress of 151.560 dynes/cm^2

From equation (64)

$$\delta = - \frac{u_w}{f(\tau w)}$$

where $f(\tau w) = \frac{1 + 3n'}{4n'} \quad \frac{8(\langle u \rangle - u_w)}{D}$

The flow behaviour index n' is obtained from the 2.2% Natrosol-250GR solution in fig. (13)

$$n' = 0.770$$

$$f(\tau w) = \frac{(1 + 3 \times 0.77)}{4 \times 0.77} (109) \ sec^{-1}$$

$$= 117.1396 \ sec^{-1}$$

Hence $\delta = - \frac{u_w}{f(\tau w)}$

$$= - \frac{0.4240}{117.1396} \ cm$$

$$= 3.8106 \times 10^{-3} \ cm$$

II Packed Bed II

(a) The calculation of shear stress chear rate for the flow of 2.2% Natrosol-250GR solution.

Density of Mercury	$\rho Hg = 13.6 \ gm/cm^3$
Porosity of Bed	$\varepsilon = 0.3806$
Hydraulic radius	$rH = 0.02452 \ cm$
Area of Bed	$A = 11.39514 \ cm^2$

Difference between pressure taps $H' = 14.7$ cm

Pressure drop across the bed $\Delta h = 35.29$ cm

Flow rate of the solution $Q = 12.416\ cm^3/sec$

$$\text{Shear rate} = \frac{2\langle u\rangle}{rH} = \frac{2}{rH}\frac{Q}{A\ \varepsilon}$$

$$= \frac{2 \times 12.416}{0.02452 \times 11.39514 \times 0.3806}\ sec^{-1}$$

$$= 233.4703\ sec^{-1}$$

$$\text{Shear stress } \tau = rH\left(\frac{-dP'}{dx}\right)$$

$$\frac{-dP'}{dx} = \frac{\Delta h\ \rho_{Hg}}{H'}$$

$$= \frac{35.29 \times 13.6}{14.7}\ gm/cm^3$$

$$= 30.24857\ gm/cm^3$$

Therefore $$\varepsilon = rH\left(\frac{-dP'}{dx}\right)$$

$$= 0.02452 \times 30.24857 \times 980\ dynes/cm^2$$

$$= 726.9034\ dynes/cm^2$$

(b) Calculation of the effective slip velocity at a shear stress of 726.9034 $dynes/cm^2$

The critical shear stress for 2.2% Natrosol-250GR from Table 2 τc = 7800 dynes/cm^2

The hydraulic radius of the bed rH = 0.02452 cm

From equation (56) and (57)

$$u_W = \frac{\xi'''(\tau w - \tau c)}{rH}$$

$\xi''' = 0.32 \times 10^{-5}$ from fig. (28) at τ = 726.9034 dynes/cm^2

$$u_W = \frac{0.32 \times 10^{-5}\ (726.9034 - 7800)}{0.02452} \text{ cm/sec}$$

$$= -\ 0.9076 \text{ cm/sec}$$

(c) Calculation of the anomalous layer thickness for 2.2% Natrosol-250GR at a shear stress of τ = 726.560 dynes/cm^2

From equation (64)

$$\delta = \frac{-\ u_W}{f\ (\tau w)}$$

$f(\tau w)$ is obtained by extrapolation in fig. (29)

$f(\tau w)$ = 965 sec^{-1}

$$\delta = \frac{0.9076}{965} \text{ cm}$$

$$= 9.4447 \times 10^{-4} \text{ cm}$$

III Calculation of the dimensionless group $(\tau/K)^s/w$ for a power-law fluid of 2.2% Natrosol-250GR solution at $\tau = 200$ dynes/cm^2

$$s = \frac{1}{n}$$

The flow behaviour index n was obtained from the slope of fig. (29) vs from the capillary tubes data n = 0.749

$$\tau = K\ f(\tau)^n$$

$$K = \frac{\tau}{f\ (\tau)^n}$$

from fig. (29) when $\tau = 200$ dynes/cm^2 is 166.9036 sec^{-1}

$$K = \frac{200}{(166.9036)\ 0.746} \text{ dynes-sec}^n/\text{cm}^2$$

$$= 4.3291 \text{ dynes-sec}^n/\text{cm}^2$$

$$w = \frac{2(\langle u\rangle - u_w)}{rH} = 57 \text{ sec}^{-1} \text{ from fig. (13)}$$

$$\text{Hence } \frac{(\tau/K)^s}{w} = \left(\frac{200/4.329}{57}\right)^{\frac{1}{n}}$$

$$= 2.9281$$

IV Ellis fluid model

Calculation of the dimensionless group $w\ \eta o/$ and $(\tau/\tau_{1/2})^{-1}$ at $\tau = 300$ dynes/cm^2 for 2.2% Natrosol-250GR solution at τ = 300 dynes/cm^2

$$w = \frac{2(\langle u\rangle - uw)}{rH} = 97 \text{ sec}^{-1} \text{ from fig. (13)}$$

ηo = 1.9404 poise obtained from table (34)

$$w = \frac{97 \times 1.9404}{300} = 0.6274$$

α was obtained from the slope of fig. (39)

$$\alpha = 1.6078$$

$\tau_{1/2}$ was obtained from fig. (38) when $\eta = \frac{\eta o}{2}$

$$\tau_{1/2} = 412 \text{ dynes/cm}^2$$

$$\left(\frac{\tau}{\tau_{1/2}}\right)^{\alpha-1} = \left(\frac{300}{412}\right)^{0.6078}$$

$$= 0.8246$$